The ENergy Roof

INTEGRATED WITH PHOTOVOLTAIC-THERMAL, HEAT PUMP, STORAGE, VENTILATION AND HEAT RECOVERY FOR A 'NUL-OP-DE-METER' RENOVATION

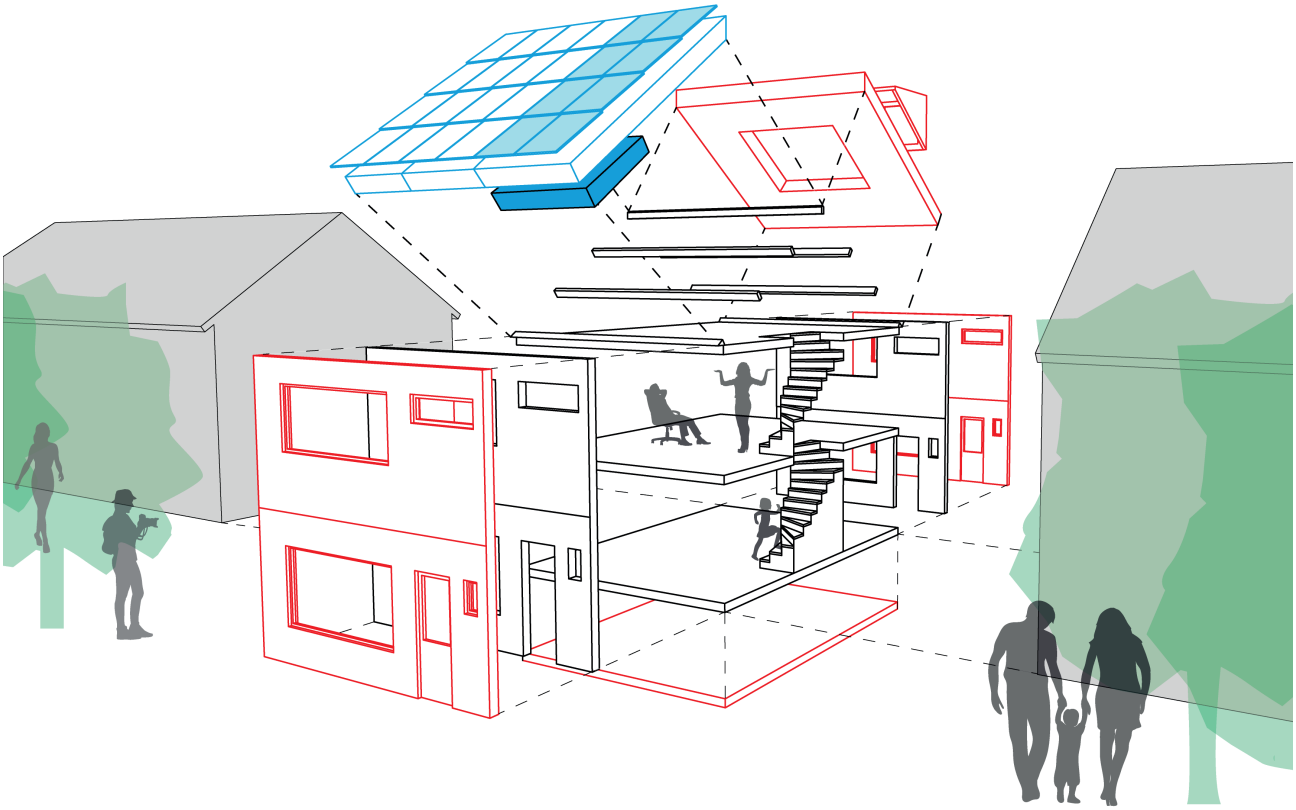

Master thesis
Stefan Hoekstra
Delft University of Technology
June 24, 2016

Graduation thesis
The ENergy Roof
This is the final report of the graduation year in the master Building Technology which is part of the Faculty of Architecture and the Built Environment at the Delft University of Technology.

Figures
The figures without acknowledgement are made by the author

Author
Wopke Stefan (W.S.) Hoekstra
4005635
W.S.Hoekstra@student.tudelft.nl
wshoekstra.91@gmail.com

First mentor
Prof.ir. P.G. (Peter) Luscuere
Architectural Engineering +Technology
Installaties

Second mentor
Ir. F.R. (Frank) Schnater
Architectural Engineering +Technology
Ontwerpen van Bouwconstructies

Third mentor
Dr.ir. W.H. (Wim) van der Spoel
Architectural Engineering +Technology
Bouwfysica

Graduation company mentor
Ir. D.J. (Dirk-Jan) Peters
Van Dorp
Adviseur Energiemanagement

External examiner
Ir. S.A. (Salomé) Bentinck
Management in the Built Environment
Real Estate Management

June 2016

Preface

This report contains the graduation thesis 'The ENergy Roof: integrated with photovoltaic-thermal, heat pump, storage, ventilation and heat recovery for a Nul-op-de-Meter renovation'. This research is part of the graduation phase in the master Building Technology at the Delft University of Technology. The aim of the thesis is to investigate how the built environment can be more sustainable.

During my student time the topic of sustainability was frequently addressed and underlined that sustainability is not only an add-on or green-washing of the project, but rather a design style that should be addressed from the beginning of every project. In the architecture projects I learned to switch between the role as designer and engineer, where my interest grew towards the second role and particularly towards the climate design. However these projects remained on paper.

I am therefore thankful to have participated in the student team of Prêt-à-Loger in which I worked together with students from many different nationalities and companies with different specialties to design, engineer and build an energy neutral home to participate the Solar Decathlon competition in 2014. This was a great experience to actually build a house and mount the installation system. In addition this project was the seed of my graduation research at the company Van Dorp, who were also part of the sponsor team of Prêt-à-Loger, therefore I am Henk Willem van Dorp grateful for giving me this graduation topic.

Furthermore I wish to express my gratitude to my first mentor Peter Luscuere for the help in defining and shaping the core of this thesis, to my mentor Wim van der Spoel for the hours of discussing the installation system and especially the modelling of the heat pump and to Frank Schnater who encouraged me to make the step towards the architectural application. It was a pleasure to work with my colleagues at Van Dorp and I especially would like to thank Dirk-Jan for the intensive supervision and helping me to understand, although partially, the world of thermodynamics.

Also I would like to thank my life partner Christien who supported me and cheered me up in the valleys of the graduation process and helped me by reading and reviewing my thesis. My parents for their support and giving me the opportunity to study. Finally, many thanks to my architecture study friends Maria, Tobias, Chiel and Onno for the many coffee breaks and great student time.

Delft, June 24, 2016

Stefan Hoekstra

Abstract

This report describes the development of the ENergy Roof: a new concept for the Nul-op-de-Meter (NoM) renovation of single family dwellings in the Netherlands. The ENergy Roof consists of innovative technology, namely a solar assisted heat pump (SAHP) connected to photovoltaic solar panels that operates as evaporator (PV-DX). Furthermore the concept integrates all the required installation components in a single roof element which allows industrialisation, high production rates, price reduction and a one-day renovation, making a NoM more attractive.

The purpose of this study is to develop the installation and control system of the ENergy Roof and to assess the technical feasibility with dynamic simulations. In the first part, a literature study has been performed to find a suitable building type for the renovation. Also the related energy demand of the dwelling is investigated. The results show that there is a large potential of 1 million post war row houses in the Netherlands with a final energy demand of 68 GJ per year whereof two third is covered by the heating demand. In accordance with the New Stepped Strategy, the dwelling was firstly wrapped in a new insulating skin and applied with a heat recovery unit, reducing the heating demand. The dwelling becomes net zero energy with the installation of the ENergy Roof, decreasing the final electrical energy demand and generating the remaining demand with solar energy. From research into the state of the art installations, the ENergy Roof system was developed. A numerical MATLAB/Simulink model was constructed in order to simulate the system's annual electrical energy input to supply the space heating and hot tap water demand of the dwelling. The model predicts the heat transfers in the panel, the operation of the SAHP and storage tanks, and includes a control strategy. Different configurations (e.g. heat pump capacity, area evaporator and storage volume) of the installation system were run and analysed.

The results show that net zero energy renovation of a post war row house can be achieved with the ENergy Roof, providing the annual heating, hot water and electricity demand. The smallest design is a 3 kW heat pump, 6 m^2 evaporator and 2 kW electrical heater, and achieves a seasonal coefficient of performance (SCOP) of 2,6. A row house with a South orientation is able to generate the annual electricity demand on a single roof surface, and East-West orientation require both sides of the roof. Increasing the evaporator area has a larger influence on the SCOP compared to increasing the heat pump capacity. Highest SCOP of 3,0 is achieved with 12 m^2 evaporator and 5 kW heat pump. A risk of the system is the ice formation on the evaporator which can occur from November till March. Further investigation of this effect is recommended.

This study has shown that the ENergy Roof is technically and financially feasible. All the installations fit in a single roof element, which can be industrially produced. The investment costs of the ENergy Roof's installations is € 15.500,- and fall within the scope of the Stroomversnelling.

Keywords: solar assisted heat pump, direct expansion, renovation, row house, thermal storage, renewable energy, nul op de meter, net zero energy, new stepped strategy

Table of contents

List of abbreviations

ASHP	Air source heat pump
BENG	Nearly zero energy (bijna energie neutraal gebouw)
CO_2	Carbon dioxide
COP	Coefficient of performance
DX	Direct expansion
EEV	Electronic expansion valve
EPBD	European Energy Performance of Buildings Directive
EPC	Energy performance coefficient (energie prestatie coefficiënt)
EPN	Energy performance norm (energie prestatie norm)
EPV	Energy performance compensation (energie prestatie vergoeding)
GJ	Giga joule (10^9 joules)
GSHP	Ground source heat pump
GWP	Global warming potential
HRU	Heat recovery unit
IEA	International Energy Agency
kW	Kilo watt (10^3 joules per second)
kWh	Kilo watt hour (or 3,6 x 10^6 joules)
kWp	Kilo watt peak (nominal power of solar module at 1000 W/m^2)
LCA	Life cycle analysis
LED	Light emitting diode
LTV	Low temperature heating (lage temperatuur verwarming)
MJ	Mega joule (10^6 joules)
MW	Megawatt (10^6 joules per second)
NoM	Net zero energy (Nul-op-de-Meter)
NSS	New stepped strategy
PV	Photovoltaic
PV-DX	Photovoltaic direct expansion
PVT	Photovoltaic thermal
R_c-value	Thermal resistance (m^2K/W)
SAHP	Solar assisted heat pump
SCOP	Seasonal coefficient of performance
U-value	Thermal heat transfer (W/m^2K)
VAT	Value added tax

1. Definition and scope

1.1 Introduction

The reduction of greenhouse gasses, such as CO_2, is an important objective against climate change. The Dutch government committed to this goal in the Kyoto protocol (2005) and aim for a reduction of greenhouse gasses with 20% in 2020. At the Climate Change Conference in Paris (2015), the world leaders decided to aim for maximum 1.5 degrees Celsius temperature rise in 2050 compared to 1990.

Why is this so important? According to the Intergovernmental Panel on Climate Change (IPCC) report, climate change will have a big impact on the world. The augmentation of CO_2, and hence the temperature, will cause catastrophes like dehydration of the soil, floods, famine and the extinction of animal races. Climate change will hit pour countries hardest. On this moment, the temperature increased already with 0,6 degree since 1990. When no actions are taken, it is expected that the temperature will increase with 4 degrees in 2050. It is clear that actions need to be taken to minimise future dangers and costs.

The major contributor to human-caused climate change is by far the burning of fossil fuels. When we continue using the fossil fuels in the current way, we won't meet the aims of the Climate Change Conference. However; the chapter of fossil fuels is closing. The sources of fossil fuels are coming closer to scarcity. Oil, natural gas, and coal are all foreseen to become radically scarce within the next decade. Thereby, the costs of excavating them from the ground are rising. There is found an alternative for fossil fuels in the use of renewables, such as solar and wind energy, which have no CO_2 emissions. The abundant energy of the sun can be harvested to generate electricity and heat. As a result of the Kyoto protocol, the renewable energy technology is developing and being applied on a large scale and becomes more affordable in contrary to the fossil fuels. This can be illustrated in the price development of photovoltaics (PV) against the application of PV in Germany and China (Figure 1-1). The solar energy even proves to be cheaper than fossil fuels in the 200 MW solar park in Dubai with 5.85 US dollar cent per kWh (Graves, 2015). The global installed PV in 2015 is 256,000 MW where the Netherlands has 1,600 MW.

Another part of the renewable energy technology are the heat pumps, which make efficient use of environmental energy, such as solar energy, ground(water) or ambient heat, to provide for heating and hot water. The average coefficient of performance for small heat pumps is around 4, where 1 part electrical energy is needed to provide 4 part thermal energy. Heat pumps are a good alternative for gas boilers since electricity is the source and thereby can be connected to PV. According to the heating and cooling roadmap of the International Energy Agency (IEA, 2011), heat pumps will significantly increase their share in space and water heating.

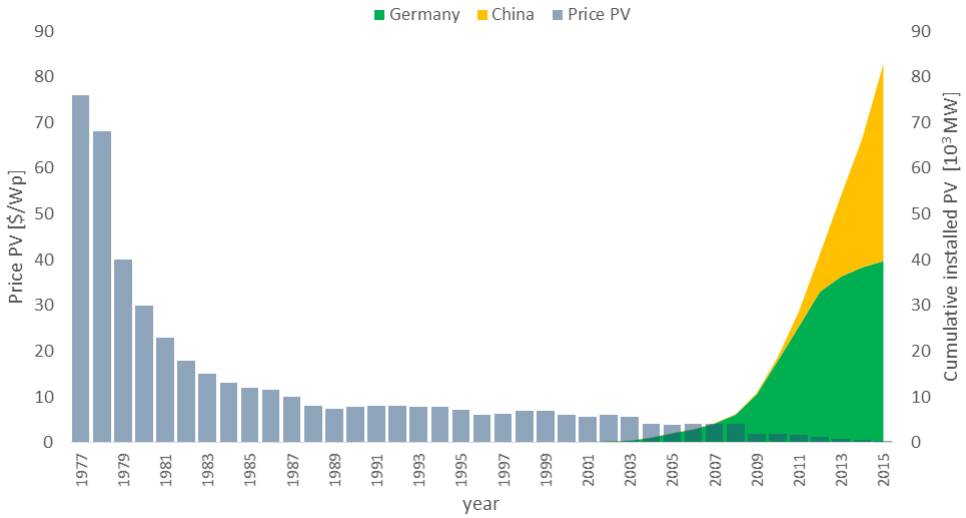

Figure 1-1 Price for crystalline silicon photovoltaic (PV) and cumulative installed PV power in Germany and China (Bloomberg, 2013)

In the Netherlands, which also has the objective to reduce the CO_2 emissions, there is a large amount of residents which consume a high amount of energy, whereby also emitting CO_2. Whereas dwellings consume 26.8% of the total final energy in the EU (Eurostat, 2015), and the Netherlands in 2015 only produced 5.2% of its energy by renewable sources (CBS, 2014), dwellings have a large share in the burning of fossil fuels and the total CO_2 emission in the Netherlands. The new build dwellings are energy efficient due to the EPC regulations, but with an annual grow of less than 1%, most high energy consuming dwellings that are present today are still there in 2050. The challenge is to find a way to renovate these existing dwellings in order to reduce their CO_2 emission.

With the program 'Energiesprong' the Dutch government aims to initiate an energy reduction on a large scale by transforming the existing dwellings into net-zero-energy. In 2013 the deal 'Stroomversnelling' was signed by 6 housing corporations and 4 building contractors (Stroomversnelling, 2016). The objective is to renovate 111.000 residents with a rental contract to net-zero-energy, also called 'Nul-op-de-Meter (NoM) renovation. The renters of high energy consuming dwellings get a sustainable and comfortable dwelling without paying more living expenses. The old energy bill is replaced by the 'Energie Presetatie Vergoeding' (EPV) and paid to the housing corporation which is used to finance the renovation investment. Extrapolating this energy bill over 30 years gives a total of 45.000 euro which can be invested in the renovation. The current NoM renovation costs are higher than this calculated budget. Integration and factory production may reduce the costs making the NoM renovation feasible.

1.2 Graduation studio and company

Within the chosen studio Climate Design the focus is on the bioclimatic design and the indoor environmental quality of buildings. The common theme of the studio, the bachelor Architecture and the master Building Technology at the Technical University of Delft is sustainability. In this research sustainability is expressed both technically, in reducing the fossil energy consumption, and socially by preserving people's homes with the refurbishment of existing dwellings. A holistic approach is key in the effort to make integrated sustainable designs.

The research project is a collaboration between the installation company Van Dorp and the TU Delft. Van Dorp is a progressive installation company and has sustainability as one of the most important priorities. A new product is being developed for the NoM renovation market where this research contributes to.

1.3 Problem statement and objective

Currently the Dutch dwellings consume a high amount of energy of which the majority have fossil fuels as source, contributing to the global CO_2 emissions. Only 1% of the total building stock are newly build low energy dwellings. For most existing dwellings it would thus be recommended to make an intervention to reduce the energy consumption and CO_2 emissions. Currently, there are some energy renovation available, however the renovations does not offer an integrated and affordable solution, for example the dwelling shown in Figure 1-2 where the PV panels are not integrated.

Figure 1-2 Non-integration of PV panels on the roof

The latest developments offer great possibilities for generating renewable energy and to combine this with high efficiency installations, such as a heat pump. For this reason, it would be a big step forward to offer an integrated renovation solution as an affordable product suitable for the NoM

renovation. Price reduction and high production rates are only possible by industrialization. In addition an integrated product give the possibility for a one-day renovation intervention. Therefore, the objective of this research project is to make an integrated roof design, including a technical and financial feasibility study, integrating photovoltaic-thermal, heat pump, ventilation, storage and heat recovery, suitable for 'Nul op de meter' renovation of Dutch dwellings.

1.4 Boundary conditions

The boundary conditions are set in order to make a clear framework in which the research can be done in the given time of a graduation project. Thereby it states clearly where it is about. Setting up the framework is essential within a graduation thesis in order to limit the scope and give a good answer to the research question.

The ENergy Roof is developed for the NoM renovation market with a certain framework. Thereby the company Van Dorp has some boundary conditions for the installations of the ENergy Roof. These conditions are listed below:

- The ENergy Roof includes the installations: direct expansion solar assisted heat pump integrated with photovoltaic panels (PV-DX SAHP), solar boiler with photovoltaic thermal (PVT), thermal storage, ventilation and heat recovery;
- The ENergy Roof excludes the installations: ground- and air source heat pump;
- All the installations are located in or near the roof;
- PV panels may extend maximum 0.5 metre beyond the existing roof and may be applied on both sides of the roof;
- The installation system is connected to a single house, not a collective system;
- The ENergy Roof is only suitable for single-family dwelling with a pitched roof;
- The ENergy Roof has to comply to the framework of the NoM-renovation;
- The annual heating demand of the dwelling is < 30 kWh_th/m^2 (according to EPV);
- The annual hot water demand is set to 11.6 MJ (according to NEN7120)
- The dwelling becomes full electric, thus without a gas connection;
- Shower heat exchanger is not included since it involves a renovation;

Due to time restrictions of this research it was not possible to include the PVT system in the simulations. Therefore the focus lies on the thermodynamic behaviour of the PV-DX panel and the SAHP. Furthermore the boundary conditions of the model are:

- Performance simulated for the Netherlands;
- Orientation North-South and East-West of the dwellings are taken into account;
- Seasonal storage is not researched, short term storage of day-night is taken into account;
- Emission system for heating is low temperature (<35 degrees Celsius);

- Solar assisted heat pump assumed performance with 90% compressor efficiency, isentropic efficiency of 65%, sub cooling and superheating of 5 Kelvin with relating thermodynamic cycles;
- Solar assisted heat pump with refrigerant R134a;
- Condensation and freezing on the panel is not taken into account in the model.

The following topics are closely related to the research, but are excluded from this research report. It is advised to take these topics into account in further development of the ENergy Roof. Life cycle analysis (LCA) and cradle to cradle certification take the materials into account with the embodied energy and the total life cycle. This can help in the decision for certain materials and give insight in the energetic payback time. The ENergy Roof can be improved with a DC grid in the dwelling, reducing the conversion losses of the PV system and smart demotics, reducing the energy consumption of the inhabitants. Furthermore introducing the capture of rainwater can improve the concept of the ENergy Roof and applying phase change materials (PCM) in the floor heating increases the storage capacity and stabilize temperatures improving the internal comfort. Finally the topic of autarky is interesting to research where the dwelling (or district) is of the grid and has its own storage capacities.

1.5 Research questions

Main research question

Is the ENergy Roof, integrated with photovoltaic-thermal, heat pump, storage, ventilation and heat recovery technically and financially feasible for a NoM renovation?

Sub research questions

1 *Which building type in The Netherlands is suitable for the ENergy Roof?*
2 *What is the energy demand of a NoM renovated dwelling?*
3 *What is the minimal required area for the evaporator in Dutch winter conditions?*
4 *What is the ENergy Roof's seasonal coefficient of performance and is NoM accomplished?*
5 *How to design the installations in a modular roof suitable for industrial production?*
6 *Is it possible to realise the installations within the financial framework of the Stroomversnelling?*

1.6 Research method

This research aims for the development and assessment of the ENergy Roof installation system for NoM renovated Dutch dwellings. An overview of the methodical approach of this research is illustrated in Figure 1-3 in four sequentially parts. The theory from the literature is used as input for the system development of the ENergy Roof after which it is simulated with calculation software MATLAB/Simulink, the output is used for the conceptual design and the concept

financial feasibility of the ENergy Roof. After the research it is planned to build a prototype of the ENergy Roof to obtain experimental data on which the model can be validated. Notice that this is not part of this research paper.

The structure of this report follows the line of approach (Figure 1-3) and is briefly described below. In chapter 2, 3 and a part of chapter 4 the literature study is presented. Chapter 4 show the system development with the hydraulic circuit. Chapter 5 and 6 includes the description of the MATLAB model with the used equations and the results from the simulations. These outputs are used for the concept design and financial feasibility in chapter 7. The conclusion and recommendation is presented in chapter 8.

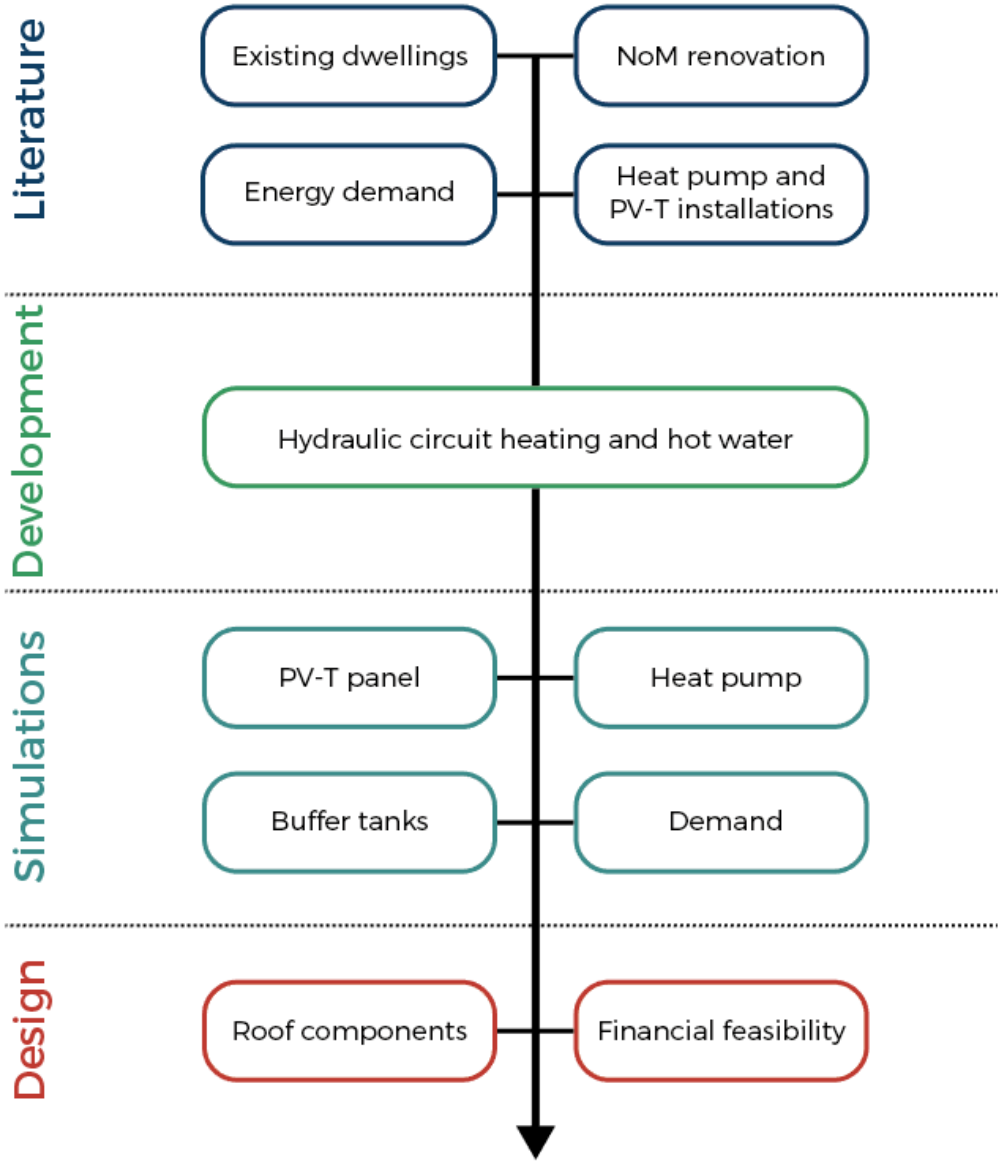

Figure 1-3 Method scheme

1.7 Relevance

Societal relevance

The societal relevance of this research into the ENergy Roof can be seen on two different levels. The first is on the global level with the collective aim to reduce the human-made CO_2 emissions underlined in the Kyoto protocol (2005) and recently the Climate Change Conference (2015). It is very urgent to act now in reducing CO_2 emissions and move from fossil to renewable energy sources in order to prevent that climate change has a catastrophic result on the planet.

The second level is the scale of the Netherlands which has a high quantity of existing low quality dwellings which consume a great amount of (fossil) energy. Besides that the dwellings have moisture and draught problems. The ENergy Roof has the potential of making the NoM renovation technical and financially feasible and can be applied on a large scale, potentially having a great impact in the reduction of the CO_2 emissions of the Netherlands. Thereby the inhabitants benefit from the intervention by improved comfort and health of their dwelling.

Scientific relevance

This study investigates the use of the photovoltaic-thermal roof as source for the heat pump to provide space heating and hot water for a Dutch dwelling. The combination of PV direct expansion and solar assisted heat pump (PV-DX SAHP) is new in the Dutch energy neutral market and has potential for the integration and price reduction of a NoM renovation. However, not much research has be done into this issue. Gaining knowledge in this system is an enrichment for the discipline.

2. Suitable dwelling NoM renovation

In the Netherlands, dwellings differ a lot in characteristics and qualities. Therefore, the Dutch building stock is analysed in order to find the suitable building type for a renovation to net zero energy, Nul-op-de-Meter (NoM), in combination with the ENergy Roof. First, it will be explained what NoM renovation is and are the related energy target, requirements and business model presented. The method New Stepped Strategy (NSS) gives us directions about the steps to come to such an energy efficient design. In the second part the building type criteria are set followed by the analysis of the building history and finally the selected building type is presented.

2.1 Nul-op-de-Meter

A Nul-op-de-Meter (NoM) dwelling produces equally or more energy than it consumes measured over a year (Stroomversnelling, 2016). This net zero energy is achieved by upgrading the dwellings façades, smart installations and sustainable energy generation, among other things. The NoM is part of the deal 'Stroomversnelling' a network organisation of ambitious building contractors, housing corporations and other partners. The aim is to upgrade the dwelling without having higher housing costs for the inhabitant. The ENergy Roof is developed within the framework of the NoM.

2.1.1 NoM programs

The program is split in rental and owner-occupied dwellings with two different business cases. The owner-occupied dwelling is based on the investment by the owner of € 45.000. This number is based on a mortgage of 30 years which is financed by the energy savings of € 175,- per month (Stroomversnelling, 2016). In the Netherlands a higher mortgage is given for energy efficiency measures (Milieu-Centraal, 2016b). In the case of a dwelling with a rental contract the housing corporation makes the investment, while the renter receives the benefit of lower energy costs. Since 2016 the housing corporation may charge an energy performance compensation (EPV) to finance the investment.

There is also a difference in NoM new build or renovation. The deal Stroomversnelling has the ambition to renovate 111.000 dwellings with a rental contract to net-zero-energy. The ENergy Roof is developed for this market as stated in the boundary conditions.

2.1.2 Requirements NoM

There are different requirements for the NoM, where one takes into account the electrical demand for appliances and the other only the building related energy for heating, hot water and ventilation. According to Stroomversnelling (2016) the definition of Nul-op-de-Meter states that the energy flows includes both building-related energy and user-related energy for domestic

appliances. The energy required is calculated based on standard climate conditions in the Netherlands and with average consumption of the dwelling as described in the Dutch norms (NEN 7120). The EPV also gives three requirements for the dwelling in order to receive a compensation (Coen, 2015), this is presented in Figure 2-1. These are the annual heating demand in kWh-thermal per square metre usable surface area, sustainable generated heat for heating demand and hot water in kWh-thermal per square metre usable surface area and finally the sustainable produced electrical energy for the auxiliary and user-related energy in kWh per square metre usable surface area. The minimal user-related energy is 1.700 kWh and maximum 2.500 kWh per dwelling. The ENergy Roof is calculated based on the demands with a compensation of € 1,40/m² per month.

Netto warmtevraag voor ruimteverwarming (Qv) [kWh_th/m²] per jaar	Minimale duurzaam opgewekte warmte voor verwarming en warm tapwater [kWh_th/m²] per jaar	Minimale productie duurzaam opgewekte energie voor gebruiksgebonden gebruik [kWh/m²] per jaar*	Maximale vergoeding [€/m²/maand]**
0 < Qv ≤ 30	Qv + 15	Ehulp + 25	1,40
30 < Qv ≤ 40	Qv + 15	Ehulp + 25	1,20
40 < Qv ≤ 50	Qv + 15	Ehulp + 25	1,00***

Figure 2-1 EPV with the requirements for the dwelling (Coen, 2015)

2.1.3 Cost NoM renovation

The costs target of € 45.000,- is split into different parts by the Stroomversnelling (Hasselaar, 2014) and presented in Figure 2-2. The total cost for the installations including monitoring and sustainable energy generation is € 15.000,-. This number is important for the ENergy Roof and will be discussed in the financial feasibility in chapter 7.

Delen	Toelichting	Eerste prijsindicatie om naar toe te werken
Opmeten		€ 500
Woning-componenten	Gevels	€ 7.000
	Dak	€ 5.000
	Installaties (incl. monitoring en duurzame energie-opwekking)	€ 15.000
	Vloer	€ 1.500
Plaatsen	Sloop kozijn, ramen en dak	€ 1.500
	Geveluitgraaf	€ 1.000
	Logistiek	€ 1.000
	Plaatsing, afbouw	€ 3.500
Cost of sales	Verkoop	€ 4.500
	Prestatiemanagement (metingen, verzekering, service)	€ 3.000
TOTAAL		**€ 43.500 incl. BTW**

Figure 2-2 Cost indication Stroomversnelling NoM renovation (Hasselaar, 2014)

The cost of the pilots are estimated to be higher than the indication of the Stroomversnelling and are around €70.000,- (Finance Ideas, 2015). Thereby recent study of Jonathan (2016) shows the average price of a NoM renovation presented on the website woonconcepten.nl is €75.000,- where the only concept which is realised in practice is the Active-House concept and cost €130.000,-.

2.1.4 Added value

The value of the NoM renovation is merely based on the savings on the energy bill. In the graduation thesis Jonathan (2016) states that the benefits of a NoM renovation involve more factors that are not taken into account by The Stroomversnelling. For private owners also the increase of value of the house (property value) and the decrease of maintenance costs is an added value. The value for public owners such as housing cooperatives has the following five cost benefits: property value increase, maintenance decrease, loss of rental booking, increase of rent and the energy performance compensation (EPV). The increased cost benefits has influence on the target price which can be higher than € 45.000 and thereby approach the current costs on the market for a NoM renovation.

The added value of the NoM renovation with ENergy Roof is not only the energy bill reduction. According to the report of Jonathan (2016) the building contractor BAM performed a NoM renovation in Soesterberg with an average price added value of € 29.000 after price indication of 10 brokers. The Prêt-a-Loger house has an increased value of € 37.000 retrieved from a virtual validation in Apeldoorn by 10 different brokers.

2.1.5 Saldering

An important condition of the NoM financial model is the 'saldering', which balances the energy delivered to the grid and the energy extracted from the grid to a maximum of the annual consumed energy. Sustainable generated energy can either be directly used by the appliances in the house, or locally stored in a battery or delivered to the grid. The compensation for the grid delivery is on the same level as the cost for extraction from the grid. The price is including the taxing and transportation costs. This 'saldering' is a stimulation for renewable energy by the government and last until 2020. According to minister Kamp there will be a transitional arrangement, but it is not certain what the new price will be. Some scenarios are presented by Stroomversnelling (2015) based on 5.500 kWh annual consumption and 30% direct use. With an energy price of 22 cent per kWh and a reduced compensation of 15 cent per kWh (instead of 22 cent), the extra costs are € 21,- per month. This has a negative effect on the financial model which is based on the € 175,- per month cost reduction. Storage technologies grow in importance in order to increase the direct use of the generated energy. This scenario assume the same annual consumption and price reduction but with energy storage technology 70% of the energy is direct

used, the extra costs are € 9,- per month. The ENergy Roof has offer the option for electrical storage.

2.1.6 Subsidies

The government supports public and private owners in the transition towards energy efficient dwellings. Housing corporation are stimulated with the stimuleringsregeling energieprestatie huursector (STEP) and fonds energiebesparing huursector (FEH) (RVO, 2014). With the STEP an application of € 2.000 and € 4.500 per dwelling if respectively 3 or 6 energy label steps are made with the renovation. This subsidy is available until end 2017. The FEH provide a low rent loan for maximum 25% of the renovation cost up to € 15.000. Minimal 3 energy label steps are required. The FEH is available until September 2019.

For house owners there is the possibility of an extra mortgage of € 27.000 to finance a NoM renovation (LenteAkkoord, 2015). And with the 'investeringssubsidie duurzame energie' (ISDE) a compensation of € 500-2.500 can be received for the purchase of a heat pump. In 2016 € 70 million subsidy is made available, every year a new budget is announced until end 2020.

2.1.7 Ambitions beyond NoM

Nul-op-de-Meter is an ambition which is ahead of the Dutch regulations for energy efficiency of dwellings. From beginning 2015 the energy performance coefficient (EPC) is set to maximum 0,4. A NoM dwelling has a EPC equal or lower than zero. Also energy labels are since 2015 mandatory for dwellings that are for sale. Label A stands for high energy efficient and G for low energy efficient dwellings. The government aims for a new energy efficiency norm for the build environment in 2020, 'bijna energie neutraal' (BENG) or nearly zero energy. This is based on the European Energy Performance of Buildings Directive (EPBD). Thereby a minimum of 50% of the primary energy consumption has to be provided with renewables as source. This is lower than the NoM ambition where 100% of the final energy is provided with renewables. However the NoM does not take energy storage into account which reduce the stress on the grid, also known as supply-load matching. Energy Plus dwellings produce more energy than consumed by the building- and user-related energy and has an electrical battery (Norber Fisch, Wilken, & Stähr, 2013). This extra energy can be used for electrical mobility. However, the dwelling requires the connection to the grid since the electrical battery is a short term storage technology and is not suitable for seasonal storage. Autarky districts are disconnected from the grid and has its own energy generation and storage where fuel cells from electrical cars can be used to level the intermittence of the renewable energy. This is a future scenario where also the embodied energy and circularity is taken into account.

2.2 *New Stepped Strategy*

The well-known strategy to design low-energy sustainable dwellings is the Trias Energetica, introduced in 1996 by E. Lysen (Novem) and developed by C. Duijvestein at the Technical University in Delft (RVO, 2013). The sequence of the 3 steps are important to come with an integral design where the joint measures enforce each other. The three steps of reduce, reuse and produce are illustrated in Figure 2-3. In the final step the remaining energy demand is produced with fossil fuel as efficiently as possible. A new methodology is introduced in 2008 by Prof.dr.ir. Andy van den Dobbelsteen where the total energy is produced with renewables and principles of circularity are introduced where waste is food (Van den Dobbelsteen, 2008). The New Stepped Strategy (NSS) is presented in Figure 2-4 and has the following steps. The start is step 0 the stocktaking of the current energy demand of a building, step 1: reduce the energy demand, step 2 reuse and recycle waste flows in the building, step 3a supply the resulting demand with renewable energy produced on the building location and step 3b let waste be food. In this research the NSS is applied where all the resulting energy demand is supplied with renewable energy on site.

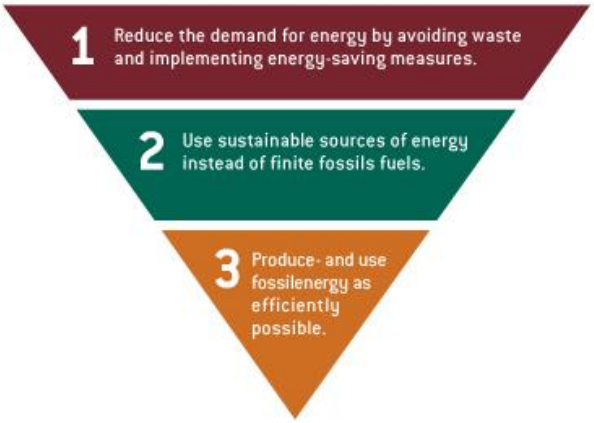

Figure 2-3 Trias Energetica (RVO, 2013)

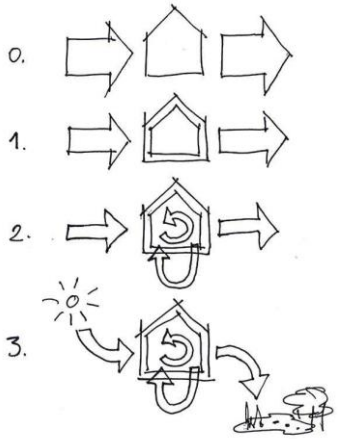

Figure 2-4 New Stepped Strategy (Van den Dobbelsteen, 2008)

2.2.1 Passive and active measures

Within the design of energy efficient buildings one make use of passive- and active measures. In the first step of the NSS and Trias Energetica the energy demand of the building is reduced. This is mainly done by architectural measures, also known for passive measures. Examples of passive measures are: orientation and shape of the building, insulation of the skin, high efficient windows with reflecting coating, fixed sun shading system, air tightness measures, night cooling by natural ventilation and heat accumulation in the building mass (e.g. Trombe wall). Based on bio climatic design, the context of the building is analysed to find the strengths and the best solutions for the climate in different seasons. These passive measures involve no installations or moving parts and are mainly applied in the reduction step. The passive measures are always prior to the active measures, which occur in step 2 and 3 of the NSS, reducing further the energy demand and

generating the remaining energy with a renewable source. An example of an active measure in step 2 is the application of mechanical ventilation with a heat recovery unit. The polluted air contains heat, which can be extracted and re-used to heat the incoming air, this is the basic of a heat recovery unit. Mechanical ventilation can be used smart in combination with the passive natural ventilation and based on fresh air demand by CO_2 sensors. A shower heat recovery pipe can also be seen as an active measure to reuse waste flows, where applying a water-saving showerhead fits in the step to reduce the demand. As can be seen the steps are sometimes overlapping and the difference between active- and passive measures are not always clear. But in general the subdivision of active and passive measures is a good exercise to design energy efficient buildings. The final step to generate sustainable energy is a typical active measure which can be divided in the generation of electricity and heat. Electrical generation for dwellings mainly involves installation such as photovoltaic panels or micro wind turbines. Also combined heat and power can be a renewable measure, if it has bio gas as source instead of fossil, providing electricity and heat. Typical sustainable installations to generate heat in a building are solar boilers, pellet heaters or heat pumps, using renewable sources as respectively the sun, wood and environmental heat. The environmental heat for the heat pump includes the ambient air, the ground, (indirect) sun and also water or geothermal. Where the photovoltaic panels can function as an autarkic system, requiring no auxiliary energy, the heat pump and solar boiler needs electricity for the pump and compressor to function. This electricity can be generated with the photovoltaics as source.

The New Stepped Strategy with the active and passive measures are used to improve the energy efficiency of existing and new build dwellings. These strategies are implemented in chapter 3. First an analyse is done of the existing dwellings as described by the NSS step 0 and a selection is made of suitable dwellings for the ENergy Roof.

2.3 Building type criteria

In this paragraph the Dutch building stock is analysed in order to find the building type that is suitable for a NoM renovation with ENergy Roof. This is done by setting up selection criteria and analysing the building stock and the history of the dwellings. The results are presented in a flow chart in chapter 2.8 with the type and number of suitable dwellings.

The selection criteria are based on the framework of NoM renovation and the boundary conditions of the ENergy Roof, as can be read in chapter 1.4 and 2.1. The NoM renovation requires renovation of dwellings where a certain energy label jump, where the energy label of the dwelling improves from label F to A, is reached in order to make the business model. Therefore the energy label is the first selection criteria. On the other hand the renovation requires a minimum construction quality of the existing dwelling. If the construction is not good enough to last another 30 years, it is not worth to invest in a renovation. Therefore the construction quality is the second

selection criteria. The boundary conditions states that the ENergy Roof requires an individual dwelling with a pitched roof in order to generate the energy. The ENergy Roof is not suitable for a collective system or a multifamily dwelling which do not have their own roof. Also single-family dwellings with a flat roof are excluded, although it may be possible to add a gabled roof with extra investment costs. The single family dwelling with a pitched roof is the third selection criteria. Industrial production and scalability are important boundary conditions of the ENergy Roof. This makes a quality improvement and cost reduction possible which is crucial to for the feasibility of NoM renovation. The factory production makes it also possible to produce fast and renovate a high amount of dwellings in a relative short period, having a large impact on the reduction of CO_2 emissions. Therefore the amount of suitable dwellings is the fourth selection criteria.

There are four criteria's to select a suitable dwelling for NoM renovation with ENergy Roof, these are: the amount of dwellings, the energy label of the dwelling, the construction quality of the dwelling and the building type single family with pitched roof.

The pitched roof dwellings with either a roof window or dormer window may form an obstacle for the ENergy Roof. The sun-side of the roof is required for the generation of energy and leaves no place for windows, but on the 'cold-side' of the roof there is. Therefore dwellings with a dormer window are not excluded. The design of the ENergy Roof takes this into account in chapter 7.

2.4 Short history of the Dutch dwellings

The ENergy Roof is suitable for the renovation of existing dwellings. In order to understand the renovation task the building history of the Dutch Dwellings is investigated. This paragraph also deals with the selection criteria 'amount' and 'energy label' of the dwellings for the NoM renovation.

In the year 2015 the Netherlands has over 7.4 million dwellings divided over private and non-private ownership. The building stock provides the Dutch population with sufficient dwellings. This was not always the case, such as in the post-war period when there was a large housing shortage. In this post-war period, between 1946 and 1980, a substantial part of the total current building stock was built, namely 3.2 million dwellings (Thijssen, 1999). According to Thijssen (1999) about 1.4 million of these dwellings are built in the social sector and from that 800.000 are single family social dwellings.

After the Second World War there was a big housing shortage in the Netherlands. The combined effect of war damage, low production during the war and the growing amount of families due to marriages and the birth explosion, e.g. baby-boom generation, the housing shortage was enormous (BouwhulpGroep, 2013). Also the lack of qualitative workers, the scarcity and high costs of building materials were part of the problem. Until the late 60's the shortage was between the 260.000-280.000 dwellings.

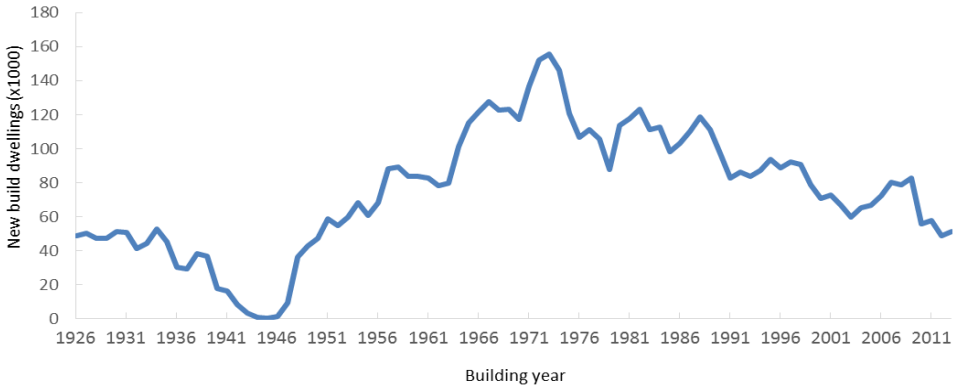

Figure 2-5 Development of new build dwellings in the Netherlands 1925-2013 (CBS, 2015)

The government supported the building companies and municipalities financially with different programs such as permitted 'Contingenten' for 'Woningwet-' and 'Premiewoningen' (BouwhulpGroep, 2013). These programs for social houses are meant for high production rates and to provide housing for all incomes. After the war the production numbers first grow slowly, from a few thousand just after the war to 38.000 in 1948, as can be seen in Figure 2-5. But from the 1960's the production machine got on speed and the production in 1962 was almost 90.000 dwellings. The grow continued until its peak in 1972 of 147.719 dwellings in one year (Bruggeman, 1980). From these dwellings a total of 113.992 were built as single-family dwellings. These production numbers are never reached again in the Netherlands. The production of dwellings slowly decreased to 94.000 in 1980 (Grotelaers, 1984) and stayed between 85.000-110.000 until 1995 (BZK, 2013). After the crisis in 2008 the numbers even dropped to 56.000 new dwellings in 2010, only one third of the production compared to 1972.

A research by Tigchelaar and Leidelmeijer (2013) clearly show the high amount of dwellings build in the period 1960-1980 compared to the periods before and after (Figure 2-6). Interesting about this figure is the combination of the quantity and energy label of the dwellings per building period. In the period 1996+ the most appearing energy labels are A and B, while before 1981 the labels D until G are dominant.

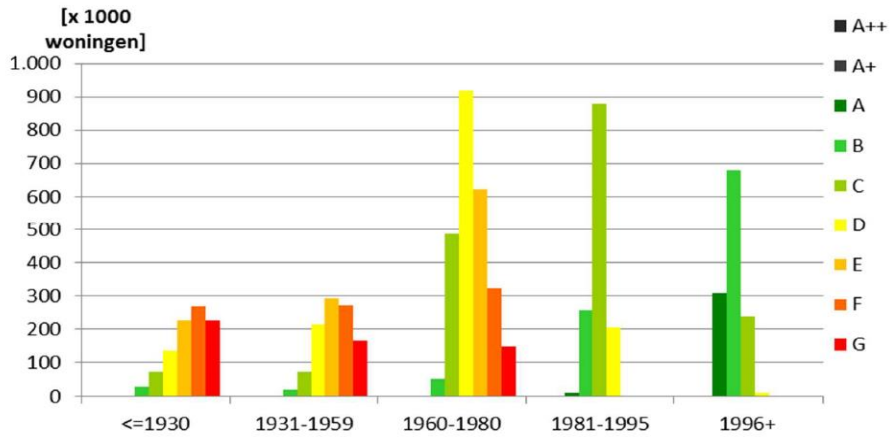

Figure 2-6 Dwellings build in the Netherlands by energy label from G to A (Tigchelaar & Leidelmeijer, 2013)

2.4.1 Conclusion

It can be concluded that in the post war period the amount of dwellings build was the highest in the Dutch history, with the building peak in 1972 with almost 150.000 new dwellings. Combining these building numbers with the energetic quality of the dwellings show that the building period 1960-1980 has high potential for the NoM renovation in the Netherlands.

2.5 History of the floorplan

In the past century big developments in the building techniques improved the construction quality of the dwellings. This paragraph deals with these developments within the Dutch building industry in the post war period and their influence on the floorplan of a single-family dwelling. The dimensions of the floorplan have effect on the size of the roof and are therefore important for the ENergy Roof.

One of the interesting developments in this period is the introduction of a new construction method, the 'systeemwoningen' or system-building (Van Elk & Priemus, 1970). The municipalities starting experimenting from 1920 but the importance mainly grew with the housing shortage after 1945. The key of this new construction method was found in repetition and prefabrication, allowing mass production of building components. The repetition and functional architecture fitted the spirit of that time. The aim was to make a better cost-quality ratio and larger production quantity, taking into account the shortage of workers in the post-war period. Where a new dwelling of 350 m^3 cost around 1.000-1.500 working hours with the traditional method, the system-building method only requires half where 650 working hours is needed. These reduced working hours and prefabrication were ideal for the fight against the housing shortage. From 1950-1975 around 450.000 dwellings with system-building were realized (BouwhulpGroep, 2013). Well known systems applied in The Netherlands are: ERA, Muwi, BMB, Rottinghuis, Vaneg, Pronto, Airey and Dura Coignet. The systems are separated in: 'stapelbouw', 'gietbouw' and 'montagebouw'. Systems were judged by the Ratiobouw which had to approve the building system (Andeweg, 2013). The systems are mainly developed for row houses and apartment buildings. According to BouwhulpGroep (2013) the Muwi system is applied in 37.831 dwellings. Knowing the construction details and assembly plan of a system-building gives an advantage in the renovation of the dwelling. These details may lack in dwellings with a traditional building method.

The Traditional building method is characterised with hand lifted blocks, small floor elements and concrete in the work poured with non-standard form work. The external walls have a constructional function, where the side facades support the floors and the front and back function for the stability. All outer walls are built as brick cavity walls with a cavity of 5-6 centimetres, mostly without insulation. From the mid-seventies new built dwellings are given a few centimetres of insulation in the cavity. Inner walls were first constructed with concrete blocks

(Pora-bocs and B2-blocks), but after 1967 the sand-lime bricks was mainly used. The ground floors were made of concrete, wood or a combination of the two, mainly seen in the two-bay dwellings. From 1966 wooden ground floors were not applied any more in single-family dwellings and are fully replaced by concrete system floors. For intermediate floors, wood is applied until 1969 and for attic floors until 1973. The large majority of the single-family dwelling roofs are built as stabled roofs with wooden purlins bearing on the sidewalls with an uninsulated roof deck. Stabled roofs occur in 87% of the researched dwellings (Bruggeman, 1980).

Until the end of the seventies the dominant building method in the Netherlands was the traditional method with had lifted blocks and wooden floors. The use of cast concrete grew in importance but remained a minority in this period. This radically changed with the introduction of mobile cranes in the late seventies. Before that the cranes required rails and a rail network was constructed on each building site. Mobile cranes made pouring concrete easier and as a result concrete constructions became the leading building method in the Netherlands (Thijssen, 1999).

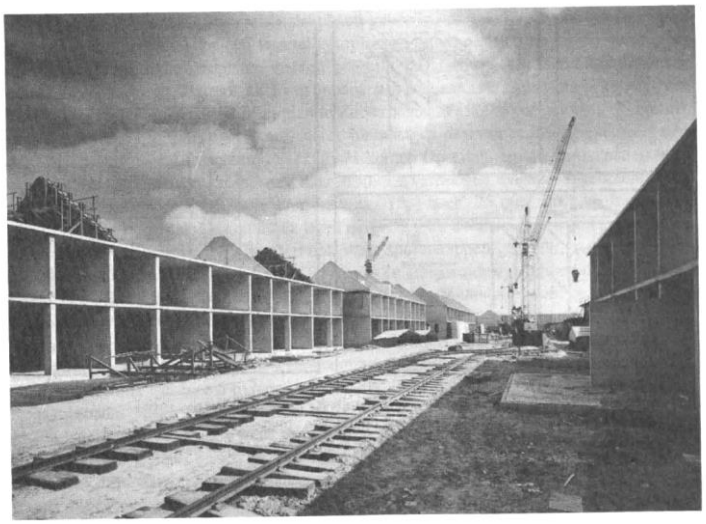

Figure 2-7 Typical building site in the Netherlands with cranes on the rails (Thijssen, 1999)

The shift from new build dwellings with two bays to single bay was made possible with the introduction of precast concrete plate floors (Bruggeman, 1980). This development had a large influence on the floorplan where the single-family dwelling became narrower. Thereby the trend of increasing floor area in the seventies made the dwellings deeper. According to the research of Bruggeman (1980) the average width of a dwelling in 1960-1971 is about 6.2 meter, whereas the average is about 5.7-5.8 meter in 1973-1977. The Depth grows in the same period from an average of 7.5-7.9 to 9.2 meter. This development is illustrated in Figure 2-8. In the same research Bruggeman points out that the amount of rooms in a dwelling dropped in this period and that open kitchens increased from 0% in 1973 to 55% in 1977.

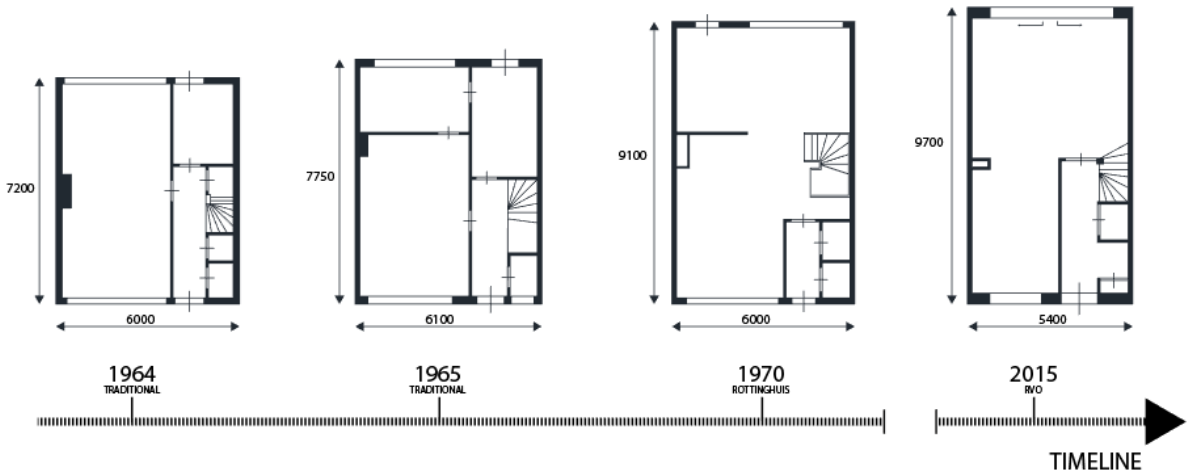

Figure 2-8 The floorplan development of the Dutch row houses

Another interesting fact in the post war period is the uniformity between dwellings in new built complexes. A new built complex in that period varied between 40 and 100 single-family dwellings. According to Thijssen (1999) the average variation of building within a complex is significant lower in the mass production period between 1957-1973 compared to the periods before and after. In this period the average variation is 1.6 per complex, while the variation before and after are respectively 3.1 and 3.4. In the post-war period the dwellings within a complex have great uniformity and differ not much from each other. This is an advantage for the NoM renovation and the ENergy Roof where one design of a prefabricated element will fit almost all the dwellings in the complex.

Conclusion

From this it can be concluded that new technologies changed the construction method applied construction materials. Most single-family dwellings in the period 1960-1980 are built according the traditional building method and 87% have a stabled roof. The construction quality of the buildings in this period are sufficient for the ENergy Roof, especially dwellings after 1973 where all the floors are made of concrete. The great uniformity between the dwellings in a complex is a large advantage for the ENergy Roof. A challenge for the ENergy Roof is the difference in floorplan width and depth of the single-family dwellings in this period.

2.6 Energy efficiency regulations

The regulations around the energy efficiency of dwellings had a large influence on the energy label of the new built dwellings. In this paragraph the evolution of these energy efficiency regulations are presented.

The first requirements for thermal insulations came into force in 1964 with the 'Model Bouwverordering' which regarded the thermal heat resistance of the roof (Van der Linden, 2015).

The insulation on the roof was at first sparingly applied with no more than 15-25 mm. In this period new dwellings had no insulation at all, not in the brick cavity wall nor under the ground floors. According to Thijssen (1999) the first time insulation in the brick cavity occurred was in 1971 with a thickness of 30 mm. In 1975 the requirements for the roof insulation became stricter and mandatory for new build dwellings (VROM, 2002). This was followed by regulations for façade insulation in 1979 and insulation of the ground floor in 1983. These regulations came in the period after the first oil crisis in 1973 where the fuel prices increased. Also the trend for more comfortable dwellings may have played a role. From 1995 the energy performance standard (EPN) was introduced and included in the Dutch Building Decree. The effect of the EPN on the energy label clearly illustrated in Figure 2-6 where only energy labels of C or better occur after 1995. In the previous regulations only measures are taken for insulations, where the EPN regards the integral energy quality of the dwelling. Points could be obtained not only for good insulation, but also for efficient installations, renewable produced energy and other subjects. The EPN was a high standard for the time, where the Netherlands was front runner in the energy efficiency building market.

In Figure 2-9 the insulation percentage of the Dutch building stock in 2012 is presented for four different building elements, respectively the roof, ground floor, façade and glass (Tigchelaar & Leidelmeijer, 2013). From this figure three conclusions are filtered. The first is that from 1981 the insulation percentage is almost 100% for the four segments. Dwellings build before this period have a much lower percentage of insulation. The second is that the building element glass has average the highest insulation percentage. Glass is a material which can be replaced relatively easy and has low investment costs. In the meantime most dwellings therefore have insulated glass and by average 80% of the dwellings between 1960 and 1980 have insulated glass. The third observation is that the floor insulation percentage is the lowest. It is also argued by Bruggeman (1980) that floor insulation is a difficult intervention and not always possible. Notice that these insulation percentages does not show the quality and thickness of the insulation materials.

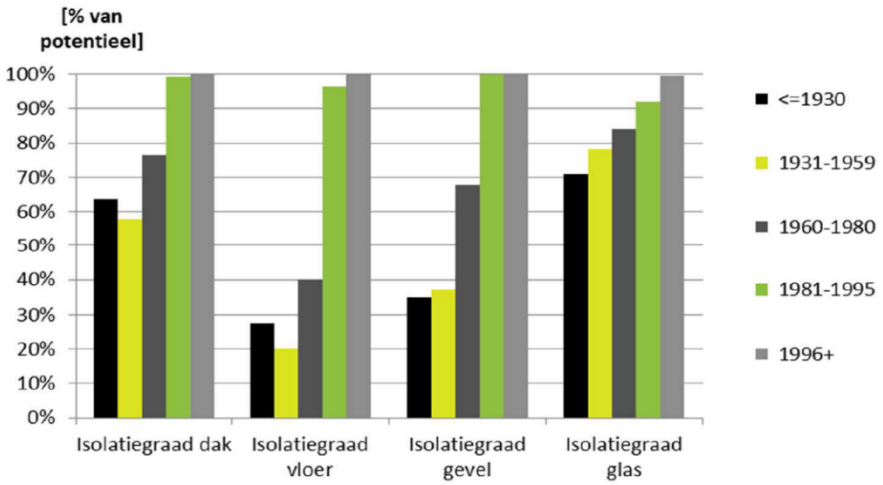

Figure 2-9 Percentage of building components which are insulated (Tigchelaar & Leidelmeijer, 2013)

Since 1995 the energy performance standard (EPN) is at force for new build dwellings and is expressed in an energy performance coefficient value (EPC). The first standard for the EPC was set on 1,4 and were since then gradually sharpened from an EPC of 1,2 in 1998 via 1,0 in 2000, 0,8 in 2006 and 0,6 in 2011 to 0,4 in 2015. For example the requirements for the thermal resistance (Rc-value) of the roof, floor and façade of a new build dwelling is raised in 2012 from 2,5 to 3,5 m^2K/W. These requirements have great effect on the thickness of the insulation and the total thickness of the façade. Also the minimum insulation value for windows and doors are tightened where the thermal transmittance (U-value) changed from 4,2 to maximum 2,2 W/m^2K.

From 2020 all new build dwellings in The Netherlands must be almost energy neutral or in Dutch 'Bijna Energie Neutraal Gebouwd' (BENG). The way to express the energy performance of the dwelling with the BENG differs from the EPC. The BENG is expressed based on 3 topics: the maximum annual final energy demand in kWh/m^2 usable area, the maximum annual primary energy demand in kWh/m^2 usable area and finally a minimal share in renewable energy in percentage. The designer or builder may choose whether to use passive or active measures.

2.5.1 Energy efficiency program for existing dwellings

From 1973, the year of the first oil crisis, the government started programs to improve the energy efficiency of existing dwellings in order to reduce the consumption of fossil fuels (VROM, 2002). This is done by providing subsidises and information (a few programs are mentioned in the following paragraph). In 1978-1990 the large scale program 'Nationaal Isolatie Programma' (NIP) had as aim to annual apply insulation measures to 200.000 existing dwellings. But according to Van der Linden (2015) the Netherlands still had in 2015 circa 500.000 dwellings with an estimation of 20 million square metres of uninsulated cavity walls. The 'Nota Energiebeleid' in the same period aimed for the improvement of the efficiency of central heating boiler and led to the introduction of improved (VR-) and high efficiency (HR-) boilers. From 1983 the renovation and improvement of the energy efficiency of the post-war dwellings got more attention. The demonstration program 'Enovatie' (1988) should show that energy saving does not lead to moisture and ventilation problems. The stimulation of market party in energy efficiency measurements of existing dwellings led to the 'Dubo Covenant' (1998-2001), 'Nationaal Akkoord Wonen' (2001-2005) and finally the energy performance test of dwellings with the EPA was applied on a big scale in 2000.

2.5.2 Conclusion

From 1965 new build dwellings are partly insulated, from 1983 insulation is mandatory for the entire skin and since 1995 there are high energy efficient standards for new build dwellings. With different energy savings programs of the government the insulation value of existing dwellings build before 1983 was partly improved. The NoM renovation brings the insulation value to a

higher value, where the greatest benefit can be achieved with dwellings with low insulation values built before 1983.

2.7 Installations in the dwellings

With the NoM renovation the installations are replaced and therefore it is interesting to know whereby the post war dwellings are equipped.

Just after the war in 1945 the single-family dwellings were exclusively heated with a decentral heating system with a gas boiler in the living room and no heating in the other rooms (Bruggeman, 1980). Most dwellings in this period have a brick laid mantelpiece in the living room. The shift from decentral gas boilers to central heating boilers with radiators took place in the mid of the sixties with high speed. Since 1965 individual central heating boilers occur in the single-family dwellings, where the boilers are mainly placed in the attic. According to Bruggeman (1980) within 7 years 100% of the subsidised new build dwellings (Woningwet) have central heating. The application of central heating in multi-story dwellings occurred earlier the 100% in 1967.

The hot water was in the post war time produced with a geyser. These installations were applied next to the gas boiler (Thijssen, 1999). A new heating system occurs with the introduction of the combi-boiler in 1972.

Mechanical ventilation does not occur on a big scale. Most dwellings have natural ventilation by opening windows or by infiltration, since the detailing was not so air tight as required today. In the research of Thijssen (1999), mechanical ventilation occurs for the first time in 1969 and appear in 22% of the single-family dwellings built between 1946-1980. The mechanical ventilation is mainly applied in the kitchen and bathroom (Thijssen, 1999).

With the 'Voorschriften van Wenken' in 1965 the subsidised dwellings, especially those in the 'Woningwet', made a clear quality improvement as well in floor space area as equipment of the dwelling (Thijssen, 1999). Dwellings built in 1964 were installed with by average 1,01 water closet and in 1965 this grew to 1,31 per dwelling. This also applies for the amount of wash-basins which grew from average 0,93 to 1,26 in 1965. The grow continued until 1975 where dwellings were installed by average with 1,52 water closets and 1,70 wash-basins.

The dwellings built in 1960-1980 do not have the same installations today as when newly build, since the installations have a life expectation of 15 to 20 years. In the research by Tigchelaar and Leidelmeijer (2013), an overview is given of the applied heating installation in Dutch dwellings in 2000, 2006 and 2012, presented in Figure 2-10. In 2012 about 70% of the dwellings have a HR-boiler with a total 5 million. The CR- and VR-boiler have been decreasing since 2000, as the decentral gas boilers ('locale verwarming'). Heat pumps are the least applied heating installation, but increased with a factor 3.5 from 2006 to 2012, the largest grow compared to the other

installations. Hot water is in 80% of the dwellings produced with a combi-boiler, including the CR-, VR- and HR-boiler (Tigchelaar & Leidelmeijer, 2013). The application of geyser and electrical boilers have strongly decreased between 2000 and 2012.

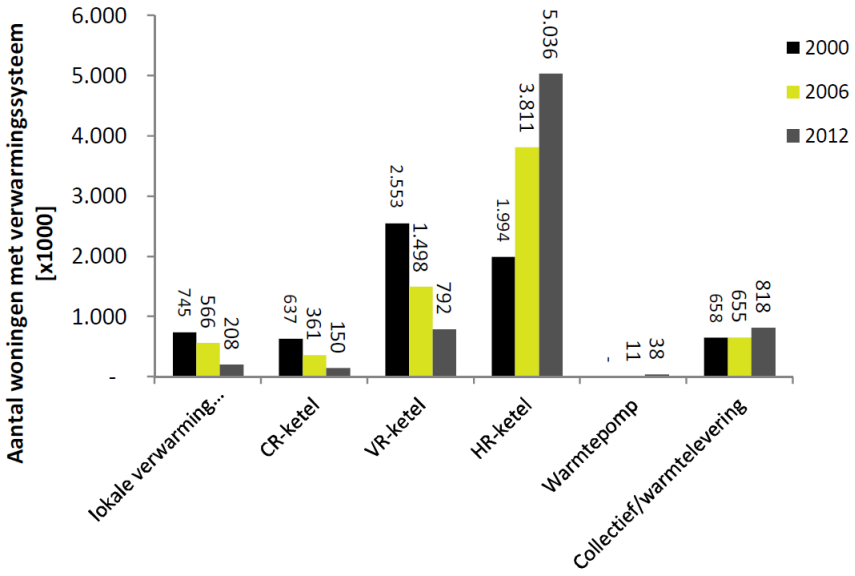

Figure 2-10 Installed heating system in dwellings in the year 2000, 2006 and 2012

Conclusion

The installations applied in the dwellings has changed a lot in the past, due to changing comfort demands, life time of installations and the technical development in this market. It can be concluded that most dwellings from 1960-1980 have a central heating system with radiators, dwellings before 1972 may still have local heating. The greatest percentage of the dwellings has a combi-boiler for heating and hot water where of the majority has a HR-boiler. Heat pumps show the largest grow but has a small share in the total heating systems of Dutch dwellings.

2.8 Flow chart selection building type

To select the building type which is most suitable for the energy roof in the NoM renovation, the four selection criteria can be evaluated: amount, construction quality, energy label and single family dwelling with gabled roof.

The combination of ***amount*** and ***energy label*** makes the building period of 1960-1980 the most interesting. In 2012 the Netherlands has 7,2 million dwellings, from which 35,6% is built in the period between 1960 to 1980 (Tigchelaar & Leidelmeijer, 2013). Due to the housing shortage and new building technology high production rates are achieved, resulting in a high quantity of new built dwellings in this period. The distribution of energy labels within the building periods shows that between 1960 and 1980 the energy labels are below average (Figure 2-6). From 1995 the new built dwellings have strict energy efficiency regulations, however before this period only

minimum or no insulation was applied. From the ***construction quality*** point of view the buildings from 1960 are suitable because of the used building method and the uniformity of the dwellings. The new techniques for concrete floors make the dwellings more resilient and suitable for bigger loads. The high quantity and uniformity of single-family complexes built in 1960 to 1980 make the NoM renovation with the ENergy Roof financially more feasible because of the possibility to produce the building elements on a large scale, which will reduce the investment costs. The second step in the flow chart is the selection of the building type of the dwelling build between 1960 and 1980 and is based on the fourth criteria: ***single-family dwelling*** with a ***gabled roof***. The researches of Bruggeman (1980) and Grotelaers (1984) show the distribution of the new build building types in this period where 70% is built as single-family dwellings and 30% as multi-story dwellings. In the period 1962-1977 the building type of row-house, semi-detached house and detached house occur within the single-family dwellings respectively with 67%, 16% and 17% (Bruggeman, 1980). It is assumed that the dwellings between 1960-1961 and 1978-1980 have the same distribution. The row-house dwellings are selected since they have the largest share and having a high uniformity. Within this group of dwellings a final selection criteria is applied which apply to the roof type. The ENergy Roof is only suitable for dwellings with a pitched roof. The research of Thijssen (1999) makes a differentiation between flat and gabled roofs of dwellings built between 1960 and 1980 in the social housing sector. From the 39 building complexes with row-houses built spread out over the Netherlands and in built in the mentioned period, 34 (87%) had gabled roofs and 5 (13%) flat roofs. All these steps are presented in the flow chart in Figure 2-11 and result in a potential of 1 million dwellings for the NoM renovation with ENergy Roof. The suitable dwellings include both mid-row-house and corner-row-house and include all the orientations. It is assumed that these dwellings meet the secondary condition of the ENergy Roof which allows no or minimal shade on the sun-side of the roof, trees that block the sun should be shortened.

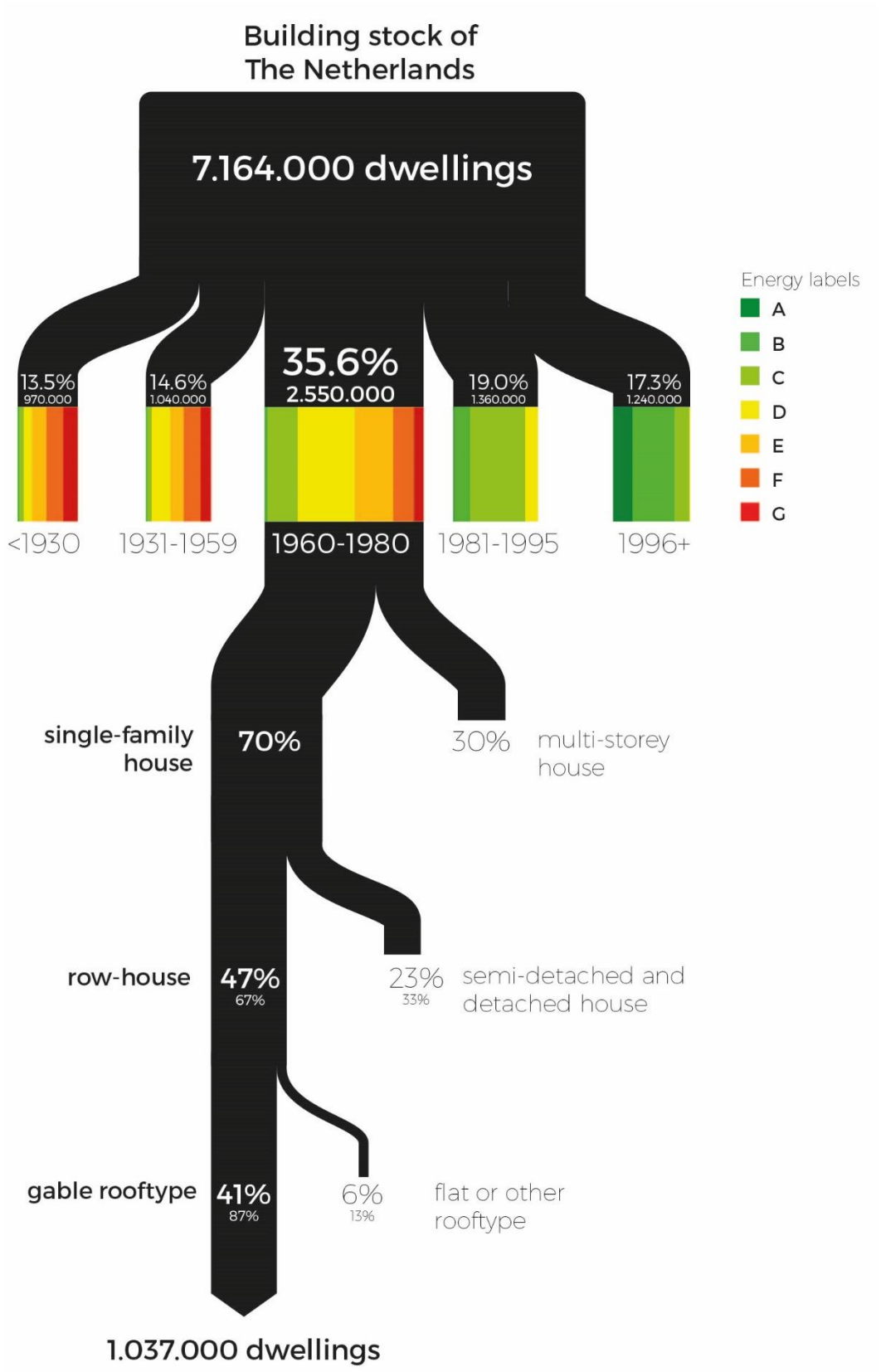

Figure 2-11 flow chart selection suitable building type for the NoM renovation with ENergy Roof

3.The energy demand of dwellings

In the previous chapter a selection is made of the suitable building type for the ENergy Roof in combination with the NoM renovation. In this chapter, the energy consumption of the existing dwelling will be mapped, as described by the New Stepped Strategy. This will be done by subdividing the energy flows into five categories: heating, hot water, ventilation, lighting and appliances. The second part of the chapter presents the energy demand of a dwelling after transformation into NoM. The aim of this chapter is to give an overview of the energy flows of a NoM renovated row house and to set the boundary conditions to which the ENergy Roof has to comply in order to become net zero energy.

3.1 Energy

In the Netherlands dwellings are generally connected to the grid for electricity and gas. The net zero energy ambition includes the annual energy consumption of gas and electricity summed. At the meter the gas and electricity enters the house where the gas is measured in cubic meters (m^3) and the electricity in kilo watt hour (kWh). Here the final energy consumption of the dwelling is measured. In order to compare the two energy flows, the energy can be expressed in joules, or mega joules (MJ). The specified energy, or calorific value, of natural gas is 31,56 MJ per cubic metre, this is the undervalue of natural gas and is exclusive condense heat. One kWh electricity is the same as 3,6 MJ, since one kW is 1000 J/S and an hour contains 3600 seconds. With these conversions the total final energy use of the dwelling can be calculated. However, there is a difference between the two types of energy, which can be explained with the primary energy.

3.1.1 Primary energy and CO_2 emission

The primary energy includes the transport and conversion losses of the electricity or gas before it enters the dwelling at the meter. With the transport and conversion process of a natural fuel, energy is 'lost' due to unusable waste heat. According to the first law of thermodynamics energy remains constant, so with 'lost' is meant the amount of energy transferred into un-useful energy, such as heat. Examples of natural fuels are coal, cruel oil, natural gas, but also solar and wind are primary energy resources. In order to compare different energy forms the primary energy is introduced. The definition of primary energy is given by Kydes (2007): "Primary energy is an energy form found in nature that has not been subjected to any conversion or transformation process". There is not an international commonly accepted primary energy factor. In the Netherlands, the norm NEN7120 give the factor is 2,56 or an efficiency of 39%. For every kWh electricity consumed at the meter, there was a total of 2,56 kWh primary energy required. In literature higher efficiencies are mentioned, such as the joint research by ECN, CBS and AgentschapNL. They presented a transparent method to calculate the primary energy factor and

the CO_2 emission factor for electricity (Harmelink, Bosselaar, Gerdes, Segers, & Verdonk, 2012). The 'gemiddelde methode' is used since it is applicable for the calculation of the total CO_2 emission of dwellings. The report presents a primary energy factor of 2,02 or an efficiency of 49,6%. Between 2000 and 2010 the primary energy factor reduced with circa 12% in the Netherlands as a result of increased application of natural gas as source for electricity production, reduction of coal, increase of combined heat and power installations and increase of electricity production by renewable energy sources (Harmelink et al., 2012). The primary energy factor for gas used in this research is 1, given by NEN7120. The CO_2 emission factor for electricity and gas are given respectively given by Harmelink et al. (2012) and NEN7120. For electricity this is 0,46 kg/kWh final energy, or 0,1278 kg/MJ and for gas this is 0,0506 kg/MJ.

3.2 Energy flows in the dwelling

The energy demand of the dwelling is based on the consumption of electricity and gas. The average consumption of a household is presented in Figure 3-1. After years of increase the electricity consumption is stabilised on 3.200 kWh per household per year. The gas consumption has a lowering trend and in 2010 a consumption of 1.600 m^3 per household per year. Dwellings built in the period 1960-1980 have a higher average consumption of 1.750 m^3 per year (Tigchelaar & Leidelmeijer, 2013).

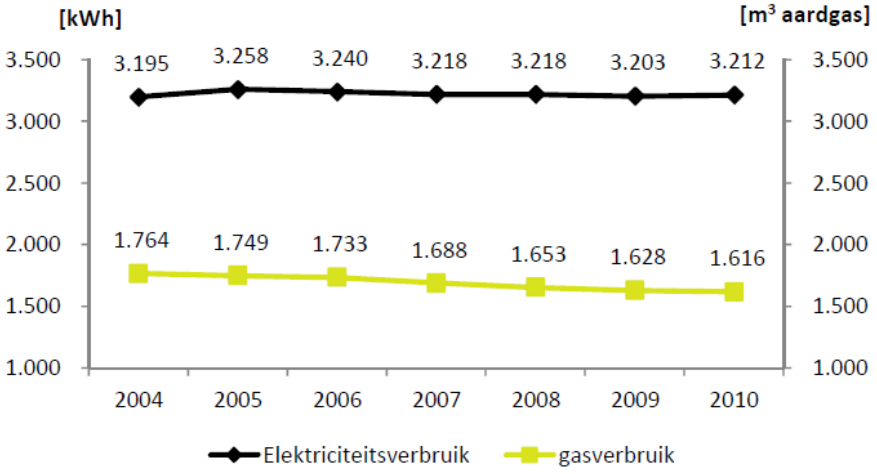

Figure 3-1 Annual final energy consumption of an average Dutch household 2004-2010

The final energy demand can be separated in user- and building related energy. With 'building related energy', all the energy required for heating, cooling, hot water, ventilation and lighting of the dwelling is meant (RVO, 2016). Lighting is in the Netherlands included and is also part of the EPC calculation. Although these energy flows are related to the building, the user also has influence on the building related energy too, such as the temperature set point, opening of windows and showering time. User related energy is all the energy used for domestic appliances,

such as television, computers, and kitchen appliances, among others. In the following part the energy flow are differentiated into five parts, regarding: heating, hot water, ventilation, lighting and appliances. Where the first four energy flows are building related energy and the final is user related energy.

A third category of energy mentioned by RVO (2016) is the material related energy, including the energy required for building, production and transport of building materials together with the maintenance and demolition of the dwelling. This category does not fall within the scope of the research and is therefore excluded. The same applies for the annual energy used for transport, such as an electrical bike or car. This may be interesting to incorporate in further research.

3.2.1 Heating

As mentioned in chapter 2.7 the majority of the Dutch dwellings have a central heating system with a gas fired combi-boiler in combination with radiator. With the average energy consumption of a post war row-house an estimation can be made of the total energy required for heating. The annual gas demand of 1750 m^3 is used for heating, hot water and cooking. Cooking requires annual average 40 m3 gas per household (Milieu-Centraal, 2015b). According to Milieu-Centraal (2015b) the ratio of gas required for heating and hot water is respectively 80% against 20% and is valid for average Dutch dwellings. Energy efficient and NoM dwellings have a ratio that approach a fifty-fifty energy distribution between hot water and heating. With these numbers the final energy for heating can be calculated using the calorific value of natural gas which result in 43.2 GJ per year. This is the final energy delivered to the meter of the dwelling, no conversion factors for the installations are taken into account.

3.2.2 Hot water

The same numbers are applicable for the hot water demand which is supplied by the combi-boiler. Calculation of 20% of the total gas consumption is required for hot water leads to 10.8 GJ final energy per year. According to Milieu-Centraal (2015a) 80% of the hot water consumption is used for showering and the other 20% for the kitchen.

3.2.3 Ventilation

Mechanical ventilation was not standard in dwellings built between 1960 and 1980 as described in chapter 2.7. In the meanwhile some dwellings may have been equipped with a ventilation system, but for this mapping it is assumed that the dwelling consumes no energy for ventilation. Therefore the annual final energy demand for ventilation is 0 GJ.

3.2.4 Lighting

The annual electricity demand of 3200 kWh is subdivided over lighting and appliances. In the Netherlands 14 % of the average electricity consumption is required for lighting (Milieu-Centraal, 2016a). This results in 1.6 GJ final energy.

3.2.5 Appliances

The remaining electrical energy consumption is used for domestic appliances, such as television, laptop, washing machine, refrigerator, amongst others. The electricity required for appliances can be calculated by extracting the percentage used for lighting. This result in 86% of the total electricity which is 2750 kWh per year or 9,9 GJ final energy. Plus the gas consumption for cooking of 40 m^3 natural gas per year or 1,3 GJ result in 11.2 GJ final energy for appliances per year.

Table 3.1 Annual final energy demand of a post-war single-family dwelling

	category	Final energy kWh	Final energy GJ	Primary energy GJ	CO_2 emission *1000 kg
1750 m^3 natural gas	heating	12000	43,2	55,2	2,8
	hot water	3000	10,8		
3200 kWh electricity	ventilation	-	-	23,3	1,5
	lighting	450	1,6		
	appliances	3100	11,2		
		18500	**66,8**	**78,5**	**4,3**

3.2.6 Total

The annual consumption of a non-renovated single-family dwelling built between 1960 and 1980 is presented in Table 3.1 where the total final energy demand is 66,8 GJ per year. The primary energy is calculated for both the electricity and gas consumption using the conversion factors presented in paragraph 3.1 and result in 78,5 GJ per year. Applying the CO_2 emission factors gives an annual emission of 4,3 ton carbon dioxide per dwelling per year. The distribution of the final energy demand of the dwelling is illustrated with a pie chart in Figure 3-2. Where the energy flow for heating is the largest and consists of two third of the total annual consumption.

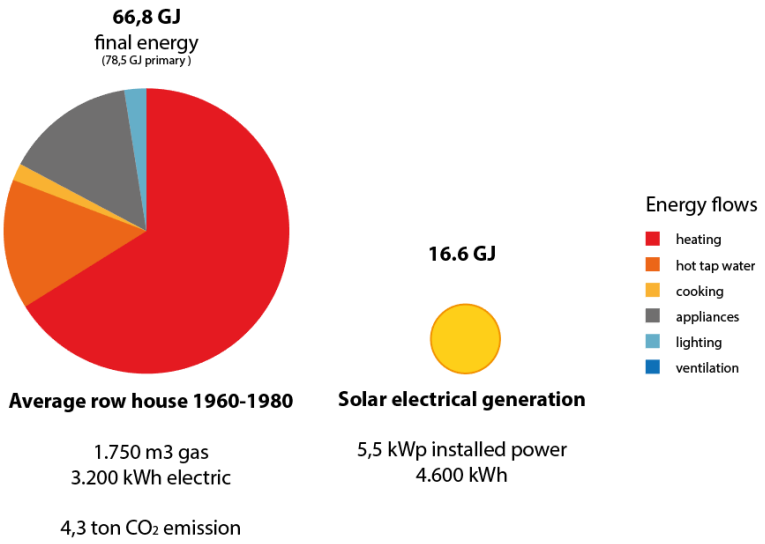

Figure 3-2 Subdivision annual energy flows of a non-renovated single-family dwelling and the potential electrical generation

3.2.7 Conclusion

The total final energy demand of an existing post-war row house is summarized in this chapter. In order to become net zero energy or NoM the total final energy demand has to be produced with renewables. In order to produce annual 66,8 GJ with PV panels, a total of 120 square metres roof surface with ideal South orientation is required. A typical Dutch row-houses has two roof surfaces of by average 30-34 square metres. This show that it is not feasible to generate all the energy on the roof of the dwelling and that it is inconvenient to place this amount of solar panels on the building site. The yellow circle in Figure 3-2 presents the potential electrical energy generation with PV panels on the roof. In order to make NoM technical and financial feasible the total energy demand of the dwelling should be reduced. This is also in line with the New Stepped Strategy. In the following paragraph the reduction of the energy demand of the different energy flows are discussed.

3.3 Energy demand NoM renovation

In this chapter the first two steps of the NSS are implemented on the five energy flows in the dwelling regarding the reduction and reuse of energy. The total energy demand after a NoM renovation is presented and compared with the potential energy generation on the dwellings roof. This sets the requirements to which the ENergy Roof should comply in order to become Nul-op-de-Meter.

3.3.1 Heating

The largest energy post of the post war row-house is the heating consumption, as illustrated in Figure 3-2. The final energy demand for heating depends on the heating losses of a dwelling and the installation. The different heat transfers with accompanied equations are illustrated in Figure 3-3 and show the gains and losses. The heat transfer losses are transmission, ventilation and infiltration where the heat gains are by solar radiation and internal gains. In order to retain a certain temperature set point within the building, a heat balance is achieved by adding a certain amount of energy provided by the heating installation. The amount of heating energy required depends on the heat losses and the external climate conditions. In order to reduce the energy demand for heating, the losses due to transmission, ventilation and infiltration should be reduced.

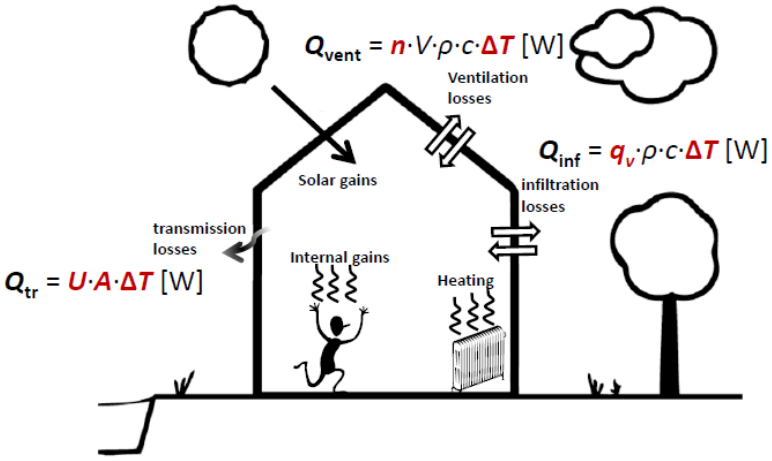

Figure 3-3 Schematic overview of the different heat transfers in a building

First the reduction of transmission losses will be discussed. In the NoM renovation the transmission losses are reduced by covering the existing dwelling with a new skin with high thermal resistance. The new skin includes insulation in the façade, roof and floor as well as high efficient glazing and window frames. These measures reduce the heat transmission, or U-value (in W/m^2K) resulting in a lower loss by transmission Q_{tr} (Figure 3-3). The surface area of the skin and the temperature difference remain the same and are represented by A and ΔT.

Reducing the heat transmission (U-value) of the dwelling leads to annual energy savings. It should be mentioned that there is a certain balance in the thickness of the insulation when the embodied energy is taken into account. According to Van den Ham (2012) an optimal can be found in the energetic payback time, taking into account the incremented thickness of the insulation. This is founded on the basic principle that the first centimetre of insulation have more impact on the energy saving than the next added centimetre. Figure 3-4 show the incremental payback time of a dwelling in the Netherlands applied with glass wool insulation which has an embodied energy of 1260 MJ/m^3 (Hammond & Jones, 2011). The calculation takes into account a heating period of 210 days with average temperature difference of 13 degrees Celsius, a heat pump with a COP of 4 and electricity conversion factor of 40%.

A thickness below 20 centimetres has a low payback time and above 30 centimetres the energetic payback time is too long. The Passive House façade has a thickness of 35 centimetres and a payback time of 29 years. The NoM renovation does not demand a certain insulation value as long as the total heat demand below 30 kWh_{th}/m^2 is reached. Based on the above mentioned argumentation a maximal insulation thickness of 21 centimetres and Rc-value of 6 Km^2/W is taken into account. The specifications of the NoM renovation is presented in Figure 3-6.

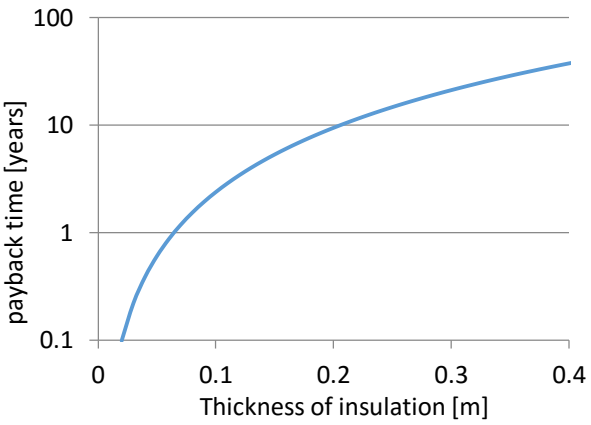

Figure 3-4 Incremental energetic payback time of glass wool insulation (Van den Ham, 2012)

Figure 3-5 Insulation according Passive-House standard ± 0.35 m and Rc 9,8 Km²/W (Van den Ham, 2012)

Second measures to reduce the heat demand is to minimize the ventilation and infiltration losses Q_{vent} and Q_{inf} (Figure 3-3). The infiltration q_v is reduced by the improvement of the air tightness of the dwelling with the new façade and roof. Ventilation losses are reduced by applying a heat recovery unit, driven by demand. The heat recovery unit extracts the heat from the exhaust air and the 'free' heat is used to preheat the incoming fresh air. With the HRU the ventilation losses can be reduced with about 83%.

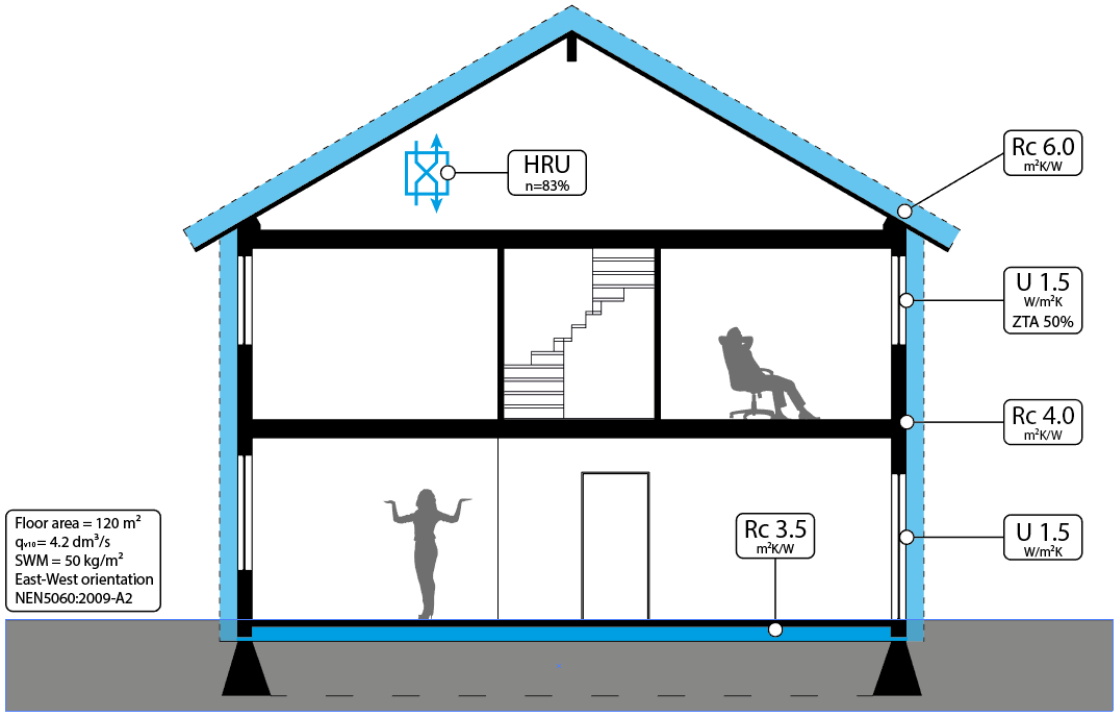

Figure 3-6 Main characteristics of a NoM renovated dwelling

The measures combined reduces the annual heating demand of the dwelling to < 30 kWh_{th}/m^2. This is a factor 3-4 reduction compared to the heating demand of an existing dwelling built in 1960 to 1980 (Table 3.2). The characteristics of the NoM renovated dwelling as described in Figure 3-6

are modelled in DesignBuilder where year simulation show a heat demand of 10.8 GJ. The DesignBuilder model is elaborated in Appendix D – DesignBuilder model.

Table 3.2 Heating demand of different dwellings

	kWh_{th}/m^2	Reference
Heating Passive House	15	Passive house demands
Heating Prêt-à-Loger	19	Prêt-à-Loger - Home with a skin (Designbuilder)
Heating EPV	**< 30**	**Energy Performance Compensation category 1**
Heating EPV	40 - 50	Energy Performance Compensation category 3
Heating dwelling 1960-1980	90	Prêt-à-Loger without skin (Designbuilder)

The heating installation supply the dwelling with the required heating demand. There are different installations to do the job, but most dwellings in the Netherlands have a gas boiler as described in paragraph 2.7. Other non-collective heating systems are: electrical heaters, heat pumps or a solar boilers. A comparison is made between these four systems in Figure 3-7 where the systems provide 100 parts of thermal energy (red) and require between the 0 and 204 parts of primary fossil energy (black). The renewable 'free' energy is illustrated with the blue and yellow arrow. The electrical boiler perform worst and has the highest amount of primary energy followed by the HR-boiler, heat pump, solar boiler and heat pump combined with PV.

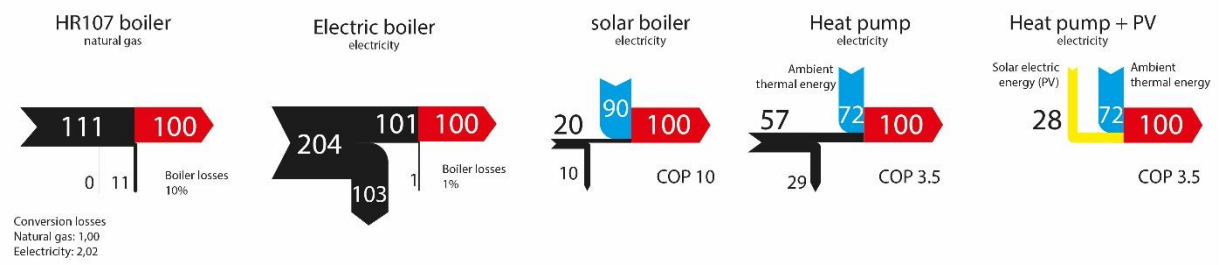

Figure 3-7 Energetic conversions primary energy to final energy

The boundary conditions of NoM renovation state that the dwelling will be full electric, thus without a gas connection, therefore the HR107 boiler is excluded. The advantage of the solar boiler and heat pump is the high coefficient of performance (COP), where respectively 10 and 28 parts of electricity are required to generate 100 parts of thermal energy. The disadvantage of the solar boiler is that it only operates with direct solar radiation and outside temperature above 0 °C, which will give problems during the winter season to generating heat and hot water. The heat pump has the ability to generate heat at low outside temperatures.

According to Trio and Schmidt (2011), the quality of energy, also known as exergy, should be taken into account matching the energy sources with the energy demands of the dwelling. The source of electricity has an energy quality of 1 and matches the demand energy quality of appliances and lighting (Figure 3-8). The energy demand for hot water and space heating has an energy quality of respectively 0,09 and 0,07, where using a source with a higher energy quality is associated with

exergy losses. Solar thermal and district heating match the energy quality for hot water and heating (Trio & Schmidt, 2011).

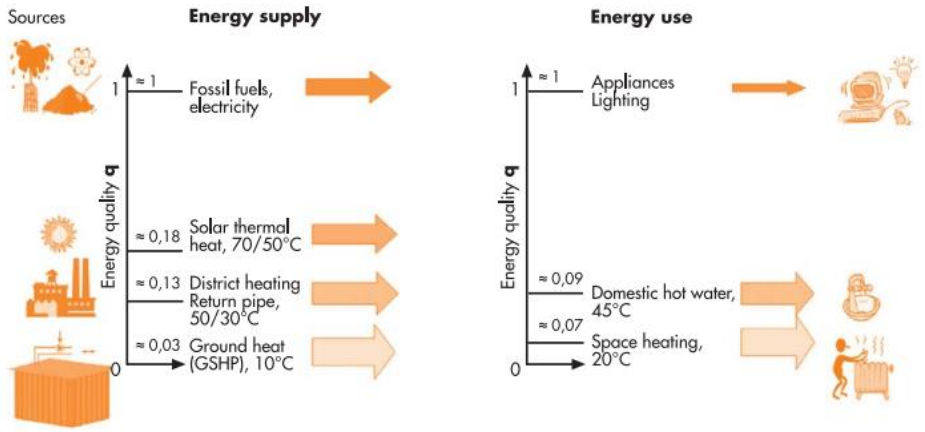

Figure 3-8 Matching of energy quality (Exergy) of demand and supply (Trio & Schmidt, 2011)

Lower temperatures for space heating lower the required energy quality and in addition improves the efficiency of a heat pump. With lower heat demand due to improved thermal resistance of the skin, lower temperature (LTV) emission systems are possible between 25 and 35°C. Three low temperature systems are selected which are suitable for the NoM renovation with ENergy Roof, these are: floor heating systems, low-H2O radiators or low temperature air heating systems. In a renovation floor heating may not always be possible, where replacing the existing radiators with low-H2O radiators is a fast and low cost alternative. But on the other hand, floor heating system with low temperature air heating may be associated with higher comfort.

Summarized, the annual heat demand of the dwelling is reduced with 75% from 43.2 GJ to 10.8 GJ with the application of a new skin and heat recovery unit. The installations used to generate the annual heat demand are a heat pump assisted with a solar boiler (for the mid- and summer season). For the calculation the assumption is made that 20% of the annual heating load is supplied with the solar boiler, mainly during the mid-season, and 80% is provided by the heat pump. A COP of 10 for the solar boiler and 3,5 for the heat pump are taken into account. With this the final energy demand for heating becomes 2.8 GJ or 745 kWh per year. The overview is presented in Table 3.3. A low temperature heating system is a condition for the ENergy Roof, but the specific system is not determined since it is dependent on the dwelling.

3.3.2 Hot water

The hot water demand is the next large thermal energy post of the dwelling, but in contrary to the heating demand, the hot water demand cannot be reduced that much. The hot water demand depends mainly on the number of inhabitants and their behaviour, where the heat demand is mainly influenced by the building. In paragraph 3.2 the hot water demand of the dwelling was calculated to be 10.8 GJ final energy, whereof 80% is used for showering according to Milieu-

Centraal (2015a) and 20% in the kitchen. The showering behaviour differs for the age, nationality and awareness of the inhabitant and fluctuate between 38 and 70 showering minutes per week, using respectively 47 and 87 litres of hot water per day for the group with the age of 65+ and the second group of 17-44 years old (Tigchelaar & Leidelmeijer, 2013). A young family with children is associated with the average hot water consumption of 216 litres per day based on 174 min of showering per week. The research into the energetic behaviour of the inhabitants in the Netherlands by VROM (2009) make a subdivision of the awareness of people and compare their showering time and amount of baths per week. Using the numbers of the volumetric flow of a normal shower head of 8,7 litres per minute and 6,9 litres per minute for a water saving shower head (Milieu-Centraal, 2015a) and 114 litres of hot water for a bath (Van Thiel, 2014) the total hot water draw per person is calculated. This show a hot water consumption of 60, 86, 88 and 145 litres hot water per person per day for respectively the category inhabitants 'water bewust', 'luxe', 'lang douchen' and 'veel in bad'. This show that there can be a large difference of the hot water consumption between different inhabitants, living in a same type of dwelling. According to the research, 49% of the Dutch population are within the category 'lang douchen' consuming 88 litres hot water per day, followed by 33% of the population that are 'water bewust' with 60 litres per day.

In the Dutch norm of NEN7120 the specified consumption of hot water is 3081 MJ per year per person or 8,44 MJ per day. With an assumed inlet temperature of 10 °C and hot water temperature of 40 °C, the average daily shower water withdrawal is 67 litres. The showering time is between the 54 and 68 minutes per week, depending on a normal- or water saving shower head.

The results from field tests show that every inhabitants consume around 1,3 kWh hot water per day as presented in Figure 3-9 (Friedel, De Jong, & Horstink, 2014). This result in average 37 litres of 40 °C hot water per person per day. Compared to the previous presented numbers this value is very low. The amount of reliable measurements in the field test is too small to generalise the results of the hot water demand, but the results are remarkable. The field test also present the use pattern of hot water during the day showing two clear peaks of hot water withdrawal in the morning and afternoon (Figure 3-10). This tap pattern is used in the simulation of the ENergy Roof in the sub-model demand as described in chapter 0.

In conclusion the hot water demand per person varies between the 37 and 145 litres per person per day and 216 litres for a young family with children. For the calculation of the hot water demand of the NoM renovated row-house the Dutch norm NEN7120 is used which shows 67 litres hot water per day and is approximately in the middle of the range of different consumptions. The hot water demand is calculated for 3 persons which result in 9,2 GJ per year.

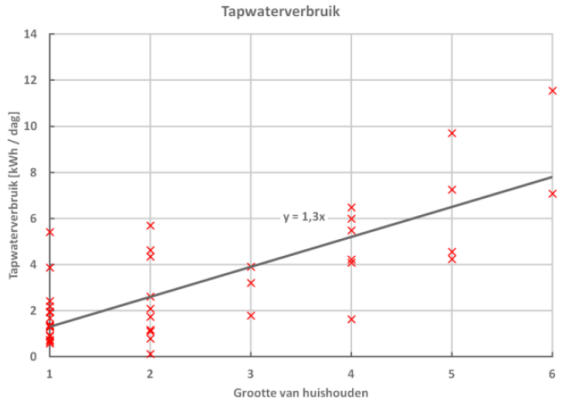

Figure 3-9 Field test of the hot water demand per household (Friedel et al., 2014)

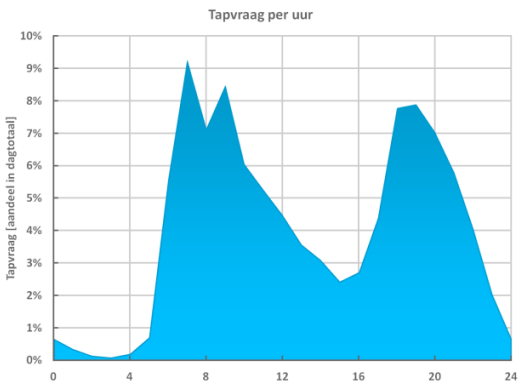

Figure 3-10 Average tap pattern of hot water during the day (Friedel et al., 2014)

The same heat pump and solar boiler supply the hot water demand of the dwelling where 50% is supplied by the heat pump and 50% by the solar boiler. The percentage of the solar boiler is higher compared to the heating because the hot water demand in the summer season is mainly supplied by the solar boiler where there is no heating demand in this time of the year. A shower heat recovery has the potential to reduce the final energy demand for hot water, but since the ENergy Roof involves a renovation, the system is difficult to install and therefore excluded. The heat pump is assumed to have a COP of 2 since it has to produce higher temperatures and the solar boiler a COP of 10. This result in an annual final energy demand for hot water of 2,8 GJ or 770 kWh.

3.3.3 Ventilation

The energy consumption by mechanical ventilation is dependent on the effective power of the ventilators installed, the occupancy time and the control strategy. In the ENergy Roof a balanced ventilation with heat recovery (HRU) is installed where the same amount of air is supplied as discharged. The ventilation has a smart control based on demand-driven CO_2 sensors in the living room and bedrooms. The air is discharged in the kitchen, toilet and bathroom. Sufficient ventilation improves the health and comfort of the inhabitants. The energy demand for ventilation is based on a market conform HRU with a maximum capacity of 350 m^3/h and low level of 75 m^3/h consuming respectively 150 and 15 W. The high maximum capacity is used during the cooking and showering hours and is assumed to be in operation for 7,5% or 1 hour and 45 minutes per day. During the remaining hours the HRU operates on low level capacity. This result in an annual consumption of 220 kWh where 100 kWh is used for the high level and 120 kWh for the low level ventilation hours.

3.3.4 Lighting

The amount of energy required for lighting is dependent on the installed power and the occupancy time. The total installed power for the lighting is depending on the efficiency of the lightbulbs and the usable floor space of the dwelling. A LED lamp can have a factor 8 lower power, compared to a light bulb or halogen lamp, e.g. a spotlight with three halogen spots have a total

power of 100W and three LED spots have a summed power of 12 W. With the NoM renovation the existing low efficient light spots are replaced with LED lights. With NEN7120 the installed power and annual energy consumption for lighting is calculated. For offices the norm takes an installed power of 16 W/m² into account, for LED the installed power is assumed to be 6 W/m². The total installed power for lighting in the dwelling is 720 W and the annual consumption is 400 kWh or 1,4 GJ.

3.3.5 Appliances

The energy consumed by appliances is difficult to predict, since it is very dependent on the devices used by inhabitants. For example an aquarium with electrical heater can add 200-400 kWh to the yearly electrical energy consumption. On the other hand, the improved energy label of new appliances has a positive influence on the reduction of energy. An older small refrigerator consume annual 270 kWh while a same sized new refrigerant consume 60 kWh per year, a reduction of 78%. Norber Fisch et al. (2013) presents an overview of the potential energy savings of domestic appliances where a larger refrigerator show approximately the same reduced percentage (Figure 3-11). With the NoM renovation the inhabitants can be stimulated to purchase high efficient domestic appliances reducing the annual energy consumption. The energy required for appliances is calculated according to the demands of the EPV which state 25 kWh/m² usable floor area with a minimum of 1750 kWh and a maximum of 2500 kWh per dwelling. An example of such an energy bundle is the NoM renovation of the builder BAM in 2015 presented in Figure 3-12. The total final energy demand for the renovated row-house is calculated for 2500 kWh or 9,0 GJ per year.

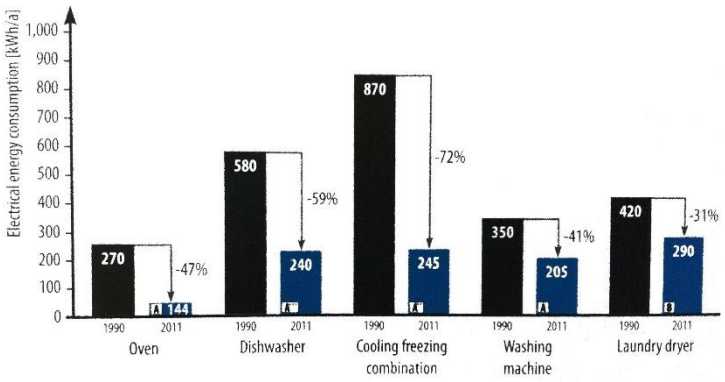

Figure 3-11 Annual electrical energy use of appliances in 1990 and 2011 (Norber Fisch et al., 2013)

Energiebundel		
Kooktoestel	251	kWh/a
Koelkast	333	kWh/a
Wasdroger	204	kWh/a
Wasmachine	170	kWh/a
Vriezer	163	kWh/a
Overige apparaten	245	kWh/a
Televisie	150	kWh/a
Audio-video	143	kWh/a
Vaatwasser	143	kWh/a
ICT	136	kWh/a
Stofzuiger	54	kWh/a
Totaal	**1992**	kWh/a
	25,5	kWh/m².a

Figure 3-12 Annual energy bundle NoM renovation Soesterberg by the BAM (OliNo, 2015)

3.3.6 Total demand

The NoM renovated dwelling with ENergy Roof becomes full electric and has an annual energy demand of 5060 kWh or 18,2 GJ. The final energy demand of the post-war row house is reduced from 66,8 GJ with more than 70%. The primary energy demand is reduced with 47% to 36,8 GJ. Due to the primary energy conversion factor for electricity the reduction is lower than for the

final energy. With the first two steps of the NSS the annual CO_2 emission is reduced from 4,3 to 2,3 ton per year. The largest energy post of the NoM dwelling is by far the energy for appliances with 50%. This shows that this post has a large influence on the total energy demand and the minimal amount of energy production. In order to become net zero energy the ENergy Roof has to produce minimal 5060 kWh per year.

Table 3.3 Annual final energy demand of a NoM renovated post-war single-family dwelling

		Final energy		Primary energy	CO_2 emission
	category	kWh	GJ	GJ	*1000 kg
Full electric	Heating*	745	2,7	33,6	2,1
	Hot water**	770	2,8		
	Ventilation	220	0,8		
	Lighting	400	1,4		
	Appliances	2500	9,0		
		4640	**16,7**	**33,6**	**2,1**

* 20% supplied by a solar boiler (COP 10) and 80% by a heat pump (COP 3,5)
** 50% supplied by a solar boiler (COP 10) and 50% by a heat pump (COP 2)

3.3.7 Electrical generation on site

The remaining energy demand of 4640 kWh has to be produced on site with renewable energy technology. The ENergy Roof is incorporated with photovoltaic (PV) panels, which convert solar waves into electricity (Figure 4-2). A part of the roof is covered with photovoltaic-thermal panels generating both electricity and heat. For this calculation the performance of a standard photovoltaic panel with mono crystalline cells are taken into account. Both sides of the roof are available to place PV panels, but it is preferred to use only one side of the roof. The boundary conditions state that the ENergy Roof may extend maximum 0,5 metre on the lower side. The annual generated electricity by the PV panels mainly depend on the total surface area of the panels, the efficiency of the panels, the system losses, the location, orientation and inclination of the panels.

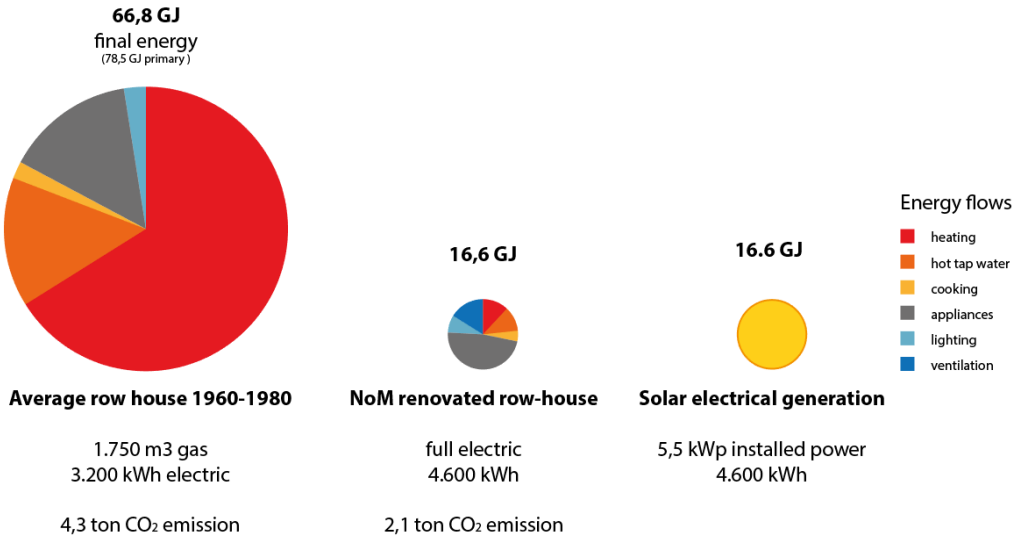

Figure 3-13 Energy flows before and after NoM renovation with potential energy generation by PV on the roof

The simplest calculation for the annual energy generation can be done using the specific yield in kWh/kWp of PV panels in the Netherlands. The average numbers of the specific yield of roof mounted PV panels are measured over a period from 1991-2010 by Sidera (2016). For an optimal orientation and inclination, the specific yield is between the 892 kWh/kWp in the east of the Netherlands and 972 kWh/kWp at the sea in the West. Using the average of 932 kWh/kWp a PV system of 5 kWp is required to produce 4640 kWh. A standard monocrystalline panel has 260 Wp and a surface area of 1,6 m^2 with an efficiency of 16%. This requires 31 m^2 of roof area or 20 PV panels with an orientation to the South and an inclination of 45 degrees. For a non-ideal orientation the average specific yield is 877 kWh/kWp (Sidera, 2016) and a roof surface of 33 m^2 is required.

Figure 3-14 Global Horizontal Irradiation (GHI) in the Netherlands (SolarGIS, 2016)

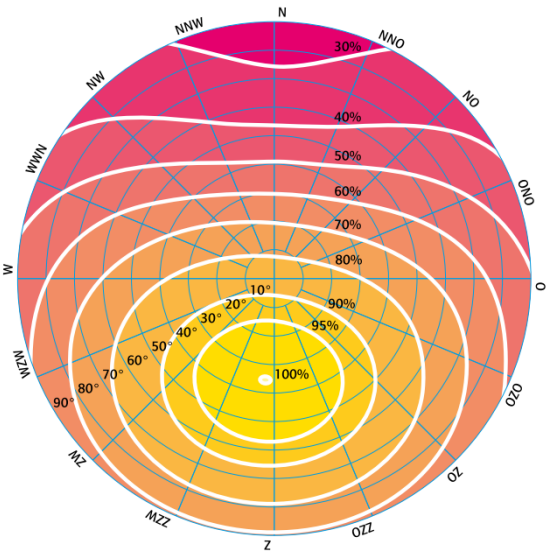

Figure 3-15 Performance ratio irradiation diagram in the Netherlands (ISSO, 2016)

The case study the post-war row house has a width of 5,8 metre, a depth of 9,1 metre where the roof has an inclination of 35 degrees. This results in a roof surface area of 32 m^2 on both sides, adding the extra extension of 0,5 metre result in 34 m^2. This shows that for an optimal orientation only one roof surface is required to become net zero and for a non-ideal orientation a roof extension is required.

A more advanced method is presented by the ISSO publication Zonne-Energie (ISSO, 2016). First the solar irradiation is calculated based on the Global Horizontal Irradiation (GHI) and the performance ratio based on the orientation as presented in Figure 3-14 and Figure 3-15. The relative 100% from the performance ratio diagram in Figure 3-15 is received from the horizontal irradiation multiplied with the 'tiltfactor' of 1,15 (ISSO, 2016). For Amsterdam the GHI is 1050

kWh/m² per year and a roof with East orientation and a slope of 35 degrees the performance ratio is 0,85, which results in 1026 kWh/m² per year. The second step is the calculation of the generated electricity based on the summed power of the panels and the system losses. The system losses includes the line losses, inverter losses and module soiling or snow and is set to 0,82 (ISSO, 2016). Taking into account the 20 PV panels of 260 Wp, a total of 4375 kWh per year can be generated on the East roof. The West roof requires another panel to generate the remaining electricity in order to become net zero energy. A dwelling with a North-South orientation with the same slope and applied PV panels to the sun-side of the roof produce a total of 5150 kWh. This shows that Nul-op-de-Meter is possible for a renovated post-war row house with ENergy Roof and that, depending on the buildings location and orientation, one or both roof surfaces are required.

3.4 Conclusion energy demand

This chapter gave an overview the different energy flows in an existing post-war row house and the energy demand after a NoM renovation with ENergy Roof. With the NoM renovation the first steps of the NSS are applied in order to reduce the energy demand of the dwelling. The final step of the NSS is the production of the remaining energy with renewables. The ENergy Roof generates renewable energy with PV panels. This chapter showed the amount PV surface area required to make the dwelling net zero energy or NoM and concluded that this is possible. Depending on the location of the dwelling in the Netherlands, the available surface area and orientation of the roof show that NoM is reached with one roof side or with both sides of the roof for PV panels.

With this the boundary conditions are set for the design of the ENergy Roof. The roof should be able to generate all the heating and hot water of the dwelling with a certain seasonal coefficient of performance (SCOP). Depending on the performance of this system the annual production of electrical energy with PV panels is higher or lower with respect to a lower or higher SCOP. The technical feasibility of the ENergy Roof, regarding the supply of heating, hot water and the total electricity generation is evaluated after a detail simulation of the system in chapter 6.

4. Installation components

The ENergy Roof consists of four essential components, which are: the photovoltaic-thermal system, a heat pump, storage technology and ventilation with heat recovery. In this chapter the background of each technology will be discussed with the dimensioning of the components. A start is made with the overview of the components in the hydraulic circuit, after which the four components will be explained in separate paragraphs.

4.1 Hydraulic circuit

The installation components of the ENergy Roof can be subdivided into a generation part and a demand part. This is presented in the hydraulic circuit in Figure 4-1 where the generation of thermal energy happens with the photovoltaic direct expansion (PV-DX) and photovoltaic thermal (PVT). The PVT is a solar boiler with automatic drain down system filled with water and provide heat for the hot water and heating demand in the summer and mid-season. The PV-DX circuit is filled with refrigerant and is connected to the solar assisted heat pump (SAHP). The heat pump provides two different temperatures suitable for the hot water and heating system and is operational in the four seasons. On the demand side the required heating is delivered for the hot water and heating circuit with their own buffer tanks. Summarized the ENergy Roof has two generation systems, two storage tanks and in total four different circuits.

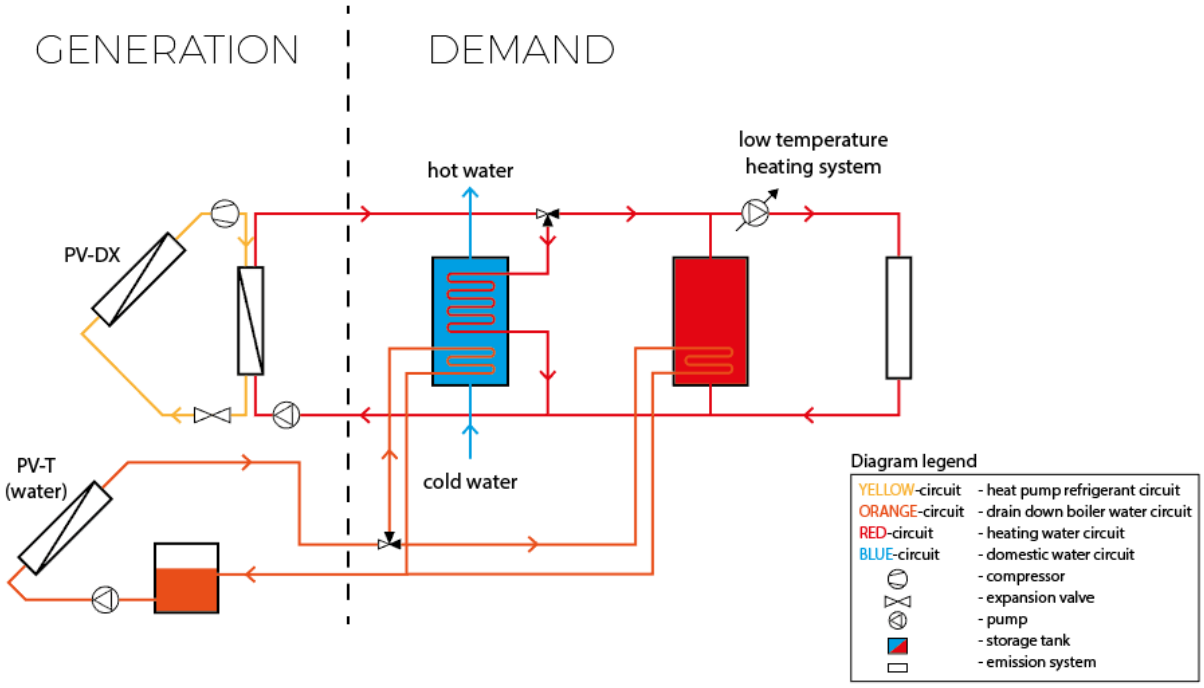

Figure 4-1 Diagram of the hydraulic circuit of the ENergy Roof

4.2 Photovoltaic-thermal

Photovoltaic panels convert solar irradiation into electricity where a large part of the solar energy is converted into heat. A graphical representation based on actual measurements of a crystalline silicon cell (Dupeyrat, 2012) shows that 74% of the incoming solar energy is wasted into heat (Figure 4-2). Whereby a large part of the incoming solar energy is unused and in addition the performance of the PV panel is decreased due to the increased temperature of the PV panel. The performance drops with about 4,5% per Kelvin above 25 °C (Zondag, De Vries, Van Helden, Van Zolingen, & Van Steenhoven, 2003).

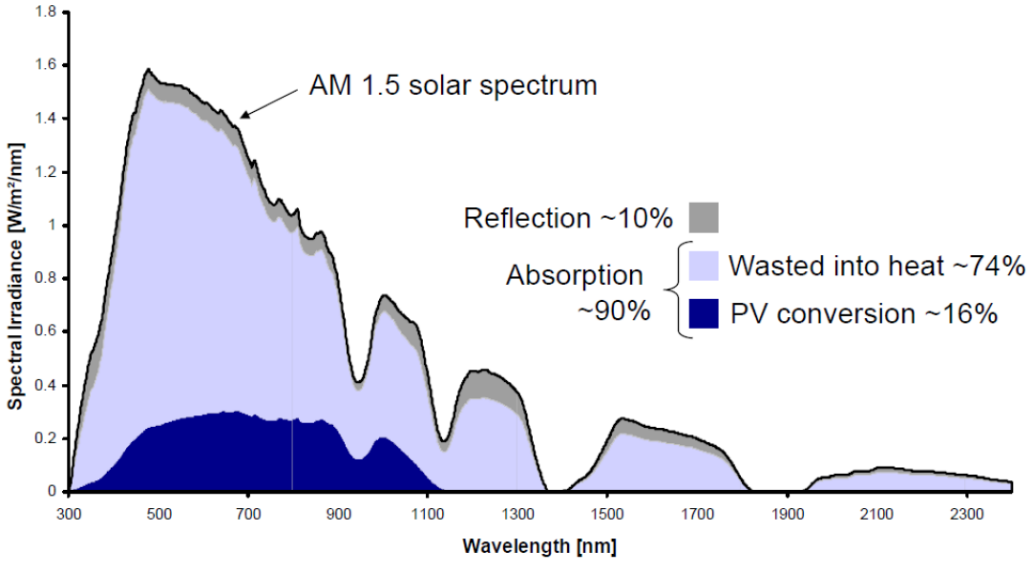

Figure 4-2 Spectral properties of a sc-Si cell with the AM 1,5 solar spectrum (Dupeyrat, 2012)

A combined PV-thermal (PVT) collector consists of a PV-laminate that functions as the absorber of a thermal collector. In this way the PVT system harvest both electrical and thermal energy from the incoming solar radiation. The main advantages of this system is the higher yield of solar energy; an area covered with PVT produces more electrical and thermal energy than a corresponding area partially covered with conventional PV and thermal collectors (Zondag et al., 2003). For an urban area with dwellings with limited roof surface, this is especially important. Depending on the system configuration, the PVT system lower the PV temperature, thereby increasing its electrical performance. Wrong configurations may lower the electrical performance of the PVT system, such as in the project of Rijksgebouwendienst (Van Helden, Roossien, & Mimpen, 2013). Other advantage of the PVT system is the architectural uniformity on a roof and finally a reduction of installation costs is possible due to the fact that only one type of system is installed.

The ENergy Roof uses two different PVT systems. The first system has a collector with water and the second a collector with refrigerant which is connected to a solar assisted heat pump (PV-DX SAHP). The water based system the fluid is warmed up by the sun and has operation temperatures

above the 25 °C and can go up to 60 °C. The system has an automatic drain down construction where the fluid runs out the panel into the tank inside when the pump shuts off. The circuit is illustrated with the orange line in Figure 4-1. The system drains down when the outside temperature drops below freezing point or when there is no solar irradiation and the outlet water temperatures does not reach above the 25 degrees. In these cases the PV-DX SAHP generates the required heat and hot water for the dwelling. Both systems can also be simultaneous in operation where the PVT preheats the water in the tank and the heat pump provides the remaining power to bring the tank to a usable temperature. In the PV-DX system the collector panel serves as an evaporator where the refrigerant evaporates due to absorbed energy from the sun or ambient air energy. The energy is delivered to the heating circuit (red line) in the condenser. The refrigerant circuit is illustrated by the yellow line in Figure 4-1. or both and delivers the energy to the heating circuit in the condenser. The functioning of a PV-DX SAHP system is described in the next paragraph. The advantage of the PV-DX, compared to the PVT system, is that the temperature of the working fluid in the absorber/evaporator is much lower. Thereby, the system can operate below zero degrees ambient temperature, where the PVT is limited due to freezing risk. In the winter the PV-DX SAHP should deliver all the heat demand of the dwelling, while in the summer and mid-seasons both systems work together. The advantage of the PVT system above the PV-DX system is the higher coefficient of performance since only a pump is in operation.

4.3 Heat pump

A heat pump works basically the same as a refrigerator, only it has the objective to heat instead of to chill. The system works with the Carnot vapour refrigeration cycle operating between a region at cold temperature T_c and higher temperature T_h (Moran & Shapiro, 1996) as presented in Figure 4-3. The heat pump extracts energy from the cold source by evaporation Q_e and with the added electrical energy E the refrigerant is compressed to a higher temperature and supplied to the hot source by condensation Q_c. The four main components of a heat pump are presented in the same figure and consist of a compressor (1-2), a condenser (2-3), an expansion valve (3-4) and an evaporator (4-1).

Let us follow the refrigerant as it passes through each component in the cycle, beginning at the inlet of the evaporator at state 4 (Figure 4-4). There are 4 processes that occur in the heat pump. All processes are internally reversible (Moran & Shapiro, 1996).

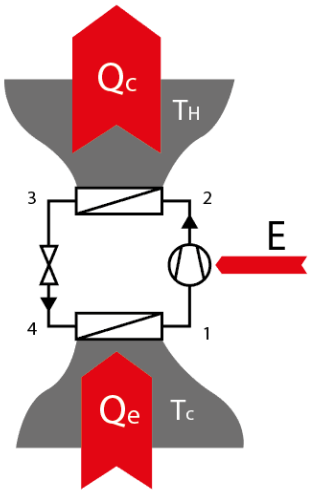

Figure 4-3 Schematic diagram of the components and energy flows within a heat pump

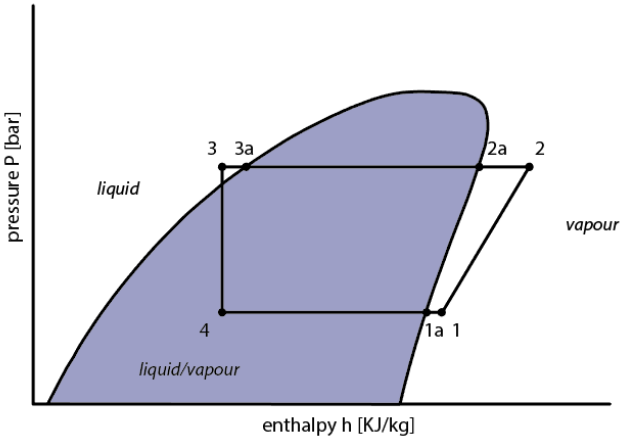

Figure 4-4 Log P-h diagram of the refrigeration cycle in a heat pump

Process 4-1: The refrigerant enters the evaporator as a two-phase liquid-vapour mixture at state 4. In the evaporator the refrigerant change phase from liquid to vapour as a result of heat transfer Q_e from the cold region to the evaporator at temperature T_c. The temperature and the pressure remain constant (isothermal process) in the process from state 4 to state 1a where it is saturated vapour (Figure 4-4). In order to ensure dry compression the refrigerant is super-heated in the saturated vapour area from state 1a to state 1. Liquid is avoided because it can damage the compressor.

Process 1-2: The saturated refrigerant vapour is then compressed adiabatically until it reaches state 2. During this process the pressure increases from P_{evap} to P_{cond} and with the pressure also the temperature increases. This process requires compressor electricity E (work).

Process 2-3: The refrigerant passes from the compressor into the condenser. The temperature drops from state 2 to state 2a until it reaches the saturated vapour border at temperature T_h. The pressure remains constant in the process from state 2a to state 3a. In the condenser the refrigerant changes phase from saturated vapour to saturated liquid at a constant temperature T_h (isothermal process) as a result of heat transfer Q_c. In the liquid phase the refrigerant undergoes sub cooling from state 3a to state 3. This is done in order to get a lower percentage of vapour (X value) in the two phase liquid/vapour state in point 4. The lower the percentage of refrigerant that is vaporised in point 4 the higher the Q_e and the better the efficiency of the heat pump.

Process 3-4: The refrigerant returns to the state at the inlet of the evaporator by expanding adiabatically through a throttling valve. In this process the pressure decreases and the temperature drops to T_c.

The coefficient of performance (COP) of a heat pump is calculated with the energy supplied to the heating system Q_c divided by the electrical energy used by the compressor of the heat pump E (Figure 4-3). For the Carnot vapour refrigeration cycle, the COP is:

$$\text{COP} = \frac{Q_c}{E} \quad (1)$$

The theoretical maximum COP of any refrigeration cycle operating between regions at T_C and T_H is calculated with equation (2).

$$\text{COP}_{carnot} = \frac{T_c}{T_H - T_c} \quad (2)$$

Actual refrigeration systems depart significantly from the ideal cycle considered above and result in a lower COP. In actual systems the heat transfers are not reversibly as presumed. The temperature of the refrigerant is below the temperature in T_C and above T_H in order to allow heat transfer to occur, resulting in a higher pressure difference and increased work in the compressor. Secondly the COP is reduced due to losses in the system such as compressor efficiency, heat loss at the compressor, isentropic efficiency and pressure loss in the lines. According to Luscuere (2015), the actual COP can be calculated by implying an efficiency factor of the compressor of approximately 0,5. However the efficiency factor differs per type of heat pump where different efficiency factors between 0,3 and 0,4 are found for air sourced heat pumps (Carrier, 2016).

$$\text{COP} = \eta \cdot \frac{T_c}{T_H - T_c} \quad (3)$$

Available heat sources

An heat pump extract heat from a cold source and supplies the heat to a hot source within a dwelling. Possible sources could be the ground, surface water, solar, ambient air or exhaust air. These different type of heat pumps are associated with different SPF. The smaller the temperature difference between the cold and hot source, the better the SPF. Ground source heat pumps (GSHP) typically have higher efficiencies than air source heat pumps (ASHP) as presented in Figure 4-5. This is because the ground is affected in a smaller degree by temperature fluctuations and provided higher temperatures for the evaporator. However, the installation costs are circa twice as high due to the installed pipes and boreholes in the ground to extract the heat.

This study investigates a heat pump with solar as main source of the heat pump (SAHP). The ASHP is excluded because of the disadvantage of an outside unit which is associated with noise pollution and high investment costs. The heat pump with exhaust air as source is not suitable for the ENergy Roof since a ventilation heat recovery unit (HRU) is applied. Solar energy is an accessible potential renewable energy source. The daily and seasonal fluctuation of solar energy highly influences the efficiency of the heat pump. Sun, Wu, Yanjun, and Ruzhu (2014) show higher efficiency of a DX-SAHP when heat from the sun is absorbed compared to an ASHP, but lower in zero solar radiation

condition (Figure 4-6). This research study focus on the integration of a DX-SAHP where the evaporator is fixed to the backside of the PV panel.

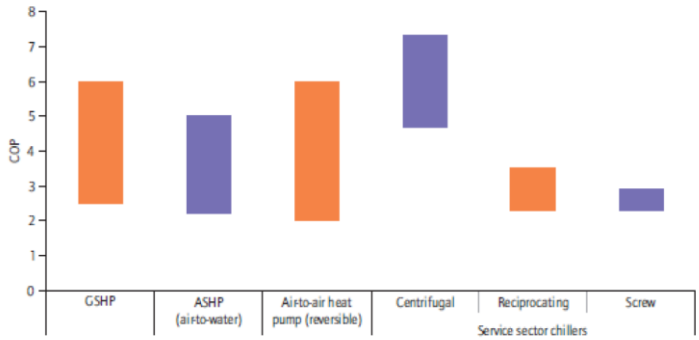

Figure 4-5 Efficiency of different heat pumps (IEA, 2011)

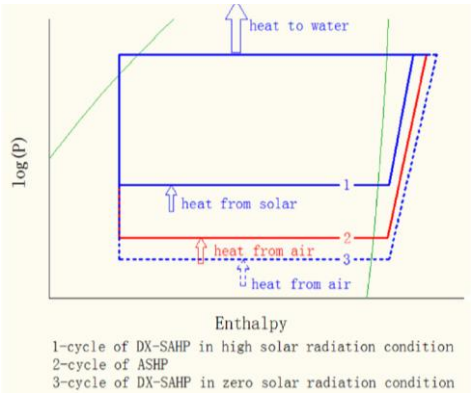

Figure 4-6 Temperature cold source of a DX-SAHP and an ASHP (Sun et al., 2014)

Roll-bond DX-evaporator

According to Sun et al. (2014) the performance of the PV-DX SAHP is significantly affected by the absorptivity and thermal conductivity between the PV and the evaporator. The geometrical structure of the flow channel is also an important factor that affects the performance of the evaporator. In this study the roll-bond panel is used as evaporator of the PV-DX panel. The roll-bond is made of two aluminium sheets and is often used in refrigerators and freezers (Rubanox, 2016). In the production process the channel networks are printed onto the aluminium sheet with graphite where after the two aluminium sheets are assembled by a rolling process. The printed inner channel can be created by pressuring the tubes. Compared to a tube-type heat exchanger the roll-bond technology is an easy and cheap manufacture process where a high conductive surface area is achieved. Roll-bond is suitable for DX-SAHP and has the following advantages: unique design flexibility for the DX-SAHP system; easy to be shaped for different applications; easy for design and fabrication; low cost for design and manufacturing; convenient for aluminium recycling (Sun et al., 2014).

Figure 4-7 Direct expansion solar assisted heat pump (DX-SAHP) with roll-bond evaporator panels (Energy Panel, 2016)

Refrigerant and compressor

The most common refrigerants used in vapour-compression refrigeration systems has been the chlorofluorocarbons (CFC's) such as Refrigerant 12 (CCI2F2). Due to the negative effects on the earth's protective ozone layer the CFCs are phased out. The refrigerant R134a contains no chlorine and is considered as an environmentally acceptable substitute for R12 with the appropriate technical specifications. The Global Warming Potential (GWP) of R134a is 1300, meaning that 1 kg of refrigerant leaking out of the system is equivalent to 1300 kg of CO_2 emission. More environmental friendly refrigerants are developed, but the disadvantage is the flammability of the refrigerant. A promising development are the HFO 1234yf with a GWP <130 which is already applied in the air-conditioning for cars. For this study the refrigerant R134a is used since it has low cost and is most commonly used for DX-SAHP.

A typical compressor will be selected suitable for a DX-SAHP and R134a with a capacity of 3-6 kW. The rotary scroll compressors is selected for this configuration since it is a commonly used compressor within this heat pump type. Reciprocating compressors are associated with noise and vibrations where centrifugal and screw compressors are mainly applied in high capacity heat pumps. Rotary vane or twin rotary are applied in fridges but are also suitable for heat pumps for 3-50 kW and may be an alternative.

The expansion valve control the pressure in the refrigeration circuit and ensures a minimal overheating of the saturated gas to ensure dry compression. The electronic expansion valve (EEV) is applied and operates with a much more sophisticated design than a conventional TXV. The EEV ensures an overheating between 3 and 6 K.

Operation mode and hydraulic circuit

The implementation of a heat pump in a domestic energy system can be done according four operation modes (ISSO 744) as presented in Figure 4-8. For this system a bivalent operation mode is selected which supplies both the heating and hot water for the dwelling. First the PVT solar boiler supplies the energy until ambient temperature drop below zero or produce water lower than 25 °C. Secondly the heat pump supplies the remaining heat demand down to a defined minimum temperature in the evaporator, after which the auxiliary system provides the remaining demand. With this configuration a smaller heat pump capacity can be selected where the auxiliary system is only in operation during a short period of the year. The auxiliary system consist of an electrical after heater.

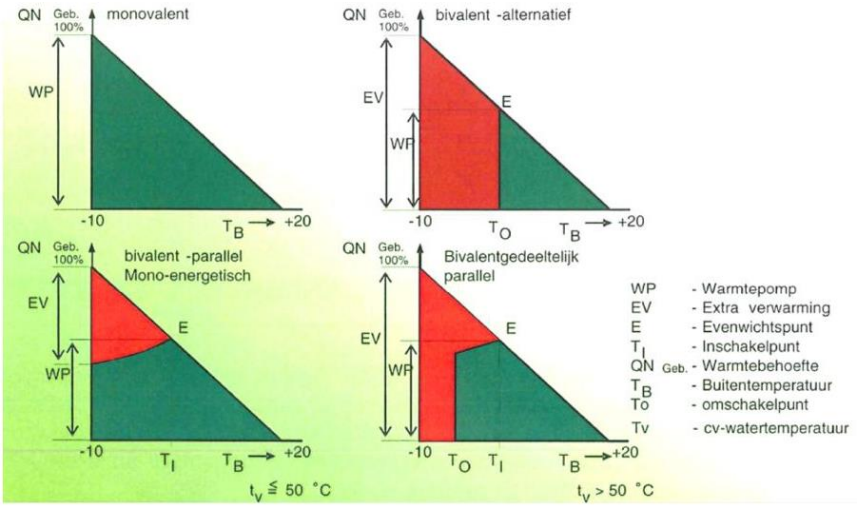

Figure 4-8 Different types of operation modes with heat pump (green) and electrical heater (red) (ISSO 744)

The alignment of the emission system to a heat pump is crucial to ensure an energy system with optimum efficiency (Van Krevel, 2000). For well insulated dwellings with small transmission losses and heat demands a low temperature emission system is suitable. Heat pumps perform better at low water temperatures but can lead faster to discomfort due to design water temperatures close to minimal room temperatures (ISSO 744). According to Van Krevel (2000) the following design rules can be applied: minimize supply water temperatures, ensure a minimum flow rate through the condenser and reduce on-off cycling of the heat pump. A minimum flow rate over the condenser is required for good heat transfer and prevent overheating within the heat pump. Frequent on-off cycling occur in a system with small buffering capacity, reducing the compressor life time. In order to maintain the number of on-off cycles of the heat pump low, the energy systems inertia can be increased by the application of a buffer tank. A parallel buffer with decoupling of the primary and secondary circuits by application of a modulating pump is applied in the heating system (ISSO 744). This provide more control and smooth operation of the heat pump. The hydraulic circuit is presented in Figure 4-9.

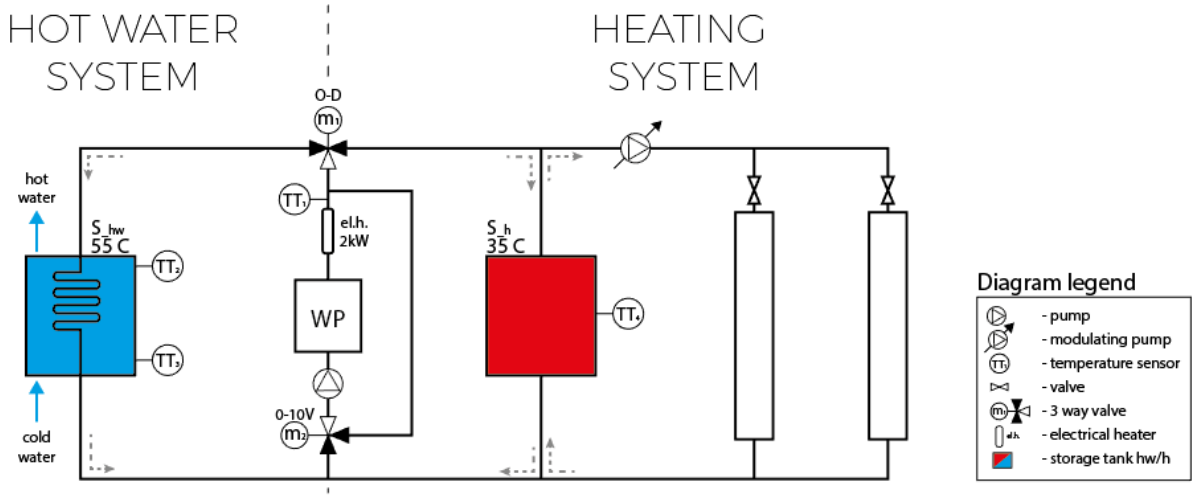

Figure 4-9 Hydraulic circuit of the hot water and heating system

4.4 Storage buffer

One may notice that a heat pump system with a capacity of 3-6 kW work totally different from a gas boiler system. A gas boiler has enough capacity to directly heat the cold water to supply the shower, where a heat pump requires a storage tank to provide enough capacity.

The ENergy Roof is applied with two types of storage buffers, one for the heating system and the other for the hot water system as presented in the hydraulic circuit in Figure 4-9. The energy storage buffers do not only provide smooth operation, but it also offers possibilities of load management where heat can be generated (and stored) at moments when renewable energy is available. The PV-DX SAHP has high efficiency and capacity when solar energy is available. The storage buffers gives the possibility to generate the heat during the day and consuming it during the night. In addition the ENergy Roof and the PV-DX panels generate electricity during the optimal SAHP operation time with high solar irradiation. The electricity is directly used by the heat pump, reducing the surplus of electricity generation, and which will lead to cost reductions. On top of that smaller losses are achieved with thermal energy storage compared to firstly storing the electrical energy where after the electrical energy is converted into heat on demand.

4.4.1 Storage heating

The heating storage tank which is a fully mixed water tank directly coupled with the heating circuit has the main function to smooth the operation of the heat pump. Water is a convenient heat storage medium with a high specific heat capacity. The temperature operation limit of the tank is set between the 23 and 35 °C. Thermal energy is supplied and taken from the tank by the heating circuit and the emission circuit, as presented in Figure 4-9. Heat is generated with the heat pump or electrical heater or both and supplied to the storage tank or directly to the heating system, depending on the flow of the modulating pump. The tank has one temperature sensor TT_4 to measure the thermal capacity of the tank. In chapter 16.16 the content of the storage tank is calculated based on the on-off cycles of the heat pump.

4.4.2 Storage hot water

The hot water storage is a stratified tank with vertical temperature layering of the water due to the effect of gravity and the buoyant force. Cold water with high-density will settle in the lower part of a tank and the hot water with low-density at the upper part. Heat is transferred between the hot and cold zone via mixing and conduction. This region is called a thermocline and reduces the usable capacity of the storage tank. Stratified water tanks can yield higher energy density than mixed water tanks. A stratified tank with a thermocline of 20% contains 2,4 times more usable energy than a mixed tank with the same volume. Best stratification occurs with a tall tank, low inlet velocities and large temperature differences between top and bottom (Dwivedi, 2009). The content of the tank is domestic water and the useful outlet temperature lies above the 40 °C, the tank is heated up to 55 °C and once a week to 60 °C to prevent the grow of legionella. A thermocline

of 20% is assumed. The storage tank of the heating circuit is assumed to be fully mixed. Due to the small temperature difference in the heating tank minimal stratification will occur.

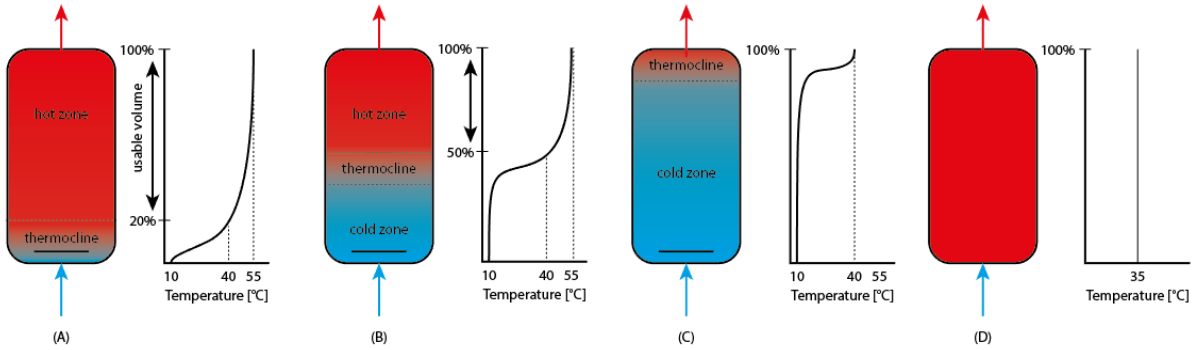

Figure 4-10 Different type of storage tanks (a) stratified tank fully loaded (b) stratified tank partly loaded (c) stratified tank empty (d) fully mixed tank fully loaded

The heating spiral circulating in the tank should be carefully placed. In order to load the hot water tank, the inlet temperature of the heating circuit should be minimal 55 °C, lower temperatures will cool the hot zone of the tank. The minimal temperature is reached with the three-way-valve m_2 with a 0-10V control which opens or closes the valve depending on the temperature in TT_1 (Figure 4-9). The flow goes over the heat pump until the temperature of 55 °C is reached. The electrical heater is used when the heat pump cannot provide the required temperature. Temperature sensors TT_3 and TT_4 measure the capacity of the tank if it is fully loaded or empty. The capacity and dimension of the tank is calculated in chapter 16.16.

4.5 Ventilation heat recovery

The ventilation heat recovery unit (HRU) is an important part of the ENergy Roof reducing the heat demand of the dwelling. The HRU is not directly part of the thermodynamic model , however it is part of the DesignBuilder model where the heat demand profile of the dwelling is simulated. The heat demand profile is an important input of the thermodynamic model.

The ventilation system supplies the dwelling with fresh air in the living and sleeping rooms and extracts the polluted air from the kitchen, toilet and bathroom. It is an balanced system where the same amount of air is supplied as is extracted. The system includes two panel filters with filtering class G4 for exhaust and a replaceable filter with filtering class F7 for supply air as shown in the diagram in Figure 4-11. Two speed controllable fans provide an air capacity up to 350 m^3/h. The heat recovery unit has an efficiency up to 94% and a bypass which can be opened if there is a need to cool the dwelling with the outside air or for frost protection. The components are integrated in a heat and sound insulated casing. The ventilation unit give the possibility to add a control unit

which includes control valves and after heaters where the air and heat is supplied in the specific rooms based on the demand. The standard ventilation unit is not equipped with this addition.

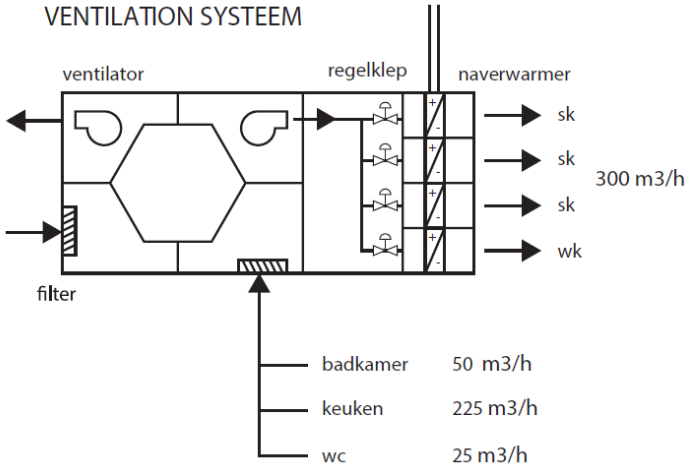

Figure 4-11 Ventilation system with heat recovery and the addition with control valves and after-heaters

5. Mathematical model

The purpose of the mathematical model is to predict the thermodynamic behaviour of the ENergy Roof in the climate of the Netherlands. The focus of the model is on the photovoltaic-direct expansion evaporative (PV-DX) panel coupled with a solar assisted heat pump (PV-DX SAHP).

This chapter describes the mathematical model which consists of four sub models, namely the panel, heat pump, storage and demand input (Figure 5-1). Each sub model is described according to the method 'steps for modelling' as described by Van Paassen (2004), these are: the purpose, system boundaries, relevant phenomena, assumptions, mathematical equations and initial values. The sub models are connected in a single MABLAB/Simulink model and simulation shows the performance of the PV-DX panel and ENergy Roof under different panel sizes, compositions and climate conditions. All the parameters used in the mathematical equations are presented in Table 10.1 in Appendix A – Parameters.

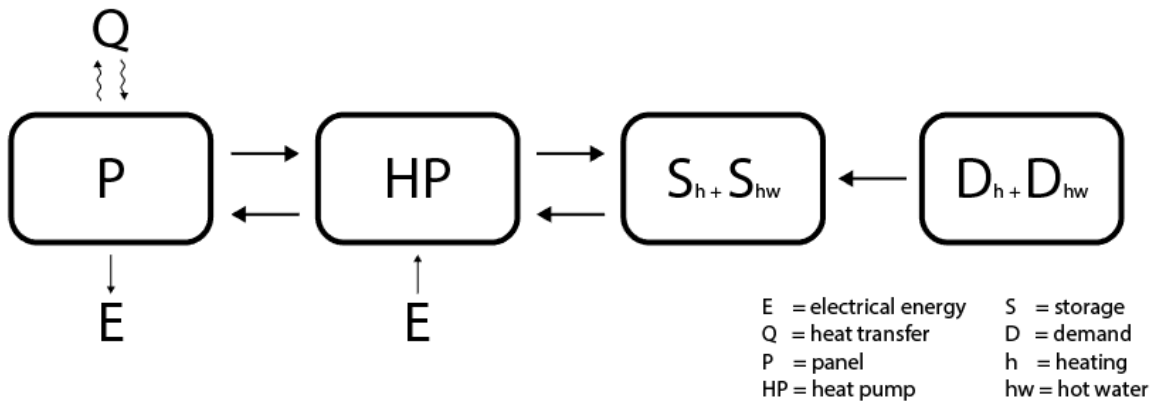

Figure 5-1 Diagram simulation model subdevided in four submodels: panel, heat pump, storage tank and demand

5.1 The Panel

The model of the panel predicts the dynamic behaviour of a PV-DX panel influenced by the environment conditions Q (e.g. wind speed, ambient temperature and irradiation) and heat pump HP (Figure 5-1). The temperature and heat fluxes vary in time and is dynamic, therefore a more complicated calculation software is used to set up a model, namely MATLAB/Simulink. A one dimensional heat conduction model is constructed with non-stationary multiple nodes with time dependence heat balances.

5.1.1 Purpose

The purpose of the model is to predict the temperature of the refrigerant flowing though the panel as function of the changing environmental conditions. The temperature of the refrigerant is

dependent on the panel characteristics and the heat transfers to and from the environment. In addition the temperature of the refrigerant in the panel is also influenced by the heat pump, this is discussed in chapter 5.2.

5.1.2 System boundaries

The system boundaries of the panel are based on the purpose of the model. The panel is separated from the environment by 2 different boundaries. The boundaries are placed at the top surface of the panel and the backside of the panel (Figure 5-3). Through these boundaries there is heat transfer to the environment. The environmental conditions are an input of the model and based on the Dutch reference climate conform NEN5060:2009 attachment A2. The climate input are hourly data of the ambient temperature, the solar irradiation, the long wave incoming radiation and the free flow wind speed at 10 metre height.

5.1.3 Relevant phenomena

The relevant phenomena of the panel model is illustrated in Figure 5-3 where there are three different heat transfer phenomena. Heat transfer in solid parts goes via conduction. Heat transfer between solid parts and air goes mainly via convection and heat transfer between solid parts goes mainly via radiation. The heat transfer is dependent on the temperature difference, surface and the heat transfer coefficient. Other phenomena's are the solar radiation and the long wave incoming radiation. Part of the solar radiation heat is absorbed in the panel, another part is reflected or converted into electricity by the PV cells. The long wave radiation loss from the panel to the sky is dependent on the properties and the temperature of the material. In addition heat transfer takes place from the inner surface of the aluminium tubes of the PV-DX panel to the refrigerant flowing through the tubes. The two-phase refrigerant entering the panel evaporates at constant temperature (isothermal process) and leaves the panel as saturated gas. The solid parts of the PV-DX panel have a low thermal mass and therefore the ability to store heat is nearly negligible compared to the solar heat.

The model with the heat transfers coefficient is based on the 1st law of thermodynamics which state the conservation of energy. A scheme with temperature nodes and resistances between the nodes is constructed in analogy with an electrical scheme in Figure 5-3. The energy conservation law is applied on each node in analogy with the Kirchhoff's current Law. Within a centrally located demarcated area or control volume an unknown temperature of a node can be calculated for every time step within the model.

5.1.4 Assumptions

The model is simplified in order to make it workable besides that not all the phenomena have a large influence on the model. Some factors are neglected or taken as constant.

The convective heat transfer between the backside of the panel and the outside air is dependent on the wind speed and temperature in the cavity between the panel and the roof. The wind speed is dependent on the characteristics of the roof (e.g. height of the cavity and openings at the bottom and top), the wind direction, the free flow wind speed and the built environment. With Computational Fluid Dynamics (CFD) simulations the heat transfer can be predicted, but this is outside the scope of this research. The heat transfer coefficient is therefore taken as a factor over the heat transfer at the top of the panel as presented by equation (10) and elaborated on in Appendix F - Convective heat transfer from the PV panel surface.

Temperature in the cavity between the panel and roof is equated with the ambient temperature. This assumption is done to simplify the model. Besides that the heat resistance from the cavity to the ambient air is very small compared to the heat resistance to the panel, which results in a small temperature difference between the cavity and the ambient air. This is again dependent on the openings in dimensioning of the cavity and in reality the air in the cavity may be lower, resulting in a reduced heat transfer to the panel. This is effect is taken into consideration with the reduced heat transfer factor.

The heat transfer coefficient between the aluminium roll-bond evaporator and the refrigerant flowing through the panel is not constant in each point of the panel owing to the geometry of the evaporator and the changing liquid-vapour state of the refrigerant. To simplify the model a single heat transfer coefficient is assumed for the entire panel, based on the average heat transfer coefficient. The heat transfer coefficient is calculated with Finite Element Method (FEM) and described in Appendix E - Heat transfer in the evaporator.

Condensation and freezing on the panel from the outside air is not taken into account. The model is a preliminary design and it is recommended to include this process in a more detailed model.

5.1.5 Mathematical equations

The dynamic calculations are based on the mathematical equations and are presented in two parts, namely the physical characteristics of the panel and secondly the heat transfers between the nodes.

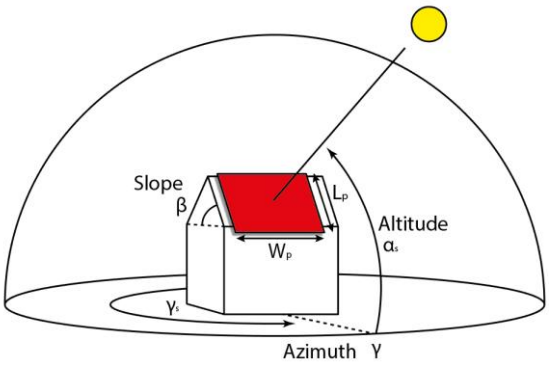

Figure 5-2 Paramaters of the ENergy Roof dimensioning

5.1.6 Physical characteristics

The surface area of the PV-DX panel is an input parameter where the maximum surface area is determined by the width and light of the technical element of the ENergy Roof. The maximum width of the element is set to 2,0 metre by the boundary conditions. The length depends on depth of the house, the slope of the roof β and the maximum extension of 0,5 metre. This gives a maximum surface area of 12 m² for the technical element of the ENergy Roof. The input parameters of A_{PV-DX} is presented in Table 10.1.

The back surface of the PV-DX panel is larger due to the relief of the tubes at the backside of the absorber. The surface is a factor larger and is represented by f_{back}. The surface of the backside of the PV-DX panel is calculated with:

$$A_{PV-DX\_b} = A_{PV-DX} \cdot f_{back} \tag{4}$$

The orientation and inclination of the panel is dependent on characteristics of the dwelling and influences the heat transfer coefficient related to the solar irradiation and the wind. Calculations are done for two orientations of the PV-DX panel: South and East based on a North-South and East-West orientation of the roof. The inclination of the panel is dependent on the slope of the and is set to 30 and 45 degrees based on the literature research.

$$\gamma_{south} = 0, \gamma_{east} = 90 \tag{5}$$

$$\beta_{30} = 30, \beta_{45} = 45 \tag{6}$$

5.1.7 Heat transfer between the nodes

The nodes are presented in the network model in Figure 5-3 and include three different heat transfers, namely convection, radiation and conduction. These three types are clarified in this section and the parameters used in the equations are presented in Table 10.1.

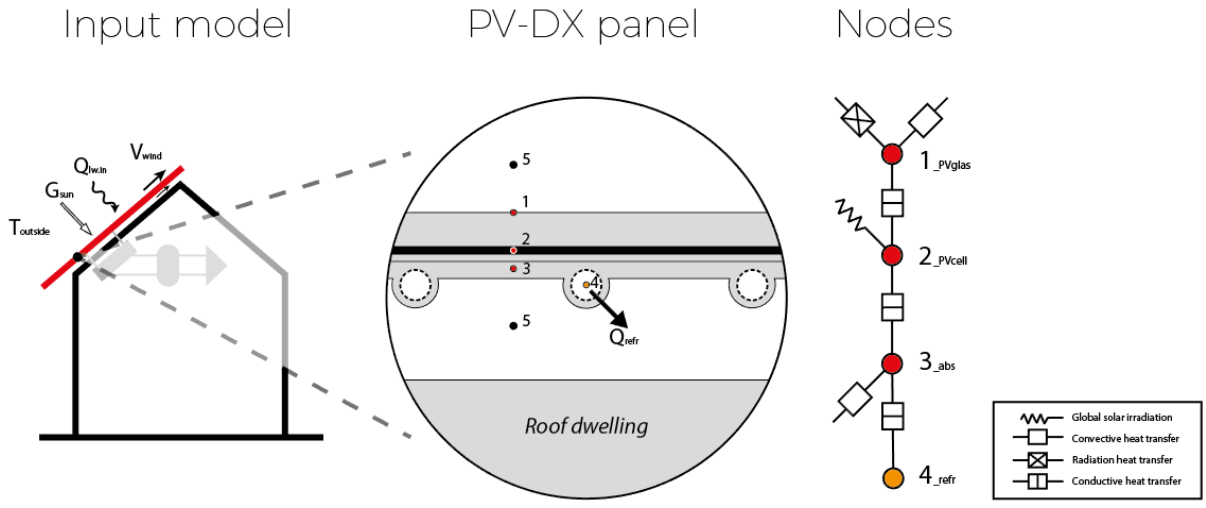

Figure 5-3 Inputs of the model with section of the PV-DX panel and the nodes with heat transfer phenomena

The convective heat transfer from the panel to the ambient represent an important portion of the overall energy balance and depend heavily on the wind induced convection. According to Mills (1999) the convective heat transfer can be calculated with equation (7). In the equation h_w represents the wind convection coefficient, including the forced and free convection. The surface and the temperature difference between the nodes is represented respectively by A and ΔT.

$$\dot{Q}_{conv} = h_w \cdot A \cdot \Delta T \tag{7}$$

The correlation of Sharples has been found as the best match for the current setup and elaborated in Appendix F - Convective heat transfer from the PV panel surface. The correlation includes both forced and free convection, therefore there is no second equation needed as done in the research of Armstrong and Hurley (2010). The wind convection coefficient of the top surface of the PV-DX panel are given by equation (8) and (9) where the free flow wind speed is represented by w (Sharples & Charlesworth, 1997).

$$h_w = 2.2 \cdot w + 8.3 \text{ (windward)} \tag{8}$$

$$h_w = 1.3 \cdot w + 8.3 \text{ (leeward)} \tag{9}$$

The wind convection coefficient at the backside of the panel differs from the front as described in paragraph 5.1.4. The arbitrary factor f_{wind} is used to calculate the heat transfer coefficient and is based on the lower wind speed, a smaller temperature difference and taking into account the chance of ice formation which will lower the heat transfer.

$$\dot{Q}_{conv\_b} = f_{wind} \cdot h_w \cdot A_{PV-DX\_b} \cdot \Delta T \tag{10}$$

The radiation heat transfer is given by two variables, the long wave incoming radiation LW_{in} and the black-body radiative heat transfer coefficient to the sky (Van der Spoel, 2015). LW_{in} is part of the input data from NEN5060:2009. Both are multiplied with the view factor to the sky, F_{sky}. In equation (11), ε represents the emissivity which is dependent on the material property. The Stefan-Boltzmann constant is represented by σ. The radiation to the sky is related to the temperature of the top surface of the panel in Kelvin. As mentioned in the paragraph 5.1.4 it is assumed that no radiation takes place between the panel and the roof, since there will be no temperature difference between the two layers.

$$\dot{Q}_{rad} = F_{sky} \cdot A_{PV-DX} \cdot (LW_{in} - \varepsilon\sigma {T_{glass}}^4) \tag{11}$$

For the conductive heat transfer the same type of equation is presented as the convective heat transfer, only with a different coefficient (Mills, 1999). In equation (12) the thermal conductivity is represented by λ and d is the material thickness.

$$\dot{Q}_{cond} = \frac{\lambda}{d} \cdot A \cdot \Delta T \tag{12}$$

The heat from the solar energy which is absorbed by the node in the solar cell is given by (Zondag et al., 2003). The solar irradiation is presented by G and given by the NEN5060:2009 for perpendicular irradiation on different inclined surfaces given in average hourly data. The effective transmission-absorption factor is represented by $\tau_{a,eff}$.

$$\dot{Q}_{sun} = \tau_{a,eff} \cdot A_{PV-DX} \cdot G \tag{13}$$

In an optical model the transmission-absorption factor of a PVT-collector is calculated for different wavelength and then integrated over the solar spectrum (Zondag et al., 2003). This study is performed for an uncovered sheet-and-tube PVT-collector which matches a PV-DX panel. The calculations present a transmission-absorption factor τ_a. The thermal efficiency is then calculated with respect to the effect of the electrical energy production, which is subtracted from the transmission-absorption factor to find the amount of thermal energy that was absorbed in the system. The electrical efficiency is a function of the temperature in the PV-cell T_{pvcell}. In equation (14), η_0 represents the electrical efficiency of the PV cell in nominal conditions (1000 W/m^2 irradiation and a temperature of 25 °C). The efficiency losses for every degrees above the nominal conditions is represented by η_t.

$$\tau_{a,eff} = \tau_a - \eta_0 \left(1 - \eta_t \left(T_{pvcell} - 25°C\right)\right) \tag{14}$$

The electrical energy produced due to the incoming solar irradiation on the PV-DX panel can be calculated with equation (15). The system losses by cables and the inverter is represented by η_{system} and the solar irradiation by G.

$$\dot{Q}_{el} = \eta_0 \left(1 - \eta_t \left(T_{pvcell} - 25°C\right)\right) \cdot \eta_{system} \cdot G \tag{15}$$

Another type of heat transfer is by the evaporation of the refrigerant in the aluminium tubes of the evaporator. The average heat transfer coefficient a_{abs_refr} is calculated with FEM and implemented as constant. This leads to equation (16) with the surface area A_{PV-DX} and temperature difference between the refrigerant T_{refr} and absorber T_{abs}.

$$\dot{Q}_{refr} = a_{abs\_refr} \cdot A_{PV-DX} \cdot \left(T_{refr} - T_{abs}\right) \tag{16}$$

All the nodes in the panel have the ability to store heat. This heat storage is given by equation (17) according to Van Paassen (2004). Where m is the mass, c_p the specific heat capacity and the temperature difference is represented by the current temperature T_n minus the temperature in the previous time step $T_{(n-1)}$.

$$\dot{Q} = m \cdot c_p \cdot (T_n - T_{(n-1)}) \tag{17}$$

5.1.8 Matrix

The different heat transfer equations of the dynamic system of the panel are represented in a matrix form. The non-stationary multi-node heat balance equations can be solved with advanced

numerical software such as MATLAB/Simulink. The heat balance is given by Van der Spoel (2015). In equation (18) the **M** is the so-called mass matrix, S the stiffness matrix which represents the heat transfer coefficients, $\underline{\boldsymbol{Q}}$ the load vector, and $\underline{\boldsymbol{T}}$ the vector with the (time-) dependent variables. The 'dot' notation, $\underline{\dot{\boldsymbol{T}}}$, denote the time derivative. This equation is called a set of ordinary differential equations (ODE).

$$\boldsymbol{M}\underline{\dot{\boldsymbol{T}}} + S\underline{\boldsymbol{T}} = \underline{\boldsymbol{Q}} \tag{18}$$

The matrices are set up according to the network model as presented in Figure 5-3. In the panel model there are 5 different nodes, so the matrices are 5 x 5 matrices. The model involves 'free' and 'bound' nodes, where the bound node has a given input and the free node will be calculated. In the model the temperature of the environment has known temperature inputs. The temperature of the refrigerant is iteratively calculated as explained in paragraph 5.2 and inserted as a known temperature in this sub-model. Because these two temperatures are known a fixed heat transfer matrix is made. The temperature of the free nodes are changing dependent on the heat transfer working on the node and the mass of the node. The heat transfer of the nodes is time dependent. The mass of the nodes remain constant and is not time dependent. Rewriting equation (18) taking into account the fixed temperatures give equation (19).

$$\underline{\boldsymbol{T}}(\boldsymbol{t}) = \boldsymbol{M}^{-1}\int_{0}^{t}\left(\underline{\boldsymbol{Q}} - \boldsymbol{S}\underline{\boldsymbol{T}} - S_{bound}\underline{\boldsymbol{T}}_{bound}\right)\boldsymbol{dt} \tag{19}$$

The S_{bound} consists of 3 rows and 2 columns, and $\underline{\boldsymbol{T}}_{bound}$ is a vector with 2 elements representing the temperature in the bound nodes (T_e and T_{refr}). Therefore the **S** is a 3 x 3 matrix. The matrix $\underline{\boldsymbol{Q}}$ is also a 3 x 3 matrix. The mass matrix **M** is a 3 x 3 matrix with positive values in the diagonal from the top left to the bottom right. The temperatures of the 3 free nodes are calculated in MATLAB/Simulink for the different time steps as presented in Figure 5-4.

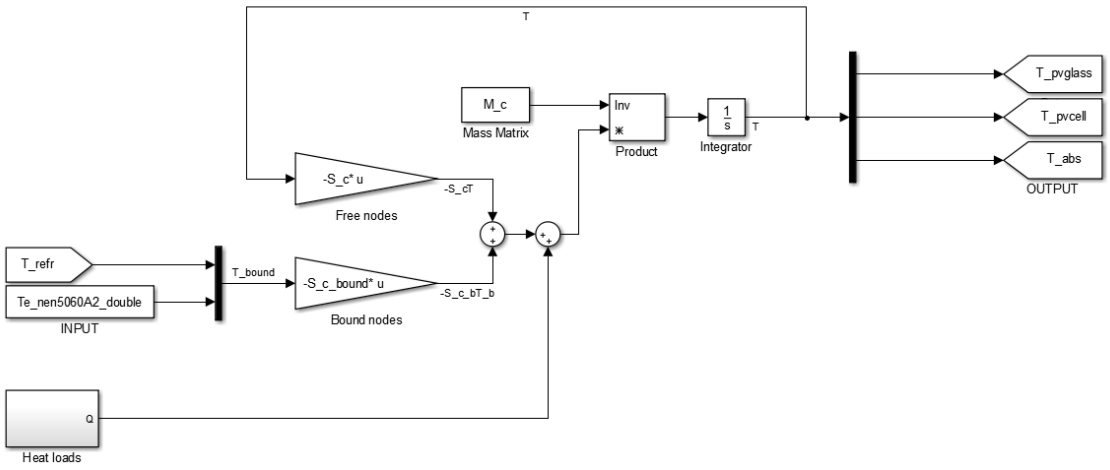

Figure 5-4 Panel model with temperature calculation in MATLAB/Simulink

5.2 Heat pump

The model of the heat pump predicts the functioning of the heat pump and is closely related to the panel model. In this chapter the solar assisted heat pump (SAHP) with refrigerant R134a is simulated. The heat pump provide heat at two different temperatures for hot water and heating of the dwelling and is connected to the storage tank.

5.2.1 Purpose

The purpose of the model is to simulate the functioning of the heat pump in different conditions. Based on the thermodynamic cycle of the refrigerant and the evaporative temperature in the panel, three outputs are predicted, namely the heat capacity Q_c, the electrical input E and the thermal energy extracted from the panel by evaporation Q_e. Two different sets of equations are presented based on the two different condensing temperature suitable for hot water and heating. The aim is to make a model which comes close to the real situation.

5.2.2 System boundaries

The system boundaries of the heat pump are based on the purpose of the model. The heat pump has 2 boundaries, one at the evaporator in the panel and the other at the condenser. The refrigerant works as medium to transport the energy. In the evaporator the refrigerant exchanges heat with the environment. In the condenser it exchanged heat with the water of the heating circuit.

5.2.3 Relevant phenomena

In the model of the heat pump there are four relevant phenomena which are described in paragraph 4.3 and illustrated in Figure 4-4. The two most important ones are the evaporation of the refrigerant in the PV-DX panel and the condensation in the condenser.

5.2.4 Assumptions

An on-off heat pump with constant volume flow is assumed. The mass flow and electrical work of the compressor are not constant. This is based on two interviews with heat pump specialists at Intercool and Carrier. The mass flow is dependent on the density of the satisfied gas entering the compressor. The electrical work is dependent on the mass flow and the delta enthalpy between state 1 and 2 (Figure 4-4).

It is assumed that the expansion valve can manage the pressure in the evaporator and the condenser. The condenser has a pressure which comply with a condensation temperature of 40 and 60 °C. The heat exchange in the condenser at the water side works with an assumed delta T of 5 Kelvin, bringing the water to 35 and 55 °C. Assumed is that there is always a sub-cooling of 5 degrees in the thermodynamic cycle of the refrigerant. The heat pump operates down to -30 °C in the evaporator where it is still able to bring up the pressure in order to condensate at 60 °C.

The efficiency of the compressor and the pressure losses in the system are represented by an efficiency factor of 0,9. Furthermore an isentropic efficiency of 0,65 is used. These factors are assumptions and taken at the safe side in order to get realistic efficiency of the heat pump. With these assumptions an efficiency factor between 0,3 and 0,4 are achieved, as presented in equation (3) which comply realistic state of the art heat pump efficiencies.

5.2.5 Mathematical equations

The mathematical equations to predict the heat pump are based on the thermodynamic cycle of the refrigerant R134a. The thermodynamic cycles are plotted using the program Coolpack and described into detail in Appendix G - Heat pump equations. The equations presented are based on a heat pump with 3 kW thermal capacity in nominal conditions (e.g. water temperature of 7 °C and air temperature of 35 °C or W7A35). This heat pump capacity is set as standard and other capacities are presented in the appendix. In this chapter the equations are subdivided in three parts. The first equations are given to calculate the heat extracted from the evaporator and the temperature of the refrigerant. The second set of equations calculate the heat exchanged to the water circuit in the condenser. Finally the equations to calculate the efficiency of the heat pump are given.

Evaporator and refrigerant temperature

The refrigerant evaporates in the absorber tubes in an endotherm process. The heat transfer in this process is calculated with equation (20). The mass flow is represented by $\dot{m}$ and the enthalpy change between the refrigerant inlet and the outlet of the panel the by $(h_1 - h_4)$. In Figure 4-4 a schematic diagram of the log p-h diagram presents the thermodynamic cycle of the refrigerant R134a. The process of evaporation is between point 4 (inlet panel) and point 1 (outlet panel).

$$\dot{Q}_e = \dot{m} \cdot (h_1 - h_4) \tag{20}$$

The thermodynamic cycles are plotted in Coolpack for different refrigerant temperatures with associated pressures in the evaporator. The thermodynamic cycle is plotted for 14 cycles from minus 30 to plus 30 °C. The condensing temperature is set as constant on 40 °C. The isentropic efficiency is set to 0.65 and the flow rate to 4,3 m³/h which is associated with a 3 kW heat pump. The points are plotted in a graph and a third-power regression line is plotted to follow the points. This results in equation (21) which predicts the heat transfer in the panel as function of the temperature of the refrigerant.

$$\dot{Q}_{e\_40} = 0.0142{T_{refr}}^3 + 1.6521{T_{refr}}^2 + 99.731T_{refr} + 2577 \tag{21}$$

For the hot water in the dwelling a higher condensing temperature is required. The same steps are taken as mentioned above, only the condensing temperature is set to a constant value of 60 °C. The 14 cycles are plotted and the regression line gives the following equation to predict the extracted heat from the panel:

$$\dot{Q}_{e\_60} = 0.0123{T_{refr}}^3 + 1.3948{T_{refr}}^2 + 81.833T_{refr} + 2062 \quad (22)$$

The heat transfer coefficients based on the refrigerant temperature in equation (16) and (20) are in balance based on the first thermodynamic law. The function can be rewritten to equation (23) in order to calculate the temperature of the refrigerant T_{refr}. This temperature is inserted as 'bound node' in the MATLAB/Simulink model of the panel as described in paragraph 5.1

$$T_{refr} = T_{abs,avg} - \frac{\dot{m}\cdot(h_1 - h_4)}{a\cdot A} \quad (23)$$

Using equation (24) and (25) the temperature of the refrigerant is calculated iterative. Two different equations are presented to calculate the T_{refr} when producing 60 and 40 degrees in the condenser.

$$T_{refr} = T_{abs,avg} - \frac{\dot{Q}_{e\_40}}{a\cdot A} \quad (24)$$

$$T_{refr} = T_{abs,avg} - \frac{\dot{Q}_{e\_60}}{a\cdot A} \quad (25)$$

Heating capacity

The heat capacity of the heat pump which supply the energy for the heating and hot water system of the dwelling are respectively represented by the equations (26) and (27). The equations are obtained with the same method described in the previous paragraph. The difference is the delta enthalpy between point 2 and 3 in the thermodynamic cycle. The same mass flow is applicable in this function.

$$\dot{Q}_{c\_40} = 0.009{T_{refr}}^3 + 1.3397{T_{refr}}^2 + 103.74T_{refr} + 3267 \quad (26)$$

$$\dot{Q}_{c\_60} = 0.0081{T_{refr}}^3 + 1.2145{T_{refr}}^2 + 95.191T_{refr} + 3029.1 \quad (27)$$

In the extreme weather conditions the evaporative temperature of the refrigerant drops together with the heat capacity of the heat pump. In these conditions the auxiliary system assist the heat pump in the production of heat for hot water and heating. The capacity of the electrical heater $\dot{Q}_{el\_h}$ is presented in Table 10.1.

Work and efficiency heat pump

The required electrical energy of the heat pump is dependent on the efficiency of the compressor η_{hp}, the heat capacity of the condenser $\dot{Q}_c$ and evaporator $\dot{Q}_e$ at a certain time. This result in equation (28).

$$\dot{W} = \frac{\dot{Q}_c - \dot{Q}_e}{\eta_{hp}} \quad (28)$$

The heat pump efficiency is calculated with the coefficient of performance (COP) and relates to the amount of heat produced compared to an amount of electrical energy required. This gives the following equation:

$$\text{COP} = \frac{\dot{Q}_c}{\dot{W}} \tag{29}$$

In order to determine the actual performance of a system over a complete heating season, the seasonal performance factor (SPF) is introduced. This is a factor of the total electrical energy input that is required to produce an amount of useful energy output (ISSO 744, 2009). This factor includes the heat losses in the tank. High tank losses result in a reduced SPF. The necessary energy involves both the work for the heat pump and the electrical heater.

$$\text{SPF} = \frac{Q_{usefull}}{Q_{necessary}} \tag{30}$$

5.3 Storage buffer tank

The model of the buffer predicts the capacity and temperature of the water in the two buffers. One sensible heat storage tank for hot water and one for heating. The capacity of the buffer can be determined with the volume of the tank, the useful temperature of the water and type of storage (e.g. stratified or mixed). Notice that the capacity has influence on the amount of start/stops of the heat pump and the time the tank can cover for the demand.

5.3.1 Purpose

The purpose of the buffer model is to predict the capacity and the temperature of the two storage tanks for heating and hot water.

5.3.2 System boundaries

The storage tank has 4 boundaries where it exchanges heat. Heat is supplied by the heat pump and electrical heater on one boundary. Heat is extracted from the tank by the input data of the dwellings demand of hot water or heating. A fourth boundary layer is the surface of the tank where the heat transfer from the tank to the environment takes place.

5.3.3 Relevant phenomena

Charging of the tank takes place by the heat pump and electrical heater. When the tank is being charged and at the same time there is a demand, firstly heat is supplied to the dwelling and the remaining heat is used to charge the tank. Charging stops when the temperature in the tank reaches the max temperature limit.

Discharging of the tank takes place when there is a heat demand. The tank will be discharged until it drops below a certain temperature level. After that the tank will be loaded again. The charging and discharging in the heating tank happens direct with the same medium. In the tank for hot water a spiral heat exchanger is applied. The final relevant phenomena is the heat transfer through the surface of the tank.

5.3.4 Assumptions

The tank for hot water is a stratified tank with an thermocline factor $f_{thermocline}$. This factor represents the thermal barrier between the cold and warm region which is mixed and unusable for hot water. The storage tank for heating is assumed to be fully mixed.

Heat loss through the surface of the tank is taken as average temperature of the tank and the heat of the outer surface of the tanks is constant 20 °C. The heat transfer coefficient of the insulation of the tank is presented in Table 10.1.

5.3.5 Mathematical equations

The volume of the cylindrical tank is calculated by multiplying the surface of circular section of the tank with the height of the tank. The volume of the tank are bound parameters which are set in Table 10.1.

$$V_{tank} = \frac{1}{4} \cdot \pi \cdot {D_{tank}}^2 \cdot h_{tank} \tag{31}$$

The surface of the tank is calculated with equation (32).

$$A_{tank} = 2 \cdot \left(\frac{1}{4} \cdot \pi \cdot {D_{tank}}^2\right) + \pi \cdot D_{tank} \cdot h_{tank} \tag{32}$$

Heating

The buffer content of the heating tank is calculated with equation (33). In the equation the minimal supply temperature, which defines the useful energy, is represented by $T_{supplymin}$. Useful means that the temperature of the water remains at a level suitable to supply a low temperature heating system. The upper temperature limit of the tank is set by $T_{upperlimit}$. The tank is assumed to be fully mixed.

$$Q_{buffercontent\_h} = V_{tank} \cdot c_p \cdot \left(T_{water} - T_{supplymin}\right) \tag{33}$$

Hot water

The buffer content for hot water differs from the equation for the heating buffer tank. The hot water tank is stratified with a thermocline factor $f_{thermocline}$.

$$Q_{buffercontent\_hw} = V_{tank} \cdot c_p \cdot (T_{water} - T_{coldwater}) \cdot (1 - f_{thermocline}) \tag{34}$$

The losses due to the conductive heat transfer can be calculated with equation (35) for both the heating and hot water tank. The surface area of the tank A_{tank} is calculated with equation (32). The heat transfer coefficient is represented by the lambda λ and the thickness d of the insulation material.

$$\dot{Q}_{tank\_losses} = \frac{\lambda}{d} \cdot A_{tank} \cdot (T_{tank} - 20°C) \tag{35}$$

The average temperature of the water in the tank can be calculated with equation (36).

$$\underline{T}(t) = M^{-1} \int_0^t \left(\underline{Q} - S\underline{T}\right) dt \tag{36}$$

5.3.6 Initial conditions

In initial conditions the buffer tanks are fully charged. For the hot water buffer the tank is set to 55 °C and for the heating tank to 35 °C.

5.4 Demand input

The fourth part of the model is the demand of the dwelling for heating and hot water. The demand is used as input in the model. The heating demand is calculated using software model of DesignBuilder where an annual simulation of a NoM renovated dwelling in Dutch climate is performed. The hot water demand is based on a family household according to NEN7120 class 3. The daily tap pattern is extracted from literature.

Heating demand Design Builder

The heat load of the NoM renovated dwelling is calculated with the software program DesignBuilder 4.6 with the computing core EnergyPlus 8.3. The user interface of DesignBuilder allows to draw the building in 3D, to specify the components and to fill in the use and installations of the zones. With a simulation the data is transferred into an input data file for EnergyPlus, which makes the calculations. The results are presented in clear information in DesignBuilder. The dynamic simulation requires hourly values of the outside temperature and radiation of the Dutch climate. In the simulation the climate data conform NEN 5060:2009 attachment A2 is used which is designed for energetic calculation of buildings in the Netherlands.

An overview of the inserted specifications of the dwelling is presented in Figure 3-6 and detailed output values of the simulation are presented in Appendix D – DesignBuilder model. Figure 5-8 shows the annual heating demand of 10 GJ where Figure 5-5 and Figure 5-6 shows the heat demand profile during the year. The maximum heat demand in the dwelling is 2,0 kW and occurred in the coldest night from 8 to 9 January.

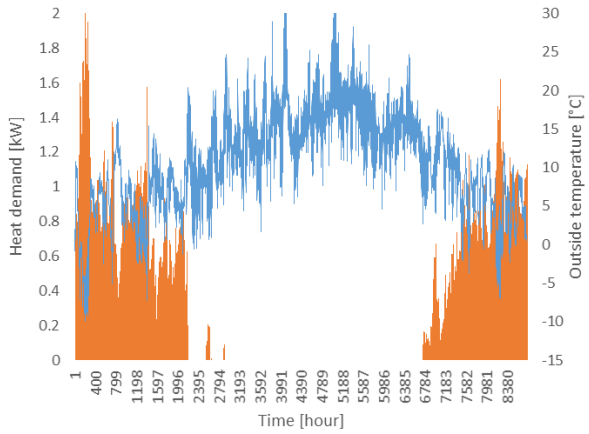

Figure 5-5 Output DesignBuilder simulation heat demand

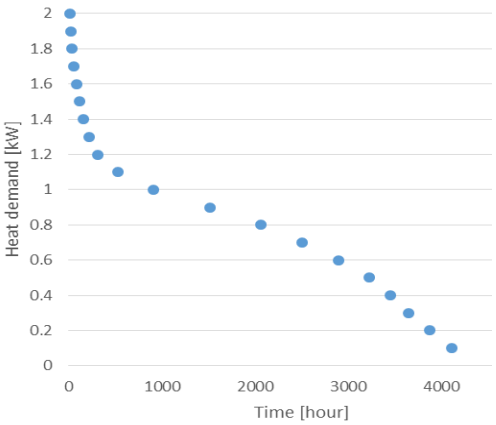

Figure 5-6 Heat demand profile 'belastingduurcurve'

Hot water

The hot water demand is calculated for the dwelling according to class 3 of the NEN7120 with an annual heat demand of 11,6 GJ. The daily heat demand is 8,85 kWh which comply with 250 litre hot water of 40 degrees per day. The hourly hot water draw is presented in Figure 5-7.

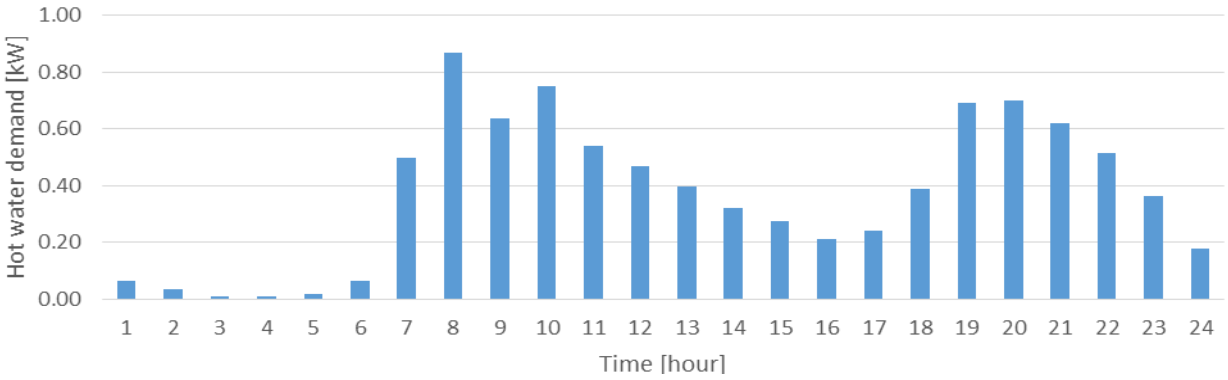

Figure 5-7 Hot water draw pattern as input of the model (Friedel et al., 2014)

Depending on the season the heat pump should deliver the heat demand for both hot water and heating. In the Figure 5-9 the heat demand for a day in three different seasons in the Netherlands are presented. The total yearly demand for heating and hot water is shown in Figure 5-8.

5.5 Control strategy

The control of the ENergy Roof is crucial for the functioning of the installations. The purpose of the control system is to provide in all cases the heating and hot water demand of the dwelling. This should be achieved with a minimal yearly primary energy consumption.

The control strategy is considered for different components, namely the heat pump, the electrical heater and both the buffer tanks. The input values which influence the control output are: the heat demand for heating and hot water, the temperatures of the TT sensors in the heating and hot

water buffer and the heat capacity of the heat pump. Important set points are the minimal and maximal temperatures in the heating and hot water tank.

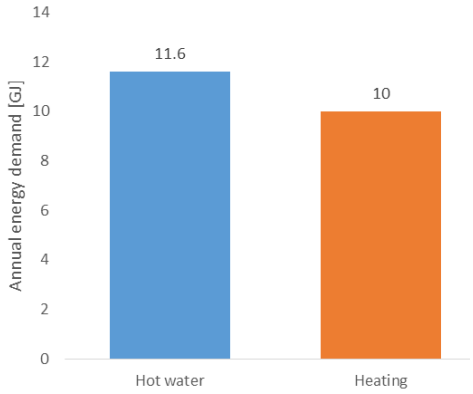

Figure 5-8 Annual demand of the dwelling

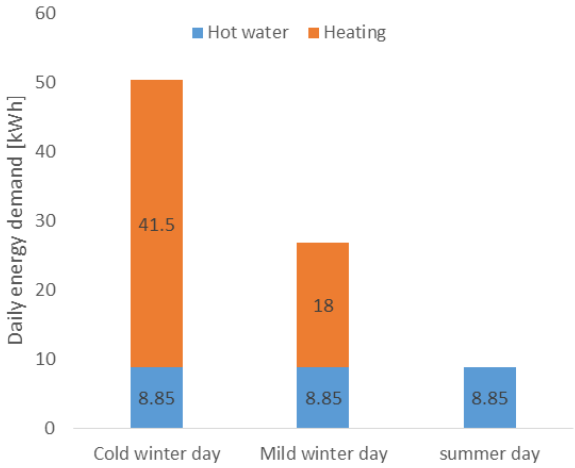

Figure 5-9 Comparison daily heat demand in different seasons

5.5.1 Heat pump

The aim of the heat pump is to provide in the heat demand and to charge the storage tanks. The generation of hot water has priority on top of the generation of heating. The heat pump has an on/off control function and can generate two different temperatures for the heating and hot water system. Notice that the heat pump has to choose which system it will provide. The heat capacity of the heat pump depends on the evaporative temperature of the refrigerant as described in paragraph 5.2.5.

The heat pump switches on when there is a heat demand which cannot be provided with the buffer. Firstly, the heat pump provides the demand and the remaining energy is used to charge the buffer. The heat pump will switch off when the buffer is fully reached.

5.5.2 Electrical heating

The electrical heater functions as a back-up system for the heat pump. If in certain conditions the heat capacity of the heat pump is not sufficient to provide in the demands of the dwelling, the electrical heater will start. In that case both systems are active. The electrical heater will switch of together with the heat pump when the buffer is fully charged.

5.5.3 Storage tanks

The storage tanks can be charged and discharged. Charging is done by the heat pump and electrical heater. Discharging happens while supplying the demand of the dwelling. Heat losses through the surface of the tank are also included. The heat demand is firstly provided with the storage tank and when the temperature drops below an under limit, the heating system switches on.

6. Analysis results

The models of the previous chapter are connected and result in the ENergy Roof system. Simulations are performed for the climate conditions of the Netherlands over a period of one year in hourly output data. The model is run with variable input parameters and the results are presented in this chapter. These variables include the heat pump capacity, the surface of the PV-DX panel, the orientation and inclination of the panel and the storage capacities. First the basic configuration of the PV-DX surface area, heat pump and buffer content are statically calculated.

6.1 Basic configuration

In this paragraph the minimal surface area of the PV-DX panel is calculated for a typical heat pump capacity. This is a steady state balance calculation in the worst case condition (e.g. winter night). In the second part the minimal buffer content is calculated based on the heat demand profile of the dwelling.

6.1.1 Minimal surface area PV-DX panel

A SAHP requires a minimal PV-DX surface area in order to be able to extract enough heat from the evaporator and not drop below the operation temperature limit of -30 °C. The minimal surface area is calculated for a 3 kW heat pump with refrigerant R134a which has a lower evaporative temperature limit of -30 °C.

The relevant phenomena on the panel are the free and forced convection, radiation due to incoming long wave radiation and black-body radiation from the panel to the sky. Since it is night there is no irradiation from the sun. Notice that for this calculation the orientation of the dwelling is not of influence. The heat resistance within the panel is very small and thereby neglected in this calculation. Snow, shadow and ice formation are also not taken into account.

The parameters in this condition are ambient temperature of -15 °C, wind speed of 1 m/s (leeward), incoming long wave radiation of 180 W/m² (NEN5060) and solar irradiation of 0 W/m². With these parameters and equations (37), and (38) the heat gain of the panel can be calculated.

$$q_{wind} = (1 + f_{wind}) \cdot (1.3w + 8.3) \quad (37)$$

$$q_{rad} = F_{sky} \cdot (LW_{in} - \varepsilon\sigma {T_{abs}}^4) \quad (38)$$

Equation (21) gives the evaporative capacity $\dot{Q}_{e\_40}$ of the 3 kW heat pump for the refrigerant temperature T_{refr} of -30 °C. The temperature of the panel T_{panel} can be calculated with equation (39) using the heat transfer coefficient between the refrigerant and the absorber panel.

$$T_{panel} = T_{refr} + \frac{\dot{Q}_{e\_40}}{a_{abs\_refr}} \quad (39)$$

The surface area of the PV-DX is based on a balance between the heat taken from the panel by the refrigerant and the heat received from the environment. With equation (40) the surface area of the panel is calculated.

$$A_{PV-DX} = \frac{\dot{Q}_{e\_40}}{q_{wind}+q_{rad}} \quad (40)$$

Using the aforementioned parameters and equations this result in a minimal surface area for a 3 kW heat pump of 6 m². The thermal heat capacity of the heat pump in these conditions is 1,1 kW. The same calculation are executed for a 4 and 5 kW heat pump where the results are presented in Figure 6-1. It can be seen that for every added kW nominal heat pump capacity an extra surface area of 4 m² is required. Also the heat capacity of the heat pump increases linear with 400W thermal capacity per added kW nominal capacity.

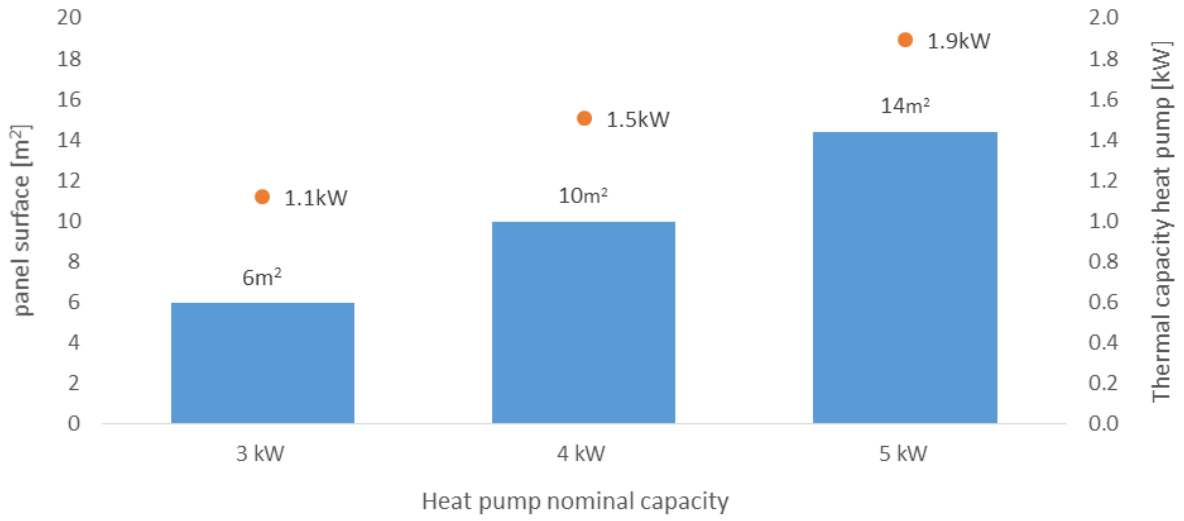

Figure 6-1 Evaporator surface and thermal capacity for different nominal heat pump capacities

In this winter conditions the highest heat demand of the dwelling is 2 kW as described in paragraph 5.4. The 3 kW heat pump delivers 1,1 kW of heat in the winter night condition. The heat pump of 5 kW can almost deliver the demand by producing 1.9 kW of heat. But the disadvantage of a larger heat pump is that it requires more surface area and has an over capacity during a large time of the year.

In order to make the system more robust an electrical heater can be added to the system which will function as back-up heater in times the heat pump cannot deliver the heat demand. These peaks in demand only occur a few hours per year (Figure 5-6). In this case a smaller heat pump will be more interesting in terms of investment cost and required surface area on the roof.

Adding more square metres of PV-DX will increase the capacity of the heat pump, where more heat will be captured from the environment which result in a higher temperature. Also the SCOP of the heat pump will improve by the addition of surface area.

Conclusion

Both the 3 and 4 kW heat pump cannot provide the heating during the peak demand, the 5 kW can almost. The peak demand does not occur that much in the Netherlands, so a 5 kW heat pump is over dimensioned for a large part of the year and has a higher investment cost than a 3 kW heat pump with an electrical back-up heater. Conversely a high capacity heat pump has a shorter loading time of the buffer tanks and add more comfort for showering (e.g. longer shower time). The addition of a 2 kW electrical heater makes the 3 kW heat pump feasible and has the lowest required surface area and investment costs, for that reason this system is set as a standard. Annual simulations with various configurations show the performance and annual electrical demand of each system and are presented in Table 6.1.

6.1.2 Minimal buffer content

The minimal buffer content has to be determined for two systems, the heating and the hot water system. The content of the heating system is based on the condition of maximum amount of start stops. The hot water buffer content has to meet two conditions. The first is the minimal shower time and the second is the capacity to store the heat for a certain time period. Both buffer contents are calculated below.

Heating buffer content

High frequency of start/stops cycles will decrease the lifetime of a heat pump. A thermal buffer in the heating system can avoid this behaviour. According to Van Krevel (2000) the amount of start/stops should be above every 20 minutes or below 3 times per hour. The minimal buffer content can be calculated with the heat demand of a winter day. On 8 January the total demand is 41 kWh (150 MJ). The amount of start/stops of the heat pump should be below the limiting value. This results in a minimal heating content $Q_{min\_content}$ in equation (41).

$$Q_{h\_min\_content} = \frac{Q_{heating\_8jan}}{x_{on/off\_hour} \cdot 24} \tag{41}$$

This results in a minimal content of 0,71 kWh. As mentioned in paragraph 5.4 the heating storage tank is fully mixed with a useful temperature range of 23 to 35 °C. With this configuration a volume of 50 litres is required. Taking into account a safety factor, the heat losses of the tank and the operation of the heat pump for hot water, a volume of 100 litres (1,63 kWh) is taken as basic buffer. A day-night storage requires 1400 litres based on 20 kWh summed heating demand during the night. This is practically (e.g. necessary space in the dwelling) and financially not feasible for a NoM renovation. Therefore the 100 litres tank is set as standard configuration.

Hot water buffer content

The hot water content can be calculated with a minimal time of showering which should be provided by the tank. Since the heat capacity of showering (15-18 kW) is much higher than can be delivered by a heat pump, a buffer is required to deliver this. The heat capacity of the shower $\dot{Q}_{shower}$ can be calculated with equation (42). In this equation v_{shower} represents the flow rate in litres per minute of 40 °C water, which is assumed to be 6,7 litres per minute as described in paragraph 3.3. The specific heat capacity of water is represented by $c_{p,water}$. The delta T is the temperature difference between the cold water of 10 °C and the showering water of 40 °C.

$$\dot{Q}_{shower} = v_{shower} \cdot c_{p,water} \cdot \Delta T \tag{42}$$

The minimal content can be calculated for a certain time per day the shower is used, represented by t_{shower} in hours. Notice that the minimal content is calculated where only the heat from the buffer is used, the heat pump and electrical heater are off.

$$Q_{\text{hw\_min}\_content} = \dot{Q}_{shower} \cdot t_{shower} \tag{43}$$

For a shower time of 25 minutes a buffer is required with a content of 6 kWh. In chapter 5.3 one may read that the buffer is stratified and with equation (33) the volume of the tank can be calculated. A volume of 150 litres with 6,27 kWh heat content is selected.

The second condition is the storage time of the buffer for a typical draw-off pattern. According to NEN7120 a family household require 8,85 kWh per day, storing this requires a volume of 212 litres. Storing the heat during non-solar hours from approximately 4 p.m. until the next day 10 a.m. requires 5,88 kWh. This can be delivered by a fully loaded tank of 150 litres. Therefore this volume is set as standard for the model.

6.2 Variations analysis

The ENergy Roof is simulated with variable inputs in order to present the technical feasibility of the different configurations. These variables include the heat pump capacity, the surface of the PV-DX panel, the orientation and inclination of the panel and the storage capacities.

6.2.1 PV-DX area and heat pump capacity

In annual simulations eight different system configurations of the ENergy Roof with varying heat pump and PV-DX are tested. All the systems provide in the heating and hot water demand of the dwelling. In Table 6.1 and Figure 6-2 the annual electrical energy consumption of these eight different systems are presented.

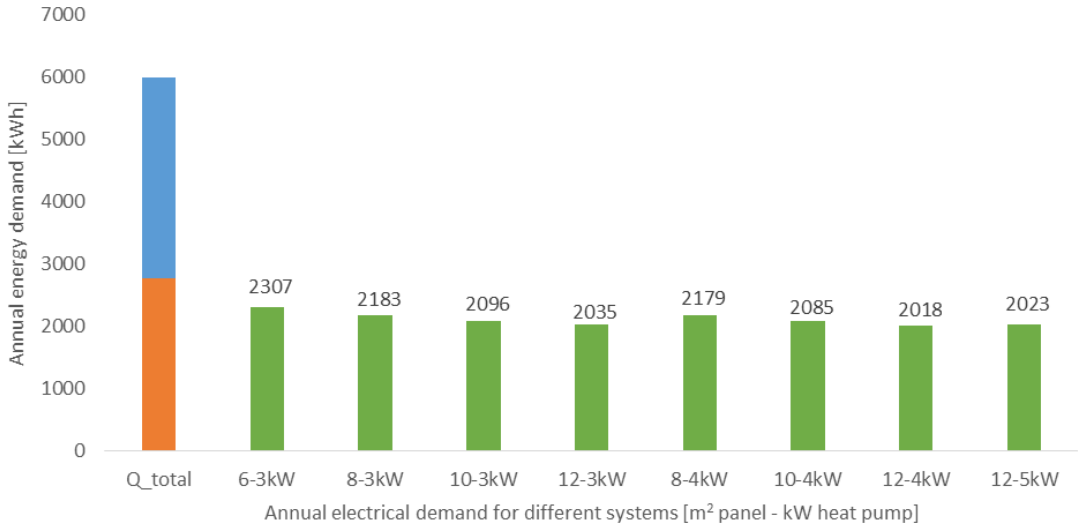

Figure 6-2 Annual electrical demand for different system configurations surface area panel and heat pump capacity

In Table 6.1 also the SCOP and the electricity produced by the PV-DX panels are presented. The feasibility of the ENergy Roof also depends on the total generated electrical energy in order to become NoM. The electrical energy demand is based on the calculations in paragraph 3.3 which show an annual demand of 3120 kWh electrical energy based on 2500 kWh for appliances, 400 kWh for lighting and 220 kWh for ventilation. This is the electrical energy demand of a NoM renovated dwelling excluding the annual demand for heating and hot water. The dwelling has a total roof area on one side of 34 m² where a part is covered by PV-DX and the other by PV. The net electrical energy produced on this side show if extra surface area is required on the other side of the roof in order to become NoM. The calculations are based on the solar irradiation file of NEN5060.

For all the systems NoM can be achieved. The dwellings with an East-West orientation require additional PV panels on the other side of the roof varying between 0,9 and 3,3 m² in different system configurations. The South orientation does not require extra PV on the other side. The total installed PV capacity is between the 5,5 and 6 kWp.

Table 6.1 Variation model output

Configurations [m²-kW]	El. demand installations [kWh/a]	Total el. demand [kWh/a]	SCOP	PV-DX [m²]	PV [m²]	Net el. East [kWh/a]	PV extra [m²]
6-3kW	2307	5427	2.6	6	28	-403	3.3
8-3kW	2183	5303	2.7	8	26	-279	2.3
10-3kW	2096	5216	2.9	10	24	-191	1.6
12-3kW	2035	5155	2.9	12	22	-130	1.1
8-4kW	2179	5299	2.8	8	26	-275	2.3
10-4kW	2085	5205	2.9	10	24	-181	1.5
12-4kW	2018	5138	3.0	12	22	-114	0.9
12-5kW	2023	5143	3.0	12	22	-119	1.0
6-3kW (S)	2284	5404	2.6	6	28	+146 (S)	-

6.2.2 Influence surface area PV-DX

In the figure below four systems are plotted which show the effect of the increased surface area of a 3 kW PV-DX SAHP. Adding two square metres of surface area from the standard 6 m² the SCOP of the heat pump increases with 5,2%. The performance increases up to 12,8% when applying 12 m² of PV-DX panel for the 3 kW heat pump.

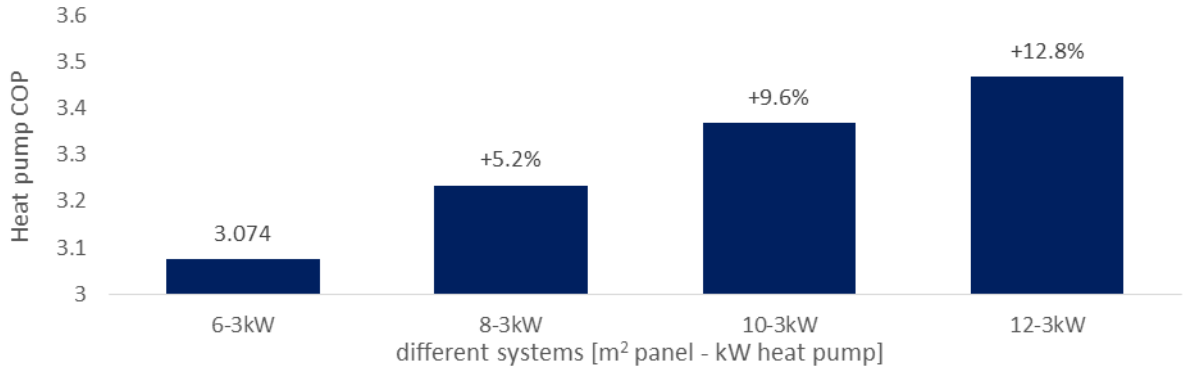

Figure 6-3 Improved SCOP of a 3 KW heat pump with increasing PV-DX surface area

6.2.3 Influence of the orientation

In this part the effect of the orientation of the roof is analysed. The standard orientation of the PV-DX is set to East. This is the worst orientation of the dwelling in which the PV-DX system should still work. The North and West roofs are not calculated because the ENergy Roof is positioned on the other side of the roof. The optimal orientation is South. The solar irradiation has the most influence on the output of the model. Mainly the produced electricity increases and the SCOP of the heat pump improves a little from 3,07 to 3,10 (Figure 6-4).

The inclination of the roof has minimal effect the performance of the system. The standard inclination is set to 30 degrees. Changing the inclination to 45 degrees the solar irradiation is reduced together with the annual produced electricity from 897 kWh to 872 kWh. The SCOP of the heat pump remain about constant.

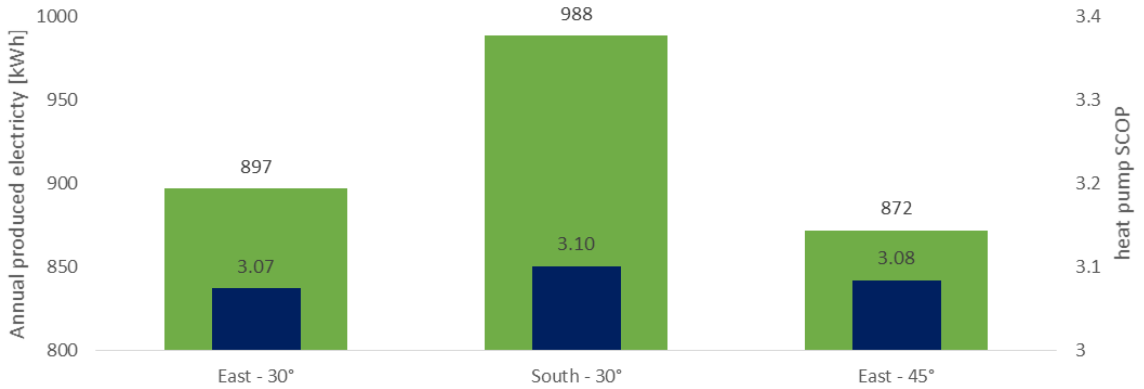

Figure 6-4 Annual electrical demand for hot water and heating (green) and SCOP of the heat pump (blue)

6.2.4 Increased storage capacity

The system may be improved by enlarging the storage capacity and connecting it with a 'smart' control which operates during optimal-hours. This is based on the fact that the heat pump has higher efficiency and capacities during solar hours where high evaporative temperatures are achieved. The standard heating storage tank has 100 litres. A simulation is done with an increased volume of 300 and 500 litres. The ideal volume would be 1400 litres in order to have a complete day-night storage, but due to limited space in the dwelling this volume is not taken into consideration.

The different volumes of the tanks are applied in the simulation of a 3 kW with 6 m² PV-DX SAHP. The control strategy remains the same where the tanks are charged when they are empty. Due to time limitation there is no smart control applied in the model. Due to the higher capacity of the storage tank the number of on/off switches of the heat pump reduces with more than 50% of a volume of 500 litres compared to 100 litres (Figure 6-5). On the other hand the annual heat losses of the system grow with 450% from 111 to 509 kWh annual. This result in an increased annual electrical consumption of the ENergy Roof system with 152 kWh or 7% from 2307 to 2459 kWh per year.

With a smart control it is expected that the annual electricity consumption will reduce due to higher efficiency of the heat pump. The above numbers show that the electrical demand of the system should be reduced with minimal 152 kWh in order to be interesting.

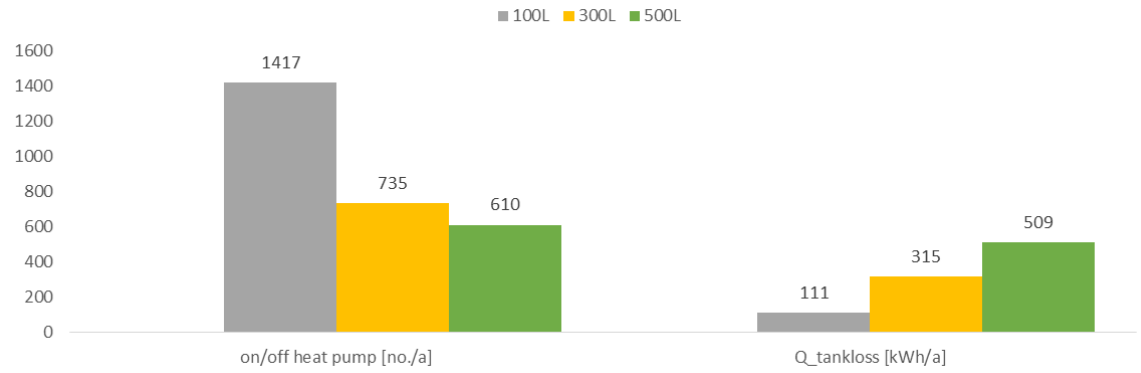

Figure 6-5 Annual simulation of 3 kW - 6 m² SAHP with different heating storage volumes

6.3 Winter and summer season

In the changing seasons of the Netherlands the PV-DX SAHP operates differently. In this paragraph more detailed data is presented of the functioning of the 3 kW with 6 m² PV-DX SAHP. Figure 6-6 show the on/off operation of the heat pump for heating hp_h and hot water hp_hw and the operation of the electrical heater el_h. The figure show a two day simulation during the winter season and present the temperature of the absorber T_abs (green). It can be seen that the line fluctuates with the operation of the heat pump and drops when the heat pump switches on. It also

follows the temperature T_e (blue) and show highest temperatures during the day when there is solar irradiation. The temperature of the absorber remain almost all the time below zero.

The dotted blue line T_e-10 represent the absorber temperature of an ASHP. This allow a comparison between the ASHP (dotted blue) and the SAHP (green). Absorber temperatures above the dotted line comply with higher heat pump efficiencies, where temperatures below the dotted line comply with lower efficiencies. It can be seen that the absorber temperatures of the SAHP are higher during the day and lower during the night compared to the ASHP.

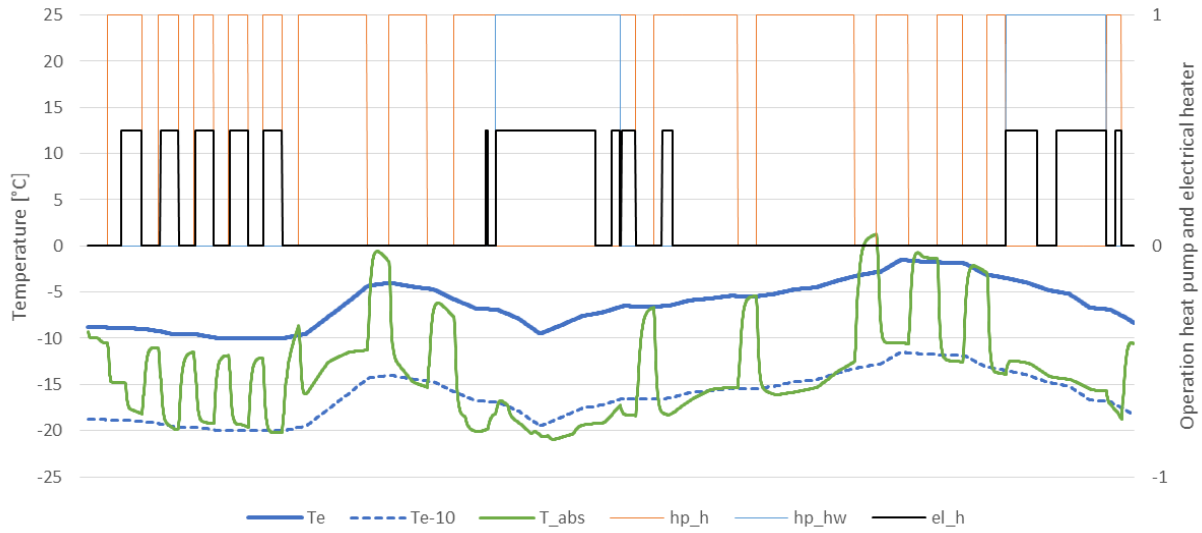

Figure 6-6 Winter simulation on 8 and 9 January of a 3 kW SAHP with 6 m² PV-DX

The same two-day simulations are performed in the mid-season and in the summer. The three different seasons are presented in Figure 6-7 and give insight in the operation of the ENergy Roof. The figure show clearly the highest operation time of electrical heater during the winter, low frequency in the mid-season and no operation during the summer. In the winter the electrical heater mainly switches on when the heat pump generates hot water. The heat pump only produces hot water during the summer where in the winter and mid-season the heat pump also supply the heating demand. The heat pump also show long operation time in the winter.

Due to higher absorber temperatures together with higher heat pump capacities it takes a shorter period to load the hot water tank in the summer than in the winter. In the winter day the hot water tank is charged during the night and takes 6 hours. In the mid-season days the average is 3 hours and 40 minutes and in the summer during the day it takes less than 2 hours.

In the winter the heat pump is mainly in operation for the heating hp_h. The time between two cycles is between 45 minutes and 1 hour and 15 minutes in the winter. During the mid-season these time may allow the ice on the panel to melt. Absorber temperature in the summer of 42 °C is reached.

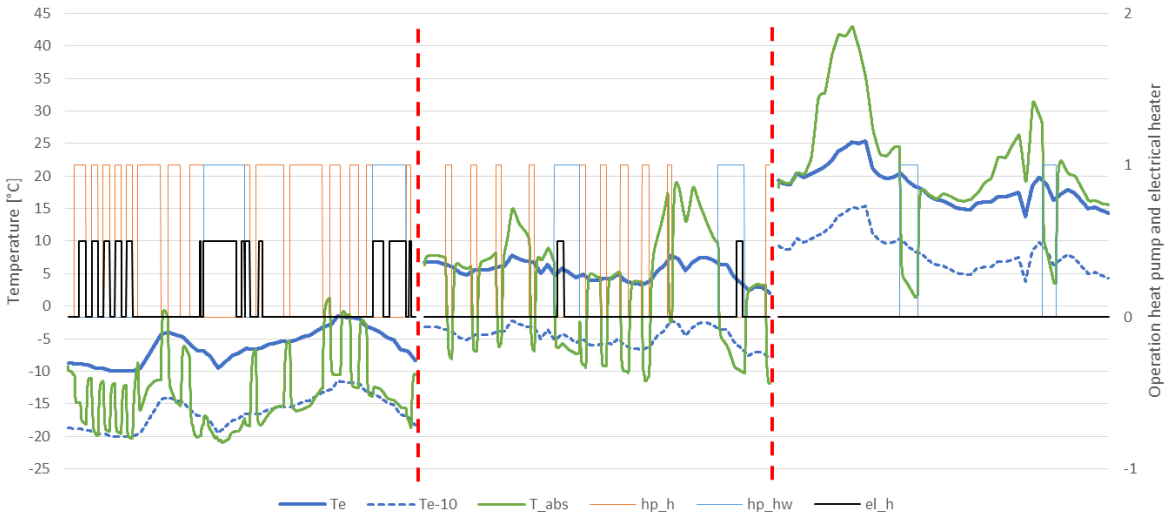

Figure 6-7 Simulation in three seasons from left to right: winter (8-9 January), mid-season (21-22 March) and summer (21-22 June)

6.4 Ice formation

In the model the phenomena of ice formation on the PV-DX panel is not simulated. It is expected that the ice formation may lead to problems for the heat transfer of the panel and the safety of the ENergy Roof because of the risk of ice falling down. Therefore the ice-formation risk time of the PV-DX panel is mapped. Ice formation can only occur when the temperature of the absorber T_abs is below 0 °C. This happens 1878 hours per year or 21% of the time. It is expected that ice will not directly form at 0 °C panel temperature, but at temperatures lower than – 5 °C. This occurs 768 hours per year or 9% and in the coldest month January this occurs 42% of the time.

The amount of hours that the panel has a risk of ice formation are illustrated per month is Figure 6-8. A distinction is made between the hours the outside temperature is below (blue) and above zero (red) for panel temperatures below zero. Outside temperatures above zero degrees have a higher risk of freezing on the panel due to the higher water content in the air. The months November until March have a high risk of ice formation and the month January has the highest risk percentage of 59%.

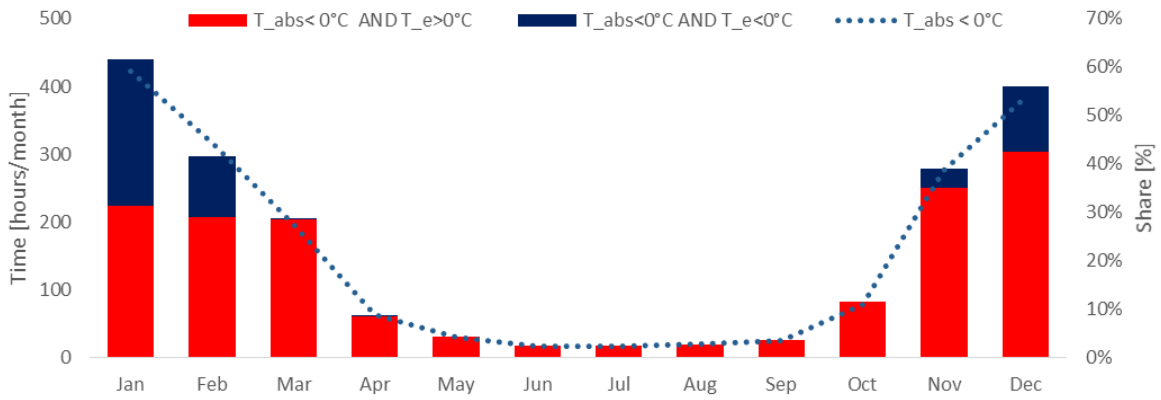

Figure 6-8 Risk of ice formation on the PV-DX panel (T_abs)

7. Financial and concept design

In this chapter the step is made towards a first concept design of the ENergy Roof together with the financial feasibility. The components of the ENergy Roof are selected based on the simulations and analysis from the previous chapters. A concept design is presented in drawings from the building scale to the installation scale. In the second part the investment costs for the ENergy Roof are presented and the financial feasibility is discussed.

7.1 Concept design

The simulation show that the NoM renovation with ENergy Roof is feasible and in this paragraph the spatial consequences of a renovation are presented starting on a large scale and ending on a small scale of the component integration in the installation-BOX. Furthermore the heat resistance in combination with the installation-BOX and construction of the ENergy Roof is calculated. Finally an indoor impression illustrates the spatial quality of the ENergy Roof with the integrated installation-BOX improving the attic of the dwelling.

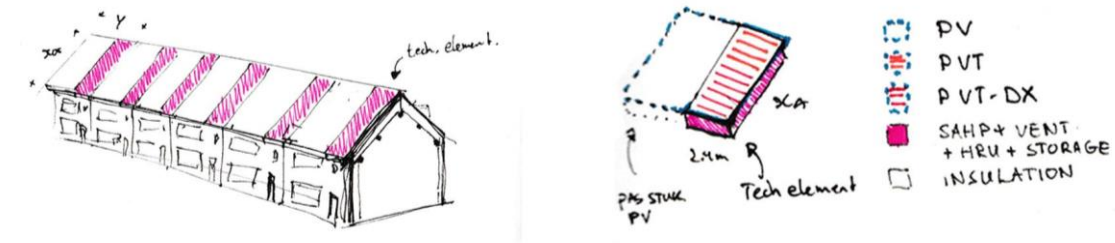

Figure 7-1 Sketch of the ENergy Roof applied on a total row of dwellings with the technical element highlighted

7.1.1 NoM renovation

The NoM renovation includes a new skin on top of the existing dwelling. In Figure 7-2 the components of a renovation are presented by number 1 till 7 where the blue elements are part of the ENergy Roof. The existing dwelling is illustrated with the black colour and elements A till C. The renovation includes new façade elements (1) with good thermal resistance and new window frames with glazing. An insulation layer is added under the ground floor (2). The existing roof and roof tiles are removed from the existing dwelling, where the wooden purlins (C) are preserved. On top of these purlins the new insulated roof panels (3) are placed where there is an option to add a new dormer window (4) on the low-solar side of the roof (e.g. North or West). The ENergy Roof includes a new roof on the high-solar side of the roof and can be subdivided in three parts. The first part is the technical roof element with PV-DX panels (5), the second part is the roof element with normal building integrated PV panels (6) and the final part is the installation BOX (7). All the roof elements have good thermal insulation with an R_c-value of 6.

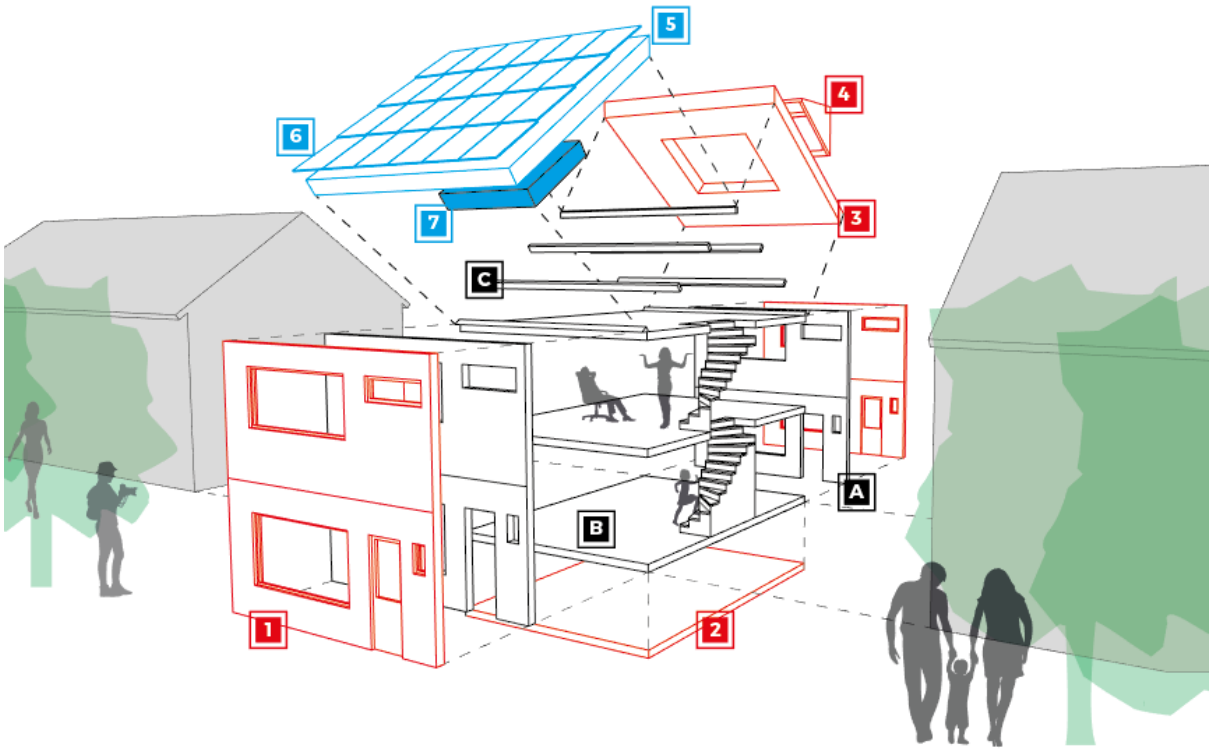

Figure 7-2 Exploded view of the existing dwelling (black) with NoM renovation (red) and ENergy Roof (blue)

7.1.2 Heat resistance of the roof

The technical roof element (5) has the installation box incorporated into the roof, resulting in a lower thickness of the insulation. In order to reach an average heat resistance of the ENergy Roof of 6 m²K/W the other elements (6) should compensate this with a higher R_c-value. In the heat resistance calculations only one direction of heat flow is considered (Van der Linden, Erdtsieck, Kuijpers - Van Gaalen, & Zeegers, 2006). Two scenarios with different insulation thicknesses are presented in Table 7.1.

Table 7.1 Scenario's for the integration of the installation box in the ENergy Roof

Scenario	1	2
Roof element	200 mm glass wool Rc 6,2 m2K/W	220 mm glass wool Rc 6,8 m2K/W
Technical roof element	120 mm PIR (at installation box) Rc 5,8 m2K/W	50 mm PIR (at installation box) Rc 4,7 m2K/W
Average roof	220 mm thickness Rc 6,0 m2K/W	240 mm thickness Rc 6,0 m2K/W
Installation Box	310 mm extend into the room 77% extends out the roof	220 mm extend into the room 55% extends out the roof
Total height (incl. solar system)	380 mm	400 mm

The more the installation box is incorporated into the roof, the less space there is to place high performing insulation (e.g. PIR). The advantage is that a smaller part of the box extends into the attic space, but the disadvantage is a lower heat resistance of the roof. Table 7.1 show two scenario's where in the first scenario the total roof thickness is 380 mm and the installation-BOX

extends 77% into the room. The second scenario has a roof thickness of 400 mm and 55% of the installation-BOX extends into the room. A choice is made for scenario 2 because of the spatial and aesthetical quality. Thereby an increased roof thickness of 20 mm is acceptable. In Figure 7-3 the roof is presented with the installation-BOX.

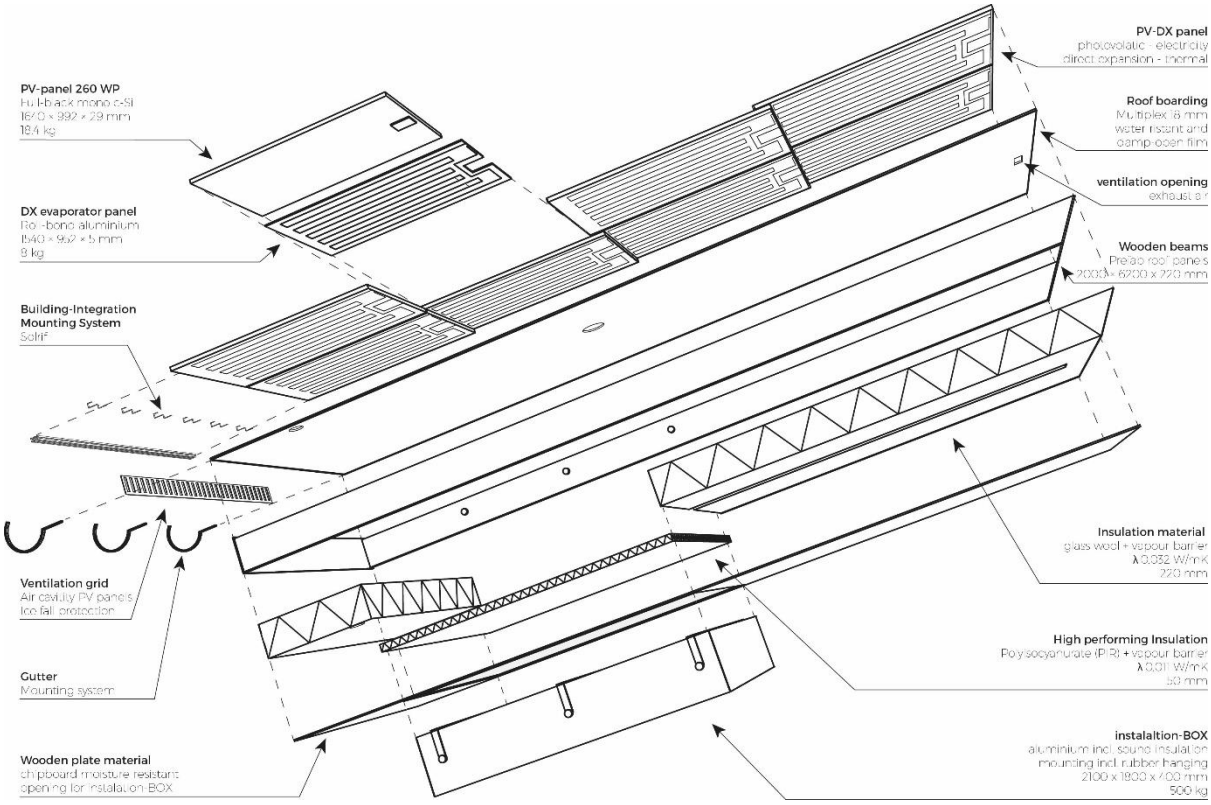

Figure 7-3 Exploded view of the technical element of the ENergy Roof (nog aan te passen + ventilation)

7.1.3 Construction of the roof

Since the existing wooden purlins of the dwelling are preserved, it should be calculated if the construction is strong enough to bear the new ENergy Roof. The purlins span horizontally between the two structural walls (Figure 7-2). The weight of the components of the ENergy Roof are summed and compared to the old roof in Table 7.2. The total weight is calculated for a surface of 32 m^2 for the old roof and 34 m^2 for the new roof since it has an extension. The weight of the insulation is neglected. The weight of the new roof is decreased with 15%. This was not expected since an installation box of 500 kg was added to the construction (Table 7.3). However replacing the heavy roof tiles with solar panels decrease the total weight drastically. Looking at the total weight of the new roof one may conclude that the existing purlin construction is sufficient to bear the new roof.

Comparing only the technical roof element of the new roof with the same surface area of the old roof, the weight is increased with 45% from 510 to 740 kg. In some situations a purlin has the be removed in order to place the installation box, in these cases the purlin has to be reinforced.

Table 7.2 Weight of the old and new roof

	Old roof	New roof
Roof tiles	41 kg/m²	-
Solar panels	-	11,4 kg/m²
Wooden roof plate	5,5 kg/m²	5,5 kg/m²
Wooden beam	-	3 x 55 kg
Installation box	-	500 kg
	1480 kg (46,5 kg/m²)	**1240 kg (36,5 kg/m²)**

The wooden beam of the technical roof is calculated with the rule of thumb which states that the height of the beam is 1/20 of the span length (Jellema, 2013). Assuming minimal one purlin between the roof-ridge and the lower purlin, the span is 2,75 metre. This result in a minimal beam height of 140 mm, the panels have a beam with a height of 220 mm which is sufficient (Table 7.1). The width is 1/4 of the height resulting in 50 mm (Jellema, 2013). The construction of the wooden beams are presented in Figure 7-3.

7.1.4 Installation-BOX

Different options for the integration of the installations into the ENergy Roof are possible. Three options are researched: (1) all the installations in the roof, (2) the important installations in the roof and the remaining behind the knee wall or (3) all the installations behind the knee wall. For the configuration of components which follow from the simulations (Table 7.3), a choice is made for the first option where all the installations are integrated in the roof. There are no restrictions from construction and thermal insulation point of view. The installation-BOX with the components are illustrated in Figure 7-4.

Table 7.3 Weight of the main components in the installation-BOX

Components	Weight	Specification
Heat pump	30 kg	3 kW capacity in nominal condition
Water tanks	350 kg	Hot water (150L), heating (100L) and drain down (30L)
Ventilation box	40 kg	Two vans and heat recovery unit
Inverter	30 kg	Operation up to 5 kW
Small materials	50 kg	Aluminium casing, pipes, valves and water pump
	500 kg	

Thereby the first option give some important advantages such as the possibility to produce the complete technical element including the installation-BOX in a factory. The factory is a clean and

protective environment with the required space and tools where the heat pump can be firmly coupled with PV-DX panels and filled with refrigerant. If the heat pump is not integrated in the roof, the coupling and filling has to be done on site which bring risks and is more costly. In addition the advantage of the roof integration is the short construction time (e.g. one-day-renovation) on the building site and cost reducing due to mass production.

The second option is more interesting if the ENergy Roof is equipped with larger tanks for more comfort or larger storage capacities (e.g. 1400 litre heating tank for day-night storage). In this configuration the water tanks can be installed behind the knee wall. The heat pump and ventilation unit are integrated in the roof.

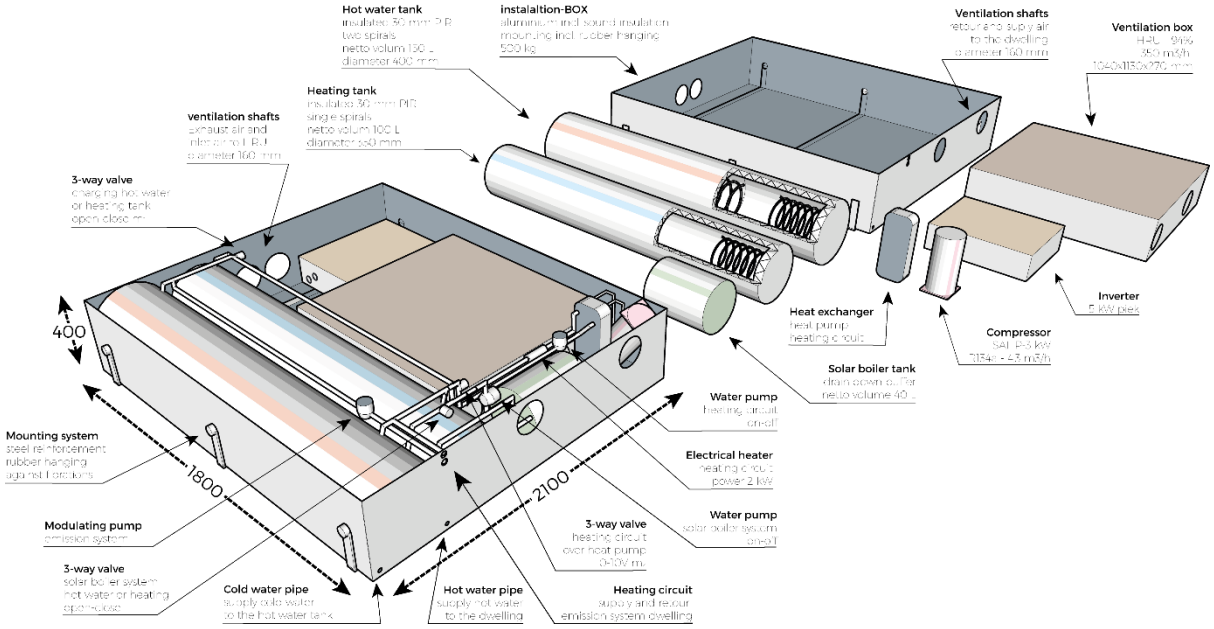

Figure 7-4 Installation box and integration of components

7.1.5 Impression of the ENergy Roof

In a Dutch dwelling the floor space is very valuable especially for row houses in the city. The ENergy Roof improves the quality of the dwelling by adding space, or better by reducing the space required for installations. This can illustrated by an impression of the attic where in the old situation the conventional installations are installed and the new situation has the ENergy Roof with integrated installation-BOX. With the renovation the attic is transformed from a low-quality storage space to a high-quality study room or bed room as presented in Figure 7-5.

Figure 7-5 Impression before (left) and after (right) NoM renovation with the ENergy Roof

7.2 Financial feasibility

The economic analysis of the total costs and benefits of the ENergy Roof result in the financial feasibility of the system. The ENergy Roof is part of the NoM renovation which has a business model based on the energy savings of the inhabitant after the renovation. According to The Stroomversnelling the target price is € 45.000 based on a monthly energy cost saving of € 175,- per month, mortgage of 30 years with 2.5% interest.

Table 7.4 Business case Stroomversnelling for NoM renovation

Component		
Energy savings		€ 175
Payback time (year|month)	30	360
Bruto savings		€ 63,000
Interest percentage (year|month)	2.50%	0.21%
Possible loan based (Present Value)		€ 44,300
Total interest		**€ - 18,700**

7.2.1 The ENergy Roof

The ENergy Roof has the focus on the installations of the NoM renovation, therefore the economic analysis is done for ENergy Roof installation components and not for the total renovation. The financial feasibility is reached when the total investment costs of the installations are below € 15.000 as presented in Figure 2-2.

The total investment cost of the ENergy Roof is based on the selected components which follow from the simulations which give a 3 kW with 6 m² PV-DX SAHP and a 2 kW electrical heater. The annual electricity demand of the dwelling is generated with the 6 m2 PV-DX and an additional PV installation of 31 m². The size of the buffer tanks are 150 and 100 litres for respectively the hot water and heating. Other installation components which are taken into account are: ventilation unit (incl. vans, heat recovery, bypass after heaters and filters), inverter (incl. cables), control

system and assembly costs. An overview of these components with the associated costs are presented in **Fout! Verwijzingsbron niet gevonden.**. With the total investment costs also a post for development costs, cover and profit and risk are taken into account. A detailed list of the investment costs can be found in Appendix B – Investment costs ENergy Roof.

Table 7.5 Overview costs components of the ENergy Roof

Component	Total price		Percentage
Solar system	€	4,720	30%
Heat pump	€	2,070	13%
Ventilation box	€	1,130	7%
Hydraulic system	€	1,060	7%
Demotics	€	730	5%
Assemblage	€	780	5%
Total factory prices	€	10,490	68%
Development cost	€	1,000	6%
Cover	€	2,620	17%
Profit and risk	€	1,400	9%
Total cost ENergy Roof	**€**	**15,500**	**100%**

The total cost of the installations are € 15.500 and is exclusive the costs for the other components for the NoM renovation. The costs for the other components and the sales costs are summed € 28.500 as presented in Figure 2-2 (Hasselaar, 2014). This results in a total investment of € 44.000 for a NoM renovation with ENergy Roof and is within the scope of the Stroomversnelling. Comparing the investment for the ENergy Roof installation with a new combined heating boiler and ventilation unit of € 2.500,- the added investment is € 12.000. This extra investment is required to become net-zero-energy from installations point of view is.

It would be interesting to compare the installation costs with other concepts of NoM renovations of the Stroomversnelling. For example the concept of the BAM (e.g. in Heerhugowaard), VolkerWessels (e.g. in Nieuw-Buijnen) or with the new concept of Factory Zero who will present their renovation in 2017. Unfortunately these numbers are not known.

7.2.2 Energy prices

The energy prices are believed to grow within the coming years, especially the price for gas. This makes the NoM renovation more attractive to invest in, since the energy bill is replaced by a fixed price for the mortgage. Especially the price for gas is believed to grow because of the expected CO_2 emission penalty and because more dwellings become all-electric which will result in higher fixed costs for the decreasing amount of people who still have a gas connection.

7.3 Social-technical value

In order to make a technical sustainable solution attractive one may take into account the social factor. The ENergy Roof is already attractive from sustainability point of view where inhabitants consume less energy and thereby have a lower negative impact on the environment (e.g. lower CO_2 emissions). But this is not the main motivation for people to choose for a NoM renovation and to make such a large investment. Key to the NoM renovation is the financial motivation and also the long term guarantee for the Nul-op-de-Meter.

The large social added value for the inhabitants is that they can stay in their home. People have an emotional attachment to their home. The NoM with ENergy Roof preserves the home and improves the house. In addition the quality of living of the inhabitant is enlarged with better thermal comfort, healthy indoor environment with fresh air, more insight in the function of the dwelling with the demotic system and no draught and mould problems. Not one size fits all solution, but prefabricated components where parts are interchangeable and satisfy with the preferences of the inhabitant (e.g. type of front door or addition of a dormer window).

There has also been some counter-messages for the NoM renovations which should be carefully dealt with in the coming projects (Renovatieprofs, 2016). Due to the improved insulation of the skin, the dwelling is sensitive to overheating in the summer. Thereby some people experience noise pollution from the ASHP external unit and also from the balanced ventilation with HRU. The ventilation is mainly negatively experienced in the bedroom and living room. Attention should be taken into the sound insulation of the ventilation system. Also to the finishing of the dwelling by the builders should be neat so that the inhabitants get a better looking dwelling after the renovation from the outside and also from the inside.

8. Conclusion

8.1 Conclusion

A literature study was performed to find the most suitable dwelling in the Netherlands for the NoM renovation with ENergy Roof. The post war row houses built between 1960 and 1980 match the selection criteria of quantity, construction quality, energy label and meet the conditions for the ENergy Roof. There is a total potential of 1 million row houses that can be renovated to NoM.

Net zero energy is achieved when the annual final energy consumption of an average post war row house of 67 GJ is reduced to zero. Literature study show that the heating demand is two third of the total annual consumption. With the first two steps of the NSS the final energy consumption is reduced with 50% by applying an insulated skin and heat recovery ventilation to the dwelling. From this starting point the ENergy Roof make the row house energy neutral and supplies the dwelling with the annual hot water, heating and electricity demand.

In conventional installation concepts for the NoM renovation, the components lack of integration and does not offer an affordable solution. An energy system was designed where all the installation components are integrated in a single roof element which allow industrialisation, high production rates, price reduction and a one-day renovation. The ENergy Roof consist of four essential components which are the photovoltaic-thermal (PVT), solar assisted heat pump (SAHP), storage technology and ventilation with heat recovery (HRU). The PVT panels harvest both electricity and heat achieving higher yield of solar energy per unit area compared to PV panels. The SAHP use the PV panel as evaporator extracting thermal energy from the panel by direct expansion (DX). The PV-DX SAHP is associated with low investment cost and high COP during solar-hours. A hydraulic system is designed where the SAHP together with a back-up electrical heater supply the low temperature heating system and hot water demand of the dwelling with two different temperatures. The heating circuit has a fully mixed storage buffer with operation temperature between 23 and 35 °C and the hot water storage buffer is a stratified tank heated up to 55 °C. The thermodynamic behaviour of the installation system is explored using a numerical MATLAB/Simulink model.

Annual simulation show that NoM is achieved with the ENergy Roof and that it provide the annual heating and hot water demand by a smallest system configuration with a 3 kW SAHP, 6 m^2 PV-DX and a 2 kW electrical heater. This configuration with East orientation achieves a SCOP of 2,6 with an annual electrical demand of 2307 kWh for the installation system and requires extra PV panels on the second side of the roof to become NoM. With a south orientation of the ENergy Roof it provides all the required electricity for NoM. The increased surface of the PV-DX has a large influence on the SCOP of the system where the increased heat pump capacity show minimal effect on the SCOP. With 12 m^2 PV-DX the system reaches a SCOP of 3,0 and with a 5 kW heat pump it

requires 2023 kWh electrical energy for the installations. The influence of the orientation and inclination of the ENergy Roof has minimal effect on the SCOP but has significant influence on the annual generated electricity. Increasing the storage capacity for the heating system from 100 to 500 litres reduces the amount of start/stops with 57% but increases the electrical demand with 150 kWh due to the increased tank losses. The electrical efficiency of the PV-DX panels increases with an annual average of 0,8% due to the cooling of the panel. A risk of the PV-DX SAHP is the ice formation on the panel when the temperatures of the evaporator drop below zero. The system has the highest risks in the months November till March where the panel is 28-59% of the time under 0 °C. After the NoM renovation with the ENergy Roof, the appliances cover more than 50% of the annual final energy demand where the post for heating demand is reduced to 16%.

All the installation components can be integrated in a single installation-BOX and fit in the technical roof element. The roof element has a total thickness of 400 mm including the PV-DX system with air cavity. The installation-Box is partly incorporated in the roof and extends with 220 mm into the attic space. Calculations show that the heat resistance R_c of 6 is achieved and that the existing wooden purlins can bear the new roof. The investment cost of the ENergy Roof's installations is € 15.500,- and falls within the scope of the Stroomversnelling. The solar system is the largest post followed by the heat pump. Depending on the cost for the new façades and roof the total investment is € 44.000,- and can be financed with the old energy bill of € 175,- per month.

In conclusion, the ENergy Roof is technical and financial feasible for a NoM renovation of 1 million row houses in the Netherlands and has the potential to reduce the national annual CO_2 emission with 2,8% compared to 2014 (4,3 million tons per year) and increase the installed national PV capacity with a factor 3,7 compared to 2015 (5500 MW nominal capacity).

8.2 Recommendations

Further investigation in the ice formation on the panel and the effect on the heat transfer and efficiency of the SAHP is recommended. It is expected that this phenomena will occur during some months of the year. The ice formation can be simulated in the existing MATLAB/Simulink model to predict the influence of this phenomena. In addition the current model can be extended with a PVT boiler and a smart control system where the heat pump operates during optimal hours. Furthermore incorporating the cooling demand of the dwelling in the model would be interesting.

Secondly, setting up a prototype of the ENergy Roof and conducting field experiments would gain additional information on the technical feasibility of the system. The effect of ice formation can be investigated and the MATLAB/Simulink model can be verified. Especially the wind convective heat transfer is an uncertainty in the current model which can be verified by field measurements. Furthermore it is recommended to research the adherence of the aluminium roll-bond evaporator to the PV panel.

Finally, the current model can be used to investigate the application of the ENergy Roof for dwellings with a different heating and hot water demand. The developed model can be used with different input files to calculate the required SAHP capacity and PV-DX surface.

9. Literature

Andeweg, M. T. (2013). *Niet-traditionele bouwmethoden uit de periode 1945-1965*.

Armstrong, S., & Hurley, W. G. (2010). A thermal model for photovoltaic panels under varying atmospheric conditions. *Applied Thermal Engineering, 30*, 1488-1495.

Bloomberg. (2013). Price per watt history for conventional (c-Si) solar cells since 1977. Retrieved from http://www.economist.com/news/21566414-alternative-energy-will-no-longer-be-alternative-sunny-uplands

BouwhulpGroep. (2013). *DOCUMENTATIE SYSTEEMWONINGEN '50 -'75*. Platform 31.

Bruggeman, L. A. (1980). *KWALITATIEVE WONINGDOCUMENTATIE (KWD) 1948-1977 enkele kwaliteitsaspecten van de nieuwbouw van woningen over de afgelopen 30 jaar*. Zoetermeer: Staatsuitgeverij 's-Gravenhage.

BZK, M. (2013). Cijfers over Wonen en Bouwen. *Ministerie van Binnenlandse Zaken en Koninkrijksrelaties*.

Carrier. (2016). Verwarming, ventilatie en airconditioning - Catalogus 2016. In U. T. C. (UTC) (Ed.), (1 ed.).

CBS. (2014). Hernieuwbare energie in Nederland. *Centraal Bureau voor de Statistiek*.

CBS. (2015). Nieuwbouw van woningen. *CBS Statline*.

Coen, M. (2015). Energie prestatie Vergoeding. *Energiesprong_Platform31*.

Dupeyrat, P. (2012). Spectral properties of a sc-Si cell. *Fraunhofer ISE*.

Dwivedi, V. (2009). *Thermal Modelling and Control of Domestic Hot Water Tank.* (Master of Science in Energy Systems and the Environment), University of Strathclyde Engineering, Glasgow, UK.

Energy Panel. (2016). Thermboil Retrieved from http://www.energypanel.es/

Eurostat. (2015). Consumption of energy. Retrieved from http://ec.europa.eu/eurostat/statistics-explained/index.php/Consumption_of_energy

Friedel, P., De Jong, A., & Horstink, M. (2014). Eindrapportage Veldtesten - Energieprestaties van 5 warmtetechnieken bij woningen in de praktijk. *EnergyMatters*.

Graves, L. (2015). UAE beats renewables cost hurdle with world's cheapest price for solar energy. *The National*. Retrieved from http://www.thenational.ae/business/energy/uae-beats-renewables-cost-hurdle-with-worlds-cheapest-price-for-solar-energy

Grotelaers, P. (1984). *DE ONTWIKKELING VAN DE NIEUWBOUWKWALITEIT VAN WONINGEN 1977-1981 analyse op basis van de Kwalitatieve Woningdokumentatie*. Delft: Delftse universitaire Pers.

Hammond, G., & Jones, C. (2011). Inventory of Carbon & Energy (ICE) version 2.0. *University of Bath*.

Harmelink, M., Bosselaar, L., Gerdes, J., Segers, R., & Verdonk, M. (2012). Berekening van de CO2-emissies, het primair fossiel energiegebruik en het rendement van elektriciteit in Nederland. *Agentschap NL*.

Hasselaar, B. (2014). *Stroomversnelling Koop – 24-uurs startbijeenkomst Innovatiecoaches*. Retrieved from http://www.sbrcurnet.nl/

IEA. (2011). Technology Roadmap Energy-efficient Buildings: Heating and Cooling Equipment. *International Energy Agency*.

ISSO 744, t. (2009). *Lucht-waterwarmtepompen in woningen*. Rotterdam: ISSO.

ISSO. (2016). *Zonne-energie – Bouwkundige- en installatietechnische richtlijnen voor zone-energiesystemen* Rotterdam: ISSO.

Jellema. (2013). Vuistregels voor het ontwerpen van een draagconstructie. *Jellema Draagconstructies I en II, deel 9*.

Jonathan, T. (2016). *The value of Zero Energy Renovations.* (Master thesis), Technical University Delft, Delft.

Kandlikar, S. G. (1991). A Model for Correlating Flow Boiling Heat Transfer in Augmented Tubes and Compact Evaporators. *Transactions of the ASME, 113*, 966-972.

Kundu, A., Kumar, R., & Gupta, A. (2014). Evaporative heat transfer of R134a and R407C inside a smooth tube with different inclinations. *Internatioinal Journal of Heat and Mass Transfer*.

Kydes, A. (2007). Primary Energy. *Encyclopedia of Earth*. Retrieved from http://www.eoearth.org/view/article/155350/

LenteAkkoord. (2015). Hogere hypotheek voor tweeverdieners en voor nul-op-de-meter. Retrieved from http://www.lente-akkoord.nl/hogere-hypotheek-voor-nul-op-de-meter/

Luscuere, P. (2015). The synergy between Low Temperature Heating and Heat Pump Technology.

Milieu-Centraal. (2015a). Bespaartips warm water. Retrieved from https://www.milieucentraal.nl/

Milieu-Centraal. (2015b). Gemiddeld energieverbruik. Retrieved from https://www.milieucentraal.nl/

Milieu-Centraal. (2016a). Bespaartips apparaten en verlichting. Retrieved from https://www.milieucentraal.nl/

Milieu-Centraal. (2016b). Financiering verbeteren eigen woning. Retrieved from https://www.milieucentraal.nl/

Mills, A. F. (1999). *Basic heat and mass transfer, second edition*. Los Angeles: Prentice hall.

Moran, M. J., & Shapiro, H. N. (1996). *Fundamentals of engineering thermodynamics* (3rd ed.). New York: John Wiley & Sons.

Norber Fisch, M., Wilken, T., & Stähr, C. (2013). *EnergyPLUS - Buildings and districts as renewable energy sources*. Leonberg: Fisch.

OliNo. (2015). Nul op de meter woning. Retrieved from http://www.olino.org/articles/2015/10/27/nul-op-de-meter-woning/

Palyvos, J. A. (2007). A survey of wind convection coefficient correlations for building envelope energy systems' modeling. *Applied Thermal Engineering, 28*(2008), 801-808.

Renovatieprofs. (2016). Kassa behandelt negatief nul op de meter project Drenthe Retrieved from https://www.renovatieprofs.nl/nieuws/

Rubanox. (2016). Roll-Bond evaporator. Retrieved from http://www.rubanox.com/

RVO. (2013). Infoblad Trias Energetica en energieneutraal bouwen. *Rijksdienst voor Ondernemend Nederland*.

RVO. (2014). Financiële steun voor het realiseren van energiebesparing bij huurwoningen. *Rijksdienst voor Ondernemend Nederland*.

RVO. (2016). Algemene Begrippen. *Rijksdienst voor Ondernemend Nederland*.

Sharples, S., & Charlesworth, P. S. (1997). Full-scale measurements of wind-induced convective heat transfer from a roof-mounted flat plate solar collector. *Solar Energy, 62*, 69-77.

Sidera. (2016). Landelijke opbrengs berekening zonnestroom. Retrieved from http://www.siderea.nl/zonne-energie/jaararchief/jaararchief.html

SolarGIS. (2016). Global Horizontal Irradiation (GHI) Maps. Retrieved from http://solargis.info/doc/free-solar-radiation-maps-GHI

Stroomversnelling. (2015). Salderen nu en in de toekomst. Retrieved from http://www.stroomversnellingkoopwoningen.nl/salderen-nu-en-in-de-toekomst/

Stroomversnelling. (2016). Wat is Stroomversnelling? Retrieved from http://stroomversnelling.nl/

Sun, X., Wu, J., Yanjun, D., & Ruzhu, W. (2014). Experimental study on roll-bond collector/evaporator with optimized-channel used in direct expansion solar assisted heat pump water heating system. *Applied Thermal Engineering, 66*, 571-597.

Thijssen, C. C. F. (1999). *BOUWCONSTRUCTIEVE ANALYSEVAN NAOORLOGSE EENGEZINSBUIZEN IN DE NON-PROFIT HUURSECTOR 1946-1980*. Delft: Delft University Press.

Tigchelaar, C., & Leidelmeijer, K. (2013). Energiebesparing: Een samenspel van woning en bewoner - Analyse van de module Energie WoOn 2012. *ECN*.

Trio, H., & Schmidt, D. (2011). Annex 49 - Low exergy systems for high-perofrmance buildings and communities. *International Energy Agency*.

Van den Dobbelsteen, A. (2008). Towards closed cycles-New strategy steps inspired by the Cradle to Cradle approach.

Van den Ham, E. (2012). Embodied energy of passive house facades. *Delft University of Technology*.

Van der Linden, A. C. (2015). *Bouwfysische aspecten rond het NA-ISOLEREN VAN SPOUWMUREN* Utrecht: Milieu Centraal.

Van der Linden, A. C., Erdtsieck, P., Kuijpers - Van Gaalen, I., & Zeegers, A. (2006). *Bouwfysica*. Utrecht/Zutphen: ThiemeMeulenhoff.

Van der Spoel, W. (2015). Playing with heat balances. *Delft University of Technology*.

Van Elk, R. S. F. J., & Priemus, H. (1970). *niet-traditionele woningbouwmethoden in Nederland*. Alphen aan de Rijn: Samsom.

Van Helden, W., Roossien, B., & Mimpen, J. (2013). Maximalisering zonne-energie per vierkante meter PVT. *VV+, februari*, 82-87.

Van Krevel, A. (2000). Installatieconcepten warmtepompen: theorie en praktijk. *Verwarming en koeling, 29*(7/8).

Van Paassen, A. H. C. (2004). Indoor climate control fundamentals. *Delft University of Technology, Process and Energy*.

Van Thiel, L. (2014). Watergebruik Thuis 2013. *TNS Nipo, Verwmin*.

VROM. (2002). Energiebesparende maatregelen in de woningvoorraad, KWR 2000 maakt balans op. *Ministerie van Volkshuisvesting, Ruimtelijke Ordening en Milieubeheer,*.

VROM. (2009). Energiegedrag in de woning - Aanknopingspunten voor de vermindering van het energiegebruik in de woningvoorraad. *Ministerie van Volkshuisvesting, Ruimtelijke Ordening en Milieubeheer,*.

Zondag, H. A., De Vries, D. W., Van Helden, W. G. J., Van Zolingen, R. J. C., & Van Steenhoven, A. A. (2003). The yield of different combined PV-thermal collector designs. *Solar Energy, 74*, 253-269.

10. Appendix A – Parameters

Table 10.1 Input parameters mathematical model

	Name	Symbol	Value	Unit	Note
Inputs (13)	External temperature	T_e	-	°C	NEN5060:2009:2A
	Long wave incoming radiation	LW_{in}	-	W/m²	NEN5060:2009:2A
	Direct solar irradiation	G	-	W/m²	NEN5060:2009:2A
	Wind speed	w	-	m/s	NEN5060:2009:2A
	Wind direction	d_{wind}	-	°	NEN5060:2009:2A
	Heat demand dwelling	Q_h	-	J/hour	DesignBuilder model
	Hot water demand dwelling	Q_{hw}	-	J/hour	NEN7120 class 3
	Surface panel	A_{PV-DX}	6/8/10/12	m	Boundary condition
	Nominal heat pump capacity	$Q_{heat\ pump}$	3/4/5	kW	Boundary condition
	Electrical heater capacity	$Q_{el.\ heater}$	2	kW	Chapter 4.3
	Volume heating tank	V_{tank_h}	100/300/500	L	Chapter 4.4
	Volume hot water tank	$V_{tank\ hw}$	150	L	Chapter 4.4
	Orientation PV-DX	γ	0/90	°	Boundary condition
	Inclination PV-DX	β	30/40	°	Boundary condition

Table 10.2 General parameters mathematical model

	Name	Symbol	Value	Unit	Note
Parameters (25)	Average heat transfer absorber	a_{abs_refr}	203	W/m²K	Appendix E
	Factor surface backside	f_{back}	1,16	-	3D model
	Factor wind backside	f_{wind}	0,25	-	Appendix F
	Efficiency factor heat pump	η_{hp}	0.9	-	Appendix G
	Diameter tank	D_{tank}	0.25	m	Boundary condition
	Insulation thickness tank	d	0,05	m	Boundary condition
	Thermal conductivity tank	λ	0,023	W/mK	Boundary condition
	Supply temperature limit heating	$T_{supplymin}$	23	°C	Chapter 4.4
	Temperature cold water	$T_{coldwater}$	10	°C	Chapter 4.4
	Thermocline layer factor	$f_{thermocline}$	0,8	-	Chapter 4.4
	Transmission-absorption factor	τ_a	0,78	-	(Zondag et al., 2003)
	Electrical efficiency of the PV cell	η_0	0,16	-	(Zondag et al., 2003)
	Efficiency losses PV cell	η_t	0.0045	K⁻¹	(Zondag et al., 2003)
	Losses by cables and the inverter	η_{system}	0.90		(Zondag et al., 2003)
	Sky factor	F_{sky}	0,8 (30°) 0,7(45°)	-	3D model
	Emissivity glass	ε	0,9	-	(Zondag et al., 2003)
	Stefan-Boltzmann constant	σ	5,578 x 10⁻⁸	W/m²K⁻⁴	(Zondag et al., 2003)
	Specific heat capacity water	c_{p_water}	4180	J/kgK	(Zondag et al., 2003)
	PV glass Thickness Thermal conductivity Density Specific heat capacity	 d λ ρ c_p	 0,003 1,8 3000 500	 m W/mK kg/m³ J/kgK	(Armstrong & Hurley, 2010)
	ARC Thickness Thermal conductivity Density Specific heat capacity	 d λ ρ c_p	 100 x 10⁻⁹ 32 2400 691	 m W/mK kg/m³ J/kgK	(Armstrong & Hurley, 2010)
	PV cell Thickness Thermal conductivity Density Specific heat capacity	 d λ ρ c_p	 225 x 10⁻⁹ 148 2330 677	 m W/mK kg/m³ J/kgK	(Armstrong & Hurley, 2010)
	EVA Thickness	 d	 500 x 10⁻⁹	 m	(Armstrong & Hurley, 2010)

	Thermal conductivity Density Specific heat capacity	λ ρ c_p	0,35 960 2090	W/mK kg/m^3 J/kgK	
	Tedlar Thickness Thermal conductivity Density Specific heat capacity	 d λ ρ c_p	 100 x 10^{-9} 0,2 1200 1250	 m W/mK kg/m^3 J/kgK	(Armstrong & Hurley, 2010)
	Adhesive Thickness Thermal conductivity Density Specific heat capacity	 d λ ρ c_p	 50 x 10^{-9} 0,085 2400 -	 m W/mK kg/m^3 J/kgK	(Armstrong & Hurley, 2010)
	Aluminium roll bond Thickness Thermal conductivity Density Specific heat capacity	 d λ ρ c_p	 0,0015 205 2700 910	 m W/mK kg/m^3 J/kgK	(Armstrong & Hurley, 2010)

11. Appendix B – Investment costs ENergy Roof

Detailed list of the investment costs for the installations of the ENergy Roof are presented below. The components costs are based on orders of 2.000 pieces and the prices are obtained from the company Van Dorp.

Table 11.1 Detailed list of investment costs

	Component	Specifications	No.	price/amount	price	total price	Reference
Solar system	PV	~ 31 m2 (37-6m2)	31	€ 100	3100	€ 4,720	Van Dorp
	inverter	ZeverSolar up to 6 kWp	1	€ 1,000	1000		Van Dorp
	cables + group		31	€ 10	310		Van Dorp
	Mounting system	Building integrated	31	€ 10	310		Van Dorp
Heat pump	PV-DX	4 x 1.60 m2	6	€ 200	1200	€ 2,070	Van Dorp
	Compressor	800 W	1	€ 500	500		Van Dorp
	Expansion valve		1	€ 150	150		Van Dorp
	Heat exchanger	refrigerant-water	1	€ 200	200		Van Dorp
	Refrigerant	1 kg R134A	1	€ 15	15		Eurorefr.
Ventilation box	Mech. fan (2x)	350 m3/h	2	€ 100	200	€ 1,130	Van Dorp
	Heat recovery	350 m3/h – 90% eff.	1	€ 128	128		Orange Climate
	Splitting unit	1-4 incl. heaters, bypass and filters	1	€ 300	300		Van Dorp
	unit box	aluminium 1x1.5m	1	€ 500	500		Van Dorp
hydraulic system	Electrical heater	2 kW	1	€ 80	80	€ 1,060	Van Dorp
	Tank hot water	150 L + 2 spirals	1	€ 350	350		Van Dorp
	Tank heating	100 L + 1 spirals	1	€ 250	250		Van Dorp
	Pump	On/off	1	€ 50	50		Van Dorp
	Pump	Moderating	1	€ 50	50		Van Dorp
	3-way valve	0-10V	1	€ 70	70		Van Dorp
	3-way valve	Open-close	1	€ 60	60		Van Dorp
	small material	pipes, etc.	1	€ 150	150		Van Dorp
Demotics	Temp sensors	4 (3 tank + 1 pipe)	4	€ 15	60	€ 730	Van Dorp
	Other sensors		1	€ 20	20		Van Dorp
	control		1	€ 250	250		Van Dorp
	el. Cables + working hours		4	€ 100	400		Van Dorp
Assemblage	installing total system in factory		8	€ 65	520	€ 780	Van Dorp
	mounting on site		4	€ 65	260		Van Dorp
Total factory prices						€ 10,490	
Development cost						€ 1,000	
Cover				25%		€ 2,620	
Profit and risk				10%		€ 1,400	
Total cost ENergy Roof						**€ 15,500**	

12. Appendix C – Detailed numbers calculations

Detailed numbers annual simulation MATLAB/Simulink

Table 12.1 Annual simulations with different configurations

Orientation and inclination	Configuration	no. hp on/off cycles	time hp on per year	% hp on per year	Q_el. Heater [kWh]	Q hp_work [kWh]	Total_el [kWh]	Q_hp condensor [kWh]	Q_demand [kWh]	Q_tankloss	scop hp	scop system	Produced electricity [kWh]
O.30	6-3kW	1417	2143	24	474.8	1832	**2307**	5630	6109	111	3.07	2.60	896.6
O.30	8-3kW	1507	1988	23	428.2	1755	**2183**	5677	6112	114	3.23	2.75	1191
O.30	10-3kW	1547	1880	21	402.9	1693	**2096**	5704	6113	115	3.37	2.86	1487
O.30	12-3kW	1581	1807	21	385.3	1650	**2035**	5722	6113	115	3.47	2.95	1782
O.30	8-4kW	1657	1622	19	339.1	1840	**2179**	5774	6114	116	3.14	2.75	1191
O.30	10-4kW	1705	1523	17	312.4	1773	**2085**	5796	6114	116	3.27	2.88	1486
O.30	12-4kW	1723	1456	17	290.1	1728	**2018**	5820	6115	117	3.37	2.97	1781
O.30	12-5kW	1837	1224	14	255.4	1767	**2023**	5856	6117	119	3.31	2.97	1781
S.30	6-3kW	1438	2113	24	465.9	1818	**2284**	5637	6109	111	3.10	2.63	988.2
O.45	6-3kW	1426	2138	24	472.3	1826	**2299**	5633	6110	112	3.08	2.61	871.9
O.30	6-3kW - S_h 300L	735	2215	25	520.7	1913	**2433**	5787	6313	315	3.03	2.47	897.4
O.30	6-3kW - S_h 500L	610	2312	26	461	1998	**2459**	6034	6507	509	3.02	2.44	898.1

Table 12.2 Risk of ice formation on the PV-DX panel with 6 m² and 3 kW heat pump

	days	T_abs < 0°C [hours/%]		T_abs< 0°C AND T_e>0°C [hours/%]		T_abs<0°C AND T_e<0°C [hours/%]		T_abs<-5 [hours/%]		T_abs<-5 AND Te>0 [hours/%]		T_e < 0 C [hours/%]	
Jan	31	440	59%	224	30%	216	29%	315	42%	131	18%	229	31%
Feb	28	297	44%	207	31%	90	13%	185	28%	129	19%	95	14%
Mar	31	205	28%	203	27%	2	0%	108	15%	105	14%	2	0%
Apr	30	63	9%	60	8%	3	0%	17	2%	18	3%	4	1%
May	31	31	4%	31	4%	0	0%	6	1%	5	1%	0	0%
Jun	30	17	2%	17	2%	0	0%	3	0%	4	1%	0	0%
Jul	31	18	2%	18	2%	0	0%	3	0%	2	0%	0	0%
Aug	31	20	3%	20	3%	0	0%	5	1%	6	1%	0	0%
Sep	30	26	4%	26	4%	0	0%	3	0%	3	0%	0	0%
Oct	31	82	11%	82	11%	0	0%	21	3%	20	3%	0	0%
Nov	30	279	39%	251	35%	28	4%	167	23%	146	20%	30	4%
Dec	31	400	54%	303	41%	97	13%	274	37%	199	27%	100	13%
Year	**365**	**1878**	**21%**	**1442**	**16%**	**436**	**5%**	**1107**	**13%**	**768**	**9%**	**460**	**5%**

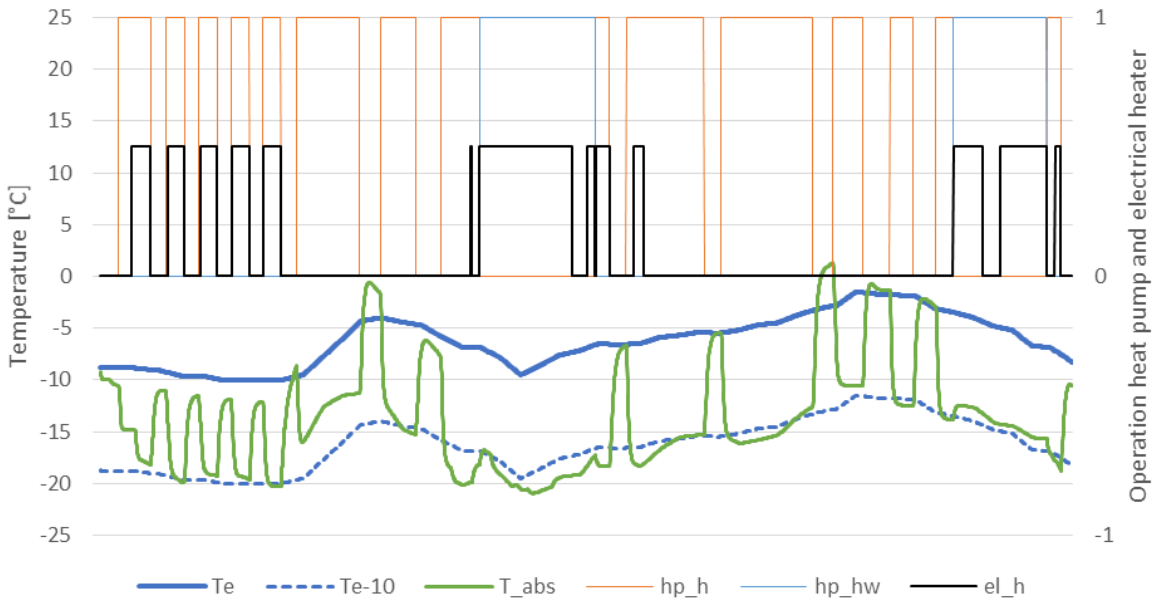

Figure 12-1 Heat pump (3 kW) with 6 m2 PV-DX two day winter simulation

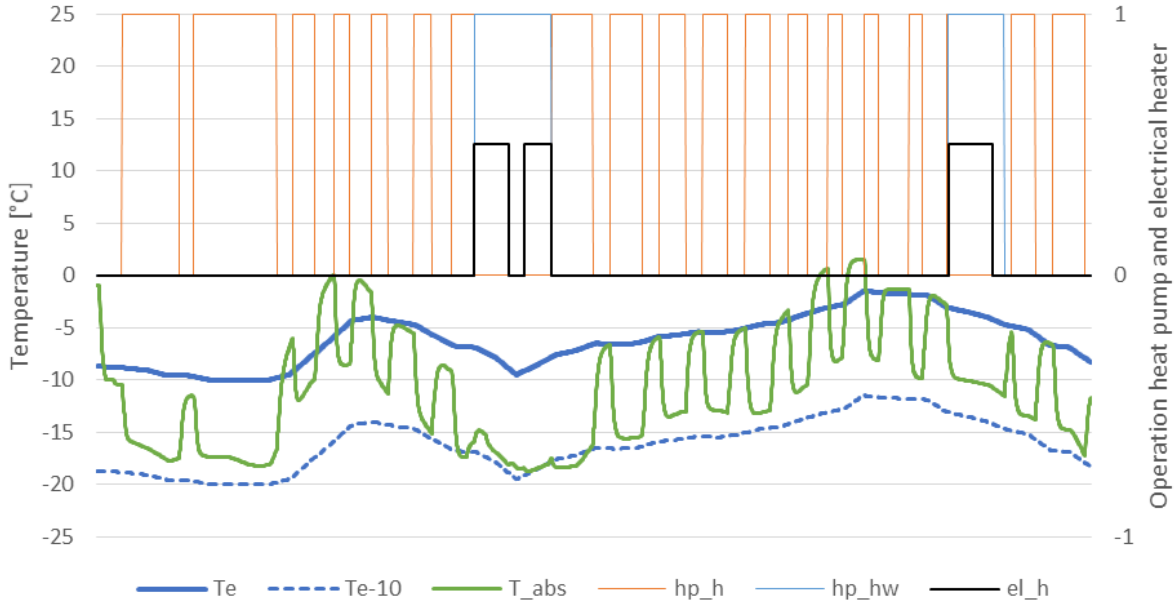

Figure 12-2 Heat pump (4 kW) with 12 m2 PV-DX two day winter simulation

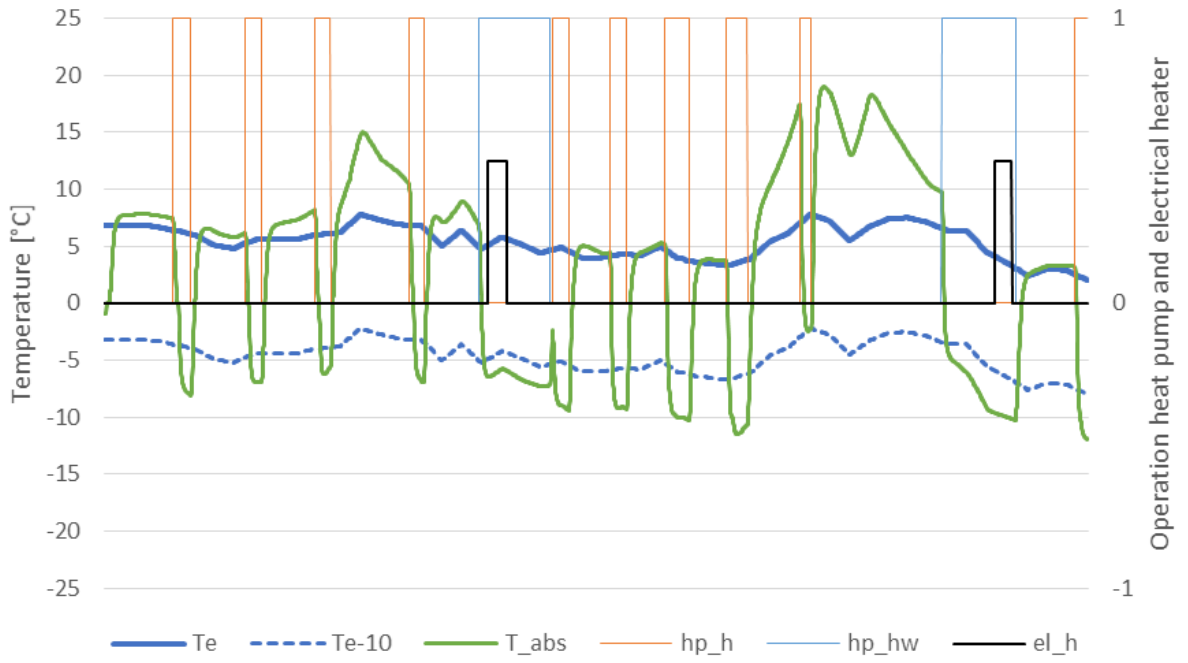

Figure 12-3 Heat pump (3 kW) with 6 m2 PV-DX two day mid-season simulation

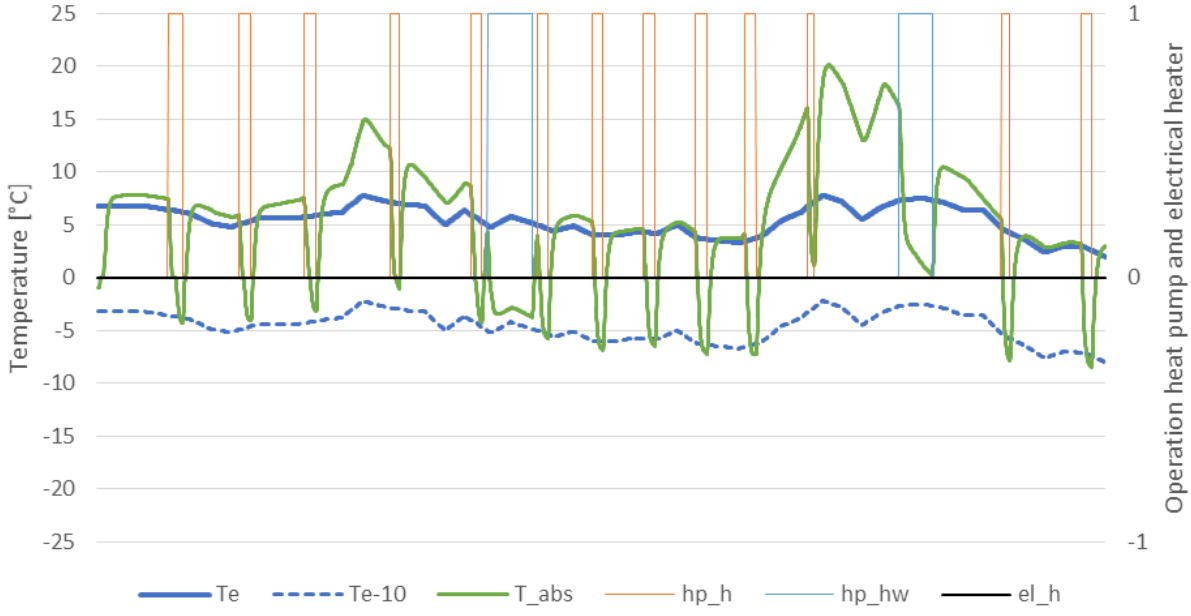

Figure 12-4 Heat pump (4 kW) with 12 m2 PV-DX two day mid-season simulation

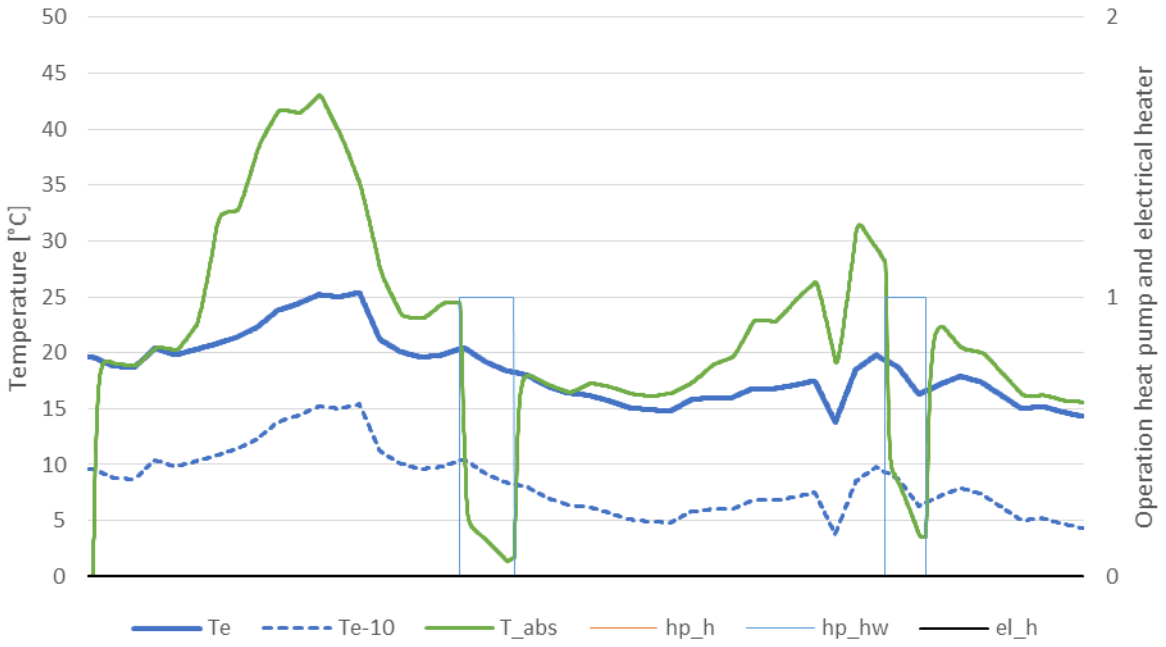

Figure 12-5 Heat pump (3 kW) with 6 m2 PV-DX two day summer simulation

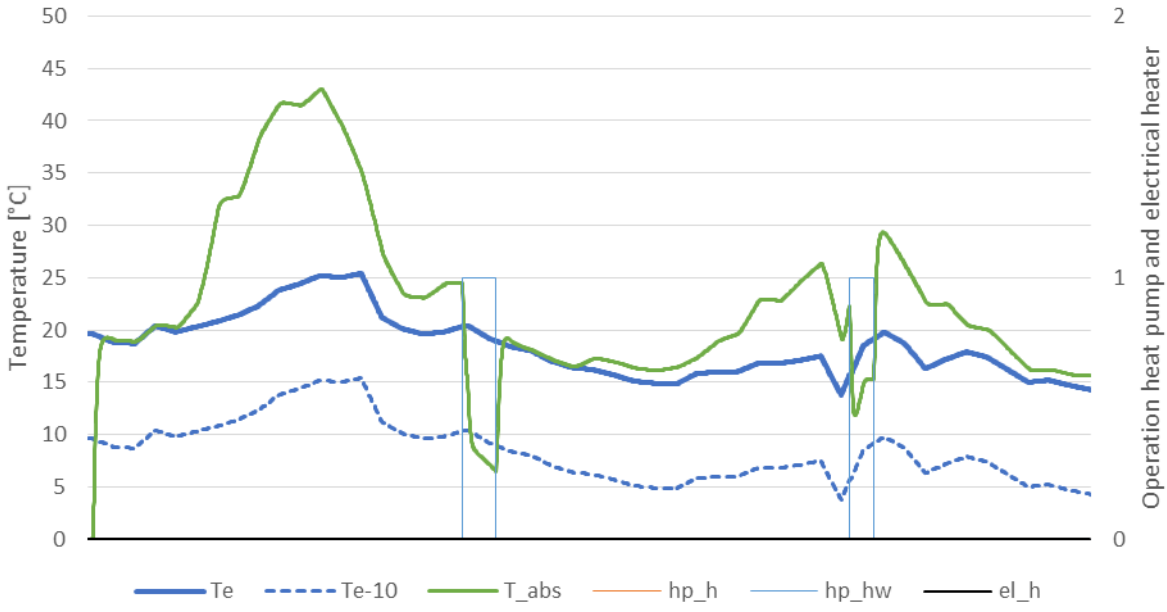

Figure 12-6 Heat pump (4 kW) with 12 m2 PV-DX two day summer simulation

Calculation heat resistance of the ENergy Roof

The following numbers are used to calculate the heat resistance R_c of the roof. The aim is to have a heat resistance higher or equal to 6 m^2K/W. Two scenarios are presented below.

Table 12.3 Scenario 1

	Width [m]	Materials	Thickness [m]	Lambda [W/mK]	Rc [m2K/W]	Note
Standard roof element (2x)	3.58	Wooden plate	0.011	0.13	0.08	multiplex
		insulation	**0.20**	0.032	6.25	Glass wool
		Wooden plate	0.011	0.13	0.08	multiplex
	0.22	2x(2 beams+2xwooden plate)			1.54	
					6.72	
Technical roof element	1.89					
		Wooden plate	0.011	0.13	0.08	
		High grade insulation	**0.12**	0.023	5.22	PIR
		Installation-BOX	0.4	1	0.4	Cover 50% of the roof element
	0.11				2.65	
		1x(2 beams+2xwooden plate)			1.54	
					4.66	
Total	**5.8**			**Rc**	**6.04**	**OK!**

Table 12.4 Scenario 2

	Width [m]	Materials	Thickness [m]	Lambda [W/mK]	Rc [m2K/W]	Note
Standard roof element (2x)	3.58	Wooden plate	0.011	0.13	0.08	multiplex
		insulation	**0.22**	0.032	6.8	Glass wool
		Wooden plate	0.011	0.13	0.08	multiplex
	0.22	2x(2 beams+2xwooden plate)			1.54	
					6.72	
Technical roof element	1.89					
		Wooden plate	0.011	0.13	0.08	
		High grade insulation	**0.05**	0.023	2.17	PIR
		Installation-BOX	0.4	1	0.4	Cover 50% of the roof element
	0.11				4.85	
		1x(2 beams+2xwooden plate)			1.54	
				Rc	**4.66**	
Total	**5.8**			**Rc**	**6.01**	**OK!**

Constructional calculations of the ENergy Roof

The following numbers are used to calculate the minimal height of the beam to take the total load of the roof. The rule of thumb stat that the height is 1/20th of the length and the width of the beam is 1/4th of the height. The span length of the beam is half of the total length and is 2,75 metre. This result in a minimal height of 140 mm. The height is minimal 200 mm, this it is sufficient.

The calculations of the weight of the roof are done with a roof area of 31,9 m^2 (5,8*5,5m) where 11 m^2 is the technical roof part and 20,9 m^2 the standard panel. The extra extension of 0,5 metre result in a roof area of 34 m^2 and is used to calculate the weight of the new roof.

	Materials	Weight [kg/m^2]	Weight [kg]	Total Weight [kg]	Weight of technical roof element [kg]
Old roof (31.9 m^2)	Roof tiles	41	-	1484	512
	Wooden plate	5,5	-		
		-	-		
New roof (34 m^2)	Wooden plate	5.5	-	1239	740
	Wooden beams	-	165		
	Insulation	-	-		
	Solar panels	11.4	-		
	Installation-BOX	-	500		

13. Appendix D – DesignBuilder model

In this appendix the DesignBuilder model used to calculate the heat demand of the dwelling is explained and the output data presented. The main specifications of the model are presented in Figure 3-6 and Figure 13-2 show the details of the skin. A 3D model of the NoM renovated row house (Figure 13-1) is constructed in DesignBuilder based on a standard house given by RVO with a total usable floor area of 120 m².

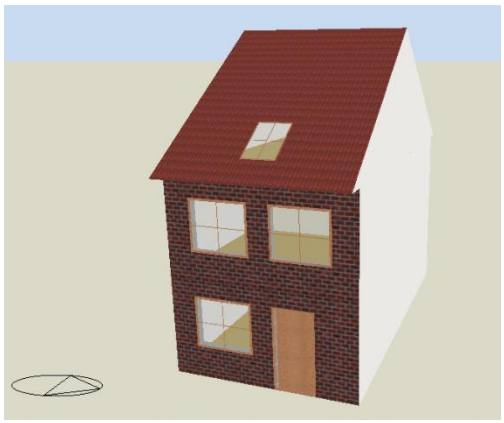

Figure 13-1 Row house 3D model in DesignBuilder

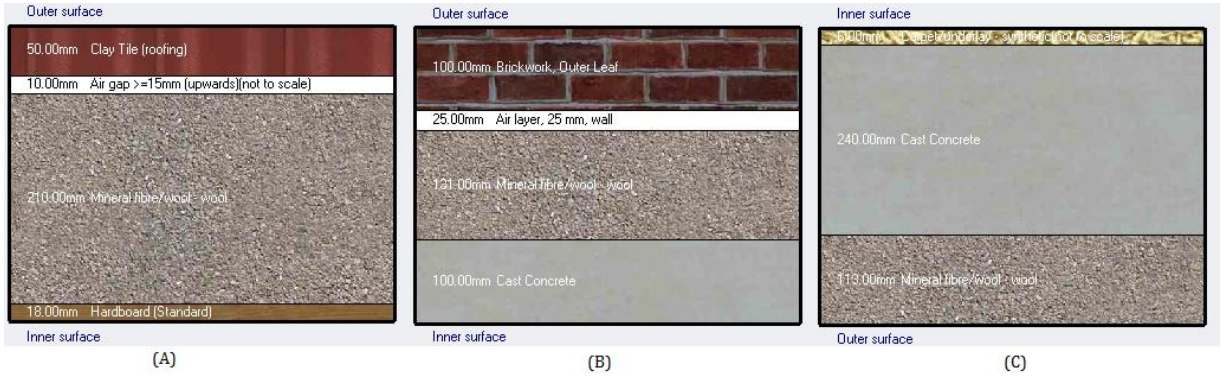

Figure 13-2 Detail of the layering (a) roof (b) facade (c) ground floor

Detail output DesignBuilder

In the figures below the detailed output of the simulation in DesignBuilder are presented. First the annual heat losses though the different components of the building are presented. In Figure 13-4 a more detailed overview of the heat gains and losses are presented. Finally Figure 13-5 show the daily heat demand of the dwelling. In this figure also the influence of the ventilation heat recovery is clearly seen. Without a heat recovery the heat demand of the dwelling will increase.

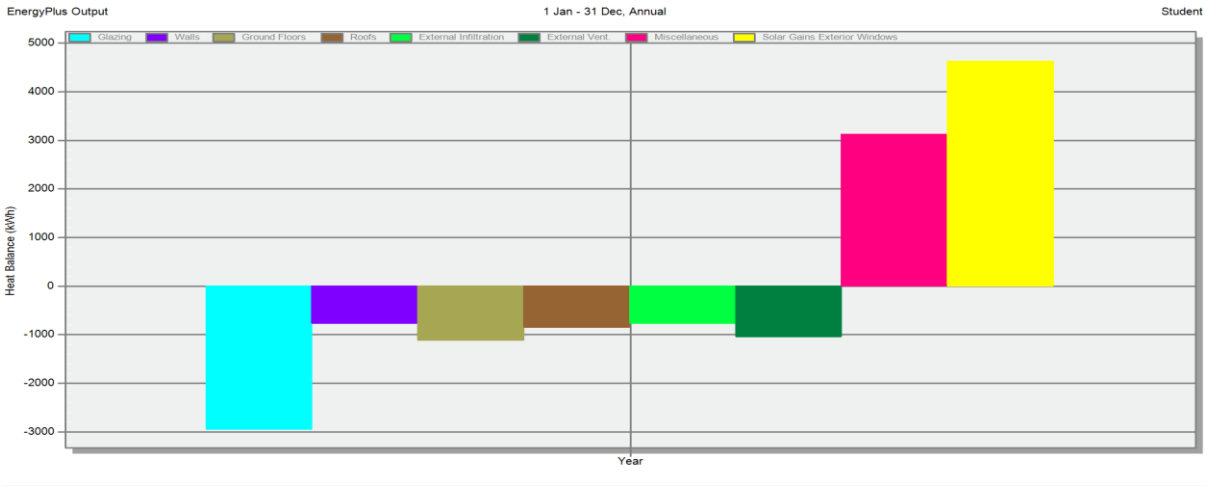

Figure 13-3 Annual heat losses and gains of the dwelling subdivided in different components

Figure 13-4 Daily heat losses and gains of the dwelling subdivided in different components

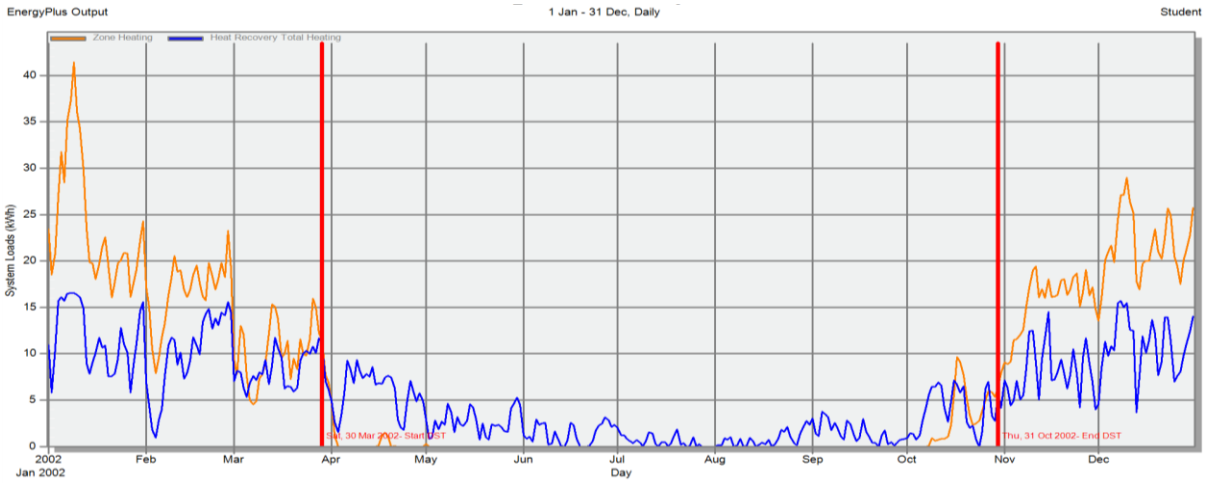

Figure 13-5 System loads of the heating system and the ventilation heat recovery

14. Appendix E - Heat transfer in the evaporator

The heat transfer in the evaporator of the PV-DX panel is very complicated. The section of the evaporator contains tubes and is not uniform (Figure 14-1). The temperature of the aluminium at a tube will be different from the place between the tubes. Secondly the refrigerant flowing through the tubes change phase from liquid-gas state to saturated gas. In this chapter a simplified heat resistance is calculated between the two nodes and used as constant in the model.

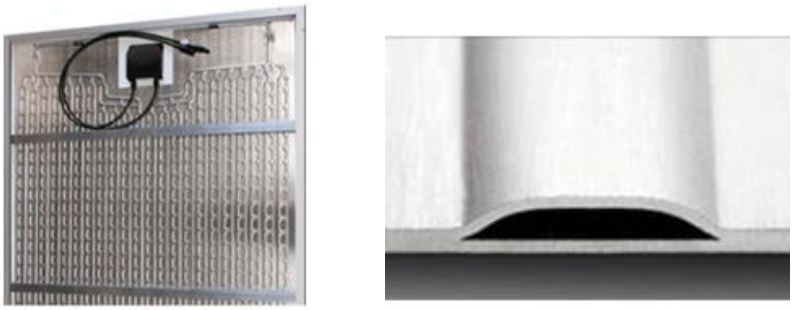

Figure 14-1 Evaporator of the PV-DX panel with section[1] (Rubanox, 2016)

Average heat resistance

The heat resistance depends on the geometry of the aluminium absorber: the thickness of the material, the diameter of the tubes and the spacing between the tubes. The geometry of the evaporator is drawn in the program THERM. This is a finite element method (FEM) and calculates the heat transfer within a material. The model shows that the heat resistance coefficient is independent on the changing temperature on the top side of the sheet (e.g. due to the irradiation) and minimal changes occur due to the changing heat transfer coefficient of the two-phase refrigerant.

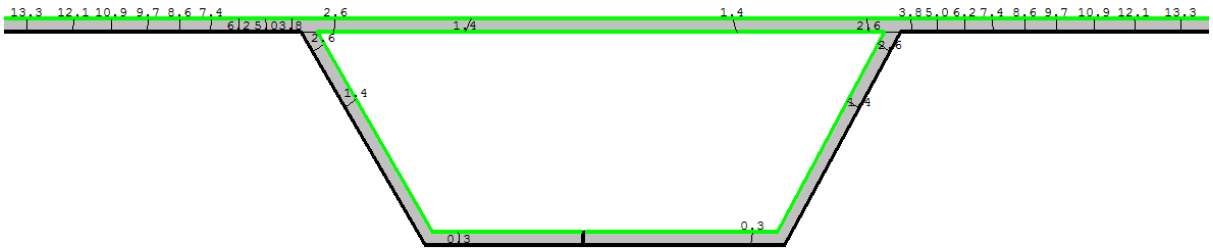

Figure 14-2 Section of the evaporator constructed in THERM

[1] (Rubanox, 2016)

Model FEM

A section of a part of the panel is constructed in THERM as presented in Figure 14-2. On the top layer a temperature of 80 degrees is set. An adiabatic layer is put on the bottom of the panel. The heat resistance at the top layer to the ambient is set to 25 W/K.m2. The inner tube has a boundary layer between 2000-4000 W/K.m2 depending on the vapour quality of the refrigerant (Figure 14-3). These heat transfer correlation is based on research on the two-phase evaporation of R134a in smooth tubes (Kandlikar, 1991; Kundu, Kumar, & Gupta, 2014). Kandlikar (1991) present an equation for the average alpha_tp of the refrigerant based on the convective- and nucleate boiling dominant regions. Assumed is a heat flux of 200 W/m^2 and a mass velocity of 3,0 kg/m^{2}s based on a 3 kW heat pump and the geometry of the panel. The material of the evaporator is aluminium and is 2 mm thick.

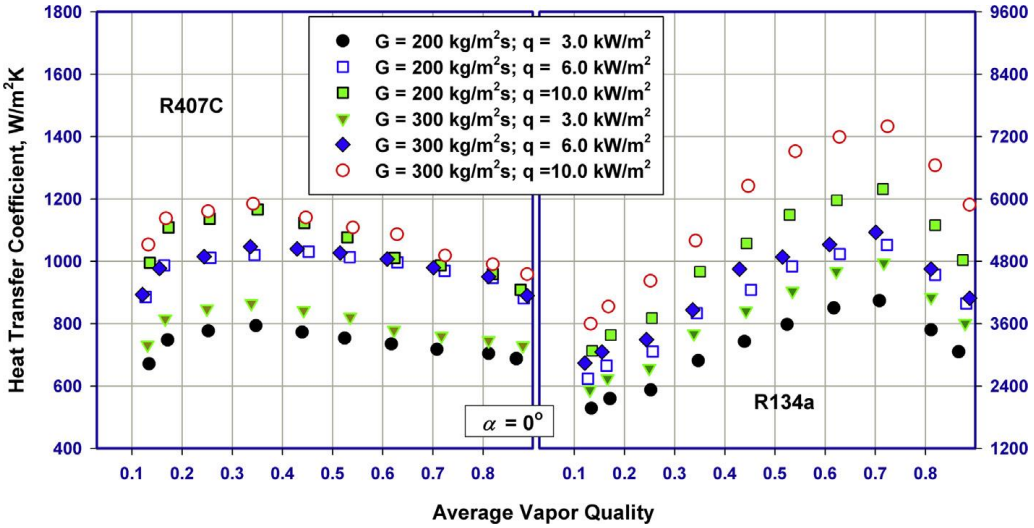

Figure 14-3 Heat transfer coefficient of R134a with changing vapour quality (Kundu et al., 2014)

Heat transfer coefficient

Based on the geometry presented in Figure 14-2 with, a distance of 270 mm between the tubes, the average heat transfer of the section is calculated. This result in 54,4 W/K heat transfer calculated over the width of the panel and 1 meter depth, recalculate this result in 203 W/m^{2}K. This value is inserted as constant in the sub model of the panel. After simulations were done the geometry of the evaporator pointed out to be different with a smaller distance of 40 mm instead of 270. New calculations show a heat transfer of 1580 W/m^{2}K. This result in a better performance of the panel since the heat transfer coefficient is increased. However it is expected that the influence on the energetic performance is minimal (<1%) since the heat transfer used in the simulations is already high. A single annual simulation show a sensitivity of 1,3% reduced electrical demand. Within the time of the graduation it was not possible to redo all the simulations. The heat transfer coefficient of 203 W/m^{2}K is therefore used in the model.

15. Appendix F - Convective heat transfer from the PV panel surface

The thermal losses to the ambient from roof mounted solar collector represent an important portion of the overall energy balance and depend heavily on the wind induced convection. Improper use of the wind convection coefficient, hw, can easily cause 20-40% errors in energy demand calculations (Palyvos, 2007). Thereby Palyvos (2007) present more than 50 different convective heat transfer correlations. For this research the report of Zondag et al. (2003) and Armstrong and Hurley (2010) provided the most correlations needed for the thermodynamic calculation of the PV-DX panel. However extra research is done to find the most suitable equation for the convective coefficient since in the first report only the free convection is taken into account and in the second report it is not clear if the equation includes the heat transfer of the back side of the panel.

Free and forced convection

According to the report Armstrong and Hurley (2010) there are two convective phenomena, the forced convection due to the wind flow over the surface and the free convection due to the temperature difference between the surface and the ambient air. On days with little or no wind, the free convective heat transfer becomes more significant.

Correlation for forced convection are developed by fundamental heat transfer theory, wind tunnel measurements and field measurements. The Nusselt relations based on wind tunnel measurements predict a small heat transfer coefficient, where the results of field measurements indicate that the measured heat transfer coefficient could be as much as 30% greater (R.J. Cole, 1977). This standard Nusselt-Jürges equation presented by McAdams is:

$$h_w = 5.7 + 3.8V_w$$

This equation is a general equation and not specific meant for a solar panel. Also the correlation does not take into account the free convection and the wind direction. Also measurements are done in wind tunnel and does not match real life situation. For this reason a study is made for the different correlations available and to select the one which is suitable for the model of the PV-DX panel.

Comparing correlations

Armstrong chooses Test as function and combines it with the free convection. However the function of Test already include free convection and the correlation does not take the wind direction into account. Palyvos makes an empirical 'average' of 36 different correlations, but this average also include correlations which are not suitable for solar panels

Table 15.1 Convective heat transfer coefficients for windspeeds of1 until 10 m/s

Wind speed	Test	Nusselt Jurges	Mc Adams	Fortuin	Armstrong	Kimura / Ito		Loveday and Taki		Palyvos		Sharples, Charlesworth	
0	8.6	5.8	5.8	5.6	8.7	12.2	12.2	8.9	4.9	7.4	4.2	8.3	8.3
1	11.0	9.6	9.4	9.4	11.1	12.2	12.2	10.9	6.7	11.4	7.7	10.4	9.5
2	13.5	13.4	13.1	13.3	13.5	12.2	12.2	12.9	8.5	15.4	11.2	12.5	10.8
3	15.9	17.2	16.7	17.1	16.0	15.7	11.5	14.9	10.2	19.4	14.7	14.6	12.0
4	18.4	20.9	20.4	20.9	18.4	18.6	12.2	16.9	12.0	23.4	18.2	16.7	13.3
5	20.8	24.7	24.0	24.8	20.8	21.3	13.0	18.9	13.8	27.4	21.7	18.8	14.5
6	23.3	27.9	27.6	27.9	23.3	23.8	13.7	20.9	15.6	31.4	25.2	20.9	15.8
7	25.7	31.5	31.3	31.4	25.7	26.1	14.4	22.9	17.3	35.4	28.7	23.1	17.0
8	28.2	34.9	34.9	34.9	28.2	28.3	15.0	24.9	19.1	39.4	32.2	25.2	18.3
9	30.6	38.3	38.6	38.2	30.6	30.4	15.7	26.9	20.9	43.4	35.7	27.3	19.5
10	33.1	41.6	42.2	41.5	33.1	32.4	16.3	28.9	22.6	47.4	39.2	29.4	20.8

A selection is made of 9 different correlations and the heat transfer at wind speed between 1 and 10 metre per second are presented in Table 15.1. The correlations have their own advantage and disadvantages. A choice is made taken into account the next considerations (a) the heat transfer coefficient is important in night situations when there is no sun (b) free convection is important when it is windless and no sun (c) ice formation on the panel will lower the heat transfer (d) wind directions are taken into account (e) The NEN5060 contain rough values for the wind speed with one decimal and average hourly data (f) the wind speeds between 1 and 5 m/s occur the most in the Netherlands (g) it is possible to spend a whole graduation report finding the appropriate convective correlation, since it is very complicate, but for now one correlation is chosen and the practise should show if this is correct.

Figure 15-1 Set up of the experimental test by Sharples and Charlesworth (1997)

Taken into account the afore mentioned considerations the equation from Sharples and Charlesworth (1997) is selected. This is based on experimental field test of a panel on a pitched roof (Figure 15-1). The correlation takes into account the wind direction and has a 'mild' heat transfer coefficient compared to other correlations, to build in safety for the reduced heat transfer because of possible ice formation. The free flow wind speed w is used in the equations:

$h_w = 2.2 \cdot w + 8.3$ (windward)

$h_w = 1.3 \cdot w + 8.3$ (leeward)

Sensitivity wind heat transfer

Taking into account the uncertainties of the wind heat transfer, the effect of a larger or smaller heat transfer can be simulated in the model. This show the sensitivity of the model towards the wind induced heat transfer. An annual simulation is done with a factor of 70% and 130% over the wind heat transfer equations. With a reduced heat transfer the efficiency of the system drops and the total electricity demand increases with 2,9%. Improving the heat transfer leads to a reduced heat demand of 0,7%.

Convection factor back side panel

The PV-DX panel is mounted on the roof with an air space in between. The convective heat transfer coefficient of the back side of the panel is lower than that of the top. The air layer has an opening on the lower and the top side of the roof, which allow convection. However the wind speed in the air cavity will be lower than outside. In addition the temperature of the air cavity will be lower than outside, resulting in a lower temperature difference and lower heat transfer. Ice formation will form a protective layer on the panel resulting in a lower heat transfer. Taking this in consideration a factor f_{wind} is used to present this reduced heat transfer. This is an arbitrary factor and in the practise this should be checked. The factor f_{wind} is set to 0,25.

The factor is used for the total heat transfer coefficient and not only for the wind speed. This result in a heat transfer on the back side between 2,1 and 7,4 W/m^{2}K for free flow wind speeds between 0 and 10 m/s. Due to lower wind speeds in the air cavity the free convection grow in influence, however the free convection is already incorporated in the equations of Sharples and Charlesworth (1997). Using the free flow heat transfer coefficient from the report of Zondag et al. (2003) and assuming a temperature difference between the panel and the air of 15 Kelvin, the heat transfer goes up to 3.5 W/m2.K. This means that the heat transfer coefficient at low wind speeds is underestimated if there is a high temperature difference between the panel and the air cavity. The wind speeds in the Netherlands is average 3,4 m/s and with f_{wind} this result in 3,2 and 3,9 W/m^{2}K for leeward and windward. This comes close to the calculated heat transfer due to free convection.

The wind speed and the heat transfer coefficient of the back side of the PV-DX panel is hard to predict. Computational Fluid Dynamic (CFD) simulations should be performed in order to calculate the heat transfer. This is not within the scope of this graduation research. In addition the input data of wind is not very detailed and is dependent on the surrounding buildings. The wind factor is used for this model where more sophisticated relation can be found in further research.

16. Appendix G - Heat pump equations

In this appendix the functioning of a heat pump with the accompanying equations are presented in the first part. The second part deals with the equations used in the Matlab model calculated with the refrigerant temperature. The program Coolpack is used to draw the thermodynamic cycles of the refrigerant. These numbers are used to calculate the heat capacity of the heat pumps with different evaporative temperatures (e.g. environmental conditions). The equations are presented for three different capacities of the heat pump.

Operation heat pump

In order to thermodynamically model the vapour-compression refrigeration systems some important features are represented below (Moran & Shapiro, 1996). A steady-state operation of the vapour-compression system is considered according to Figure 4-4. Beginning with the evaporator where a refrigeration effect is achieved as a result of evaporation of the refrigerant. For a control volume enclosing the refrigerant side of the evaporator give:

$$\dot{Q}_e = \dot{m} \cdot (h_1 - h_4) \tag{44}$$

Where $\dot{m}$ is the mass flow rate of the refrigerant, the enthalpy change from state 4 to state 1 is represented by $h_1 - h_4$ and the heat transfer rate $\dot{Q}_e$ is referred to as the refrigeration capacity in Watts.

The refrigerant leaving the evaporator is compressed to a relative high pressure and temperature by the compressor from state 1 to state 2. The equation for the mass and energy rate balance for a control volume enclosing the compressor, assuming no heat transfer to or from the compressor give:

$$\dot{W}_c = \frac{\dot{m} \cdot (h_2 - h_1)}{\eta_{comp}} \tag{45}$$

Next the refrigerant passes through the condenser where heat is transferred from the refrigerant to the region T_H due to condensation of the refrigerant. For a control volume enclosing the refrigerant side of the condenser, the heat transfer is:

$$\dot{Q}_c = \dot{m} \cdot (h_2 - h_3) \tag{46}$$

Finally the refrigerant enters the expansion valve and expands to the evaporator pressure from state 3 to state 4. The irreversible adiabatic expansion is modelled as a throttling process, for which:

$$h_3 = h_4 \tag{47}$$

Using the quantities and expressions introduced above, the coefficient of performance of the vapour-compression refrigeration system is

$$\text{COP} = \frac{\dot{Q}_c}{\dot{W}_c} \tag{48}$$

Coolpack

These equations are the basis to simulate the performance and the capacity of a heat pump. In the program Coolpack is used to draw the thermodynamic cycle of the refrigerant. Coolpack is a simulation tool for refrigeration developed by the Technical university of Denmark. A cycle is plotted in the pressure – enthalpy diagram (log P-H diagram) of R134a such as presented in Figure 4-4. The log P-H diagram of R134a can be found in Appendix H – Log P-H diagram R134a.

Enthalpy change

For the simulation an on-off heat pump with a constant volumetric flow is assumed. Thereby an overheating of 5 Kelvin and sub cooling of 5 Kelvin is assumed. The expansion valve controls the pressure in the evaporator. The compressor has a isentropic efficiency of 0,65. The minimal evaporative temperature is -30 °C corresponding to 0,9 bar and the maximum temperature simulated in the evaporator is 35 °C corresponding to 8,9 bar. Higher temperatures will result in saturated vapour and with the same volume the pressure goes up to 10 bar for 80 °C.

Taking this assumptions into account 28 cycles are plotted in Coolpack, 14 for a condensing temperature of 40 °C for heating and 14 cycles at a condensing temperature of 60°C for the hot water. The enthalpy change for the different evaporative temperatures are presented in Table 16.1 and Table 16.2. These delta enthalpy values remain the same for the different heat pump capacities.

Table 16.1 Enthalpy change for 40 °C condensing temperature (Coolpack)

Evaporative T_refr [°C]	-30	-25	-20	-15	-10	-5	0	5	10	15	20	25	30	35
Evaporator 1-4 [KJ/Kg]	134	138	141	144	147	150	153	156	159	162	165	167	170	173
Compressor 1-2 [KJ/Kg]	81	74	67	60	53	47	41	35	29	24	19	14	9	4
Condenser 2-3 [KJ/Kg]	216	211	207	203	200	197	194	191	188	186	183	181	179	177

Table 16.2 nthalpy change for 60 °C condensing temperature (Coolpack)

Evaporative T_refr [°C]	-30	-25	-20	-15	-10	-5	0	5	10	15	20	25	30	35
Evaporator 1-4 [KJ/Kg]	104	107	110	113	116	119	122	125	128	131	134	137	140	142
Compressor 1-2 [KJ/Kg]	99	91	83	76	70	63	57	51	46	40	35	30	25	20
Condenser 2-3 [KJ/Kg]	202	198	194	190	186	183	180	177	174	171	169	167	165	163

Capacity heat pumps

The ENergy Roof model includes three capacities of heat pump where the 3 kW heat pump is set as standard. This is the capacity at nominal conditions at air temperature of 7 °C and water temperature of 35 °C (A7W35). It is assumed that in an ASHP the refrigerant temperature lies 10 degrees below the outside temperature, thus in nominal conditions at -3 °C. With this the mass flow of a 3 kW heat pump can be calculated with equation (46) and Table 16.1. Knowing the mass flow we can calculate the volumetric flow of the refrigerant in this condition. Notice that the volumetric flow is constant for all the evaporative temperatures, where the mass flow and density of the refrigerant changes. The volumetric flow V is calculated using equation (49) and Table 16.3.

$$\dot{m} = \frac{V}{v \cdot 3600} \left[\frac{kg}{s}\right] \quad (49)$$

For a 3 kW heat pump this result in a volumetric flow of 4,3 m^3/h. The 4 kW and 5 kW heat pump has a volumetric flow of respectively 5,8 and 7,3 m^3/h. Once the volumetric flow is calculated the mass flow can be calculated for all the evaporative temperatures. Since the density of the refrigerant changes, also the mass flow changes, see equation (49). The density v is obtained from Coolpack and presented in Table 16.3. In the same table the calculated mass flows are presented for the three heat pump capacities.

Table 16.3 Density and mass flow of refrigerant R134a of various evaporative temperatures

T_refr [°C]	-30	-25	-20	-15	-10	-5	0	5	10	15	20	25	30	35
v [m^3/kg]	0.230	0.185	0.150	0.123	0.101	0.084	0.071	0.060	0.051	0.043	0.037	0.032	0.027	0.024
$\dot{m}$ [kg/s] 3 kW - HP	0.005	0.006	0.008	0.010	0.012	0.014	0.017	0.020	0.024	0.028	0.032	0.038	0.044	0.050
$\dot{m}$ [kg/s] 4 kW - HP	0.007	0.009	0.011	0.013	0.016	0.019	0.023	0.027	0.032	0.037	0.044	0.051	0.059	0.068
$\dot{m}$ [kg/s] 5 kW - HP	0.009	0.011	0.014	0.016	0.020	0.024	0.029	0.034	0.040	0.047	0.055	0.064	0.074	0.086

Knowing the mass flow and the delta enthalpy for the different evaporative temperatures the functioning of the heat pump can be predicted. Using equation (44), (45), (46) and (48) respectively the evaporating capacity, the electrical compressor, the condensing capacity and COP of the heat pump is calculated. An additional efficiency η_{comp} of 0,9 for the compressor is inserted, which result in a higher electrical demand of the compressor and a lower COP of the heat pump. For the 3 kW heat pump also the total efficiency is calculated in order to compare this with the state of the art heat pumps, which have an efficiency between 0,3 and 0,4 (Carrier, 2016). The result of the 3 kW heat pump are presented in Table 16.4. The other tables are presented in the end of the appendix.

Table 16.4 Specifications heat pump 3kW capacity and 40 °C condensing temperature

T_refr [°C]	-30	-25	-20	-15	-10	-5	0	5	10	15	20	25	30	35
$\dot{Q}_e$ [W]	699	889	1120	1398	1729	2122	2585	3127	3759	4492	5339	6314	7432	8712
$\dot{W}_c$ [W]	470	530	589	644	694	734	763	776	768	736	674	576	436	247
$\dot{Q}_c$ [W]	1122	1366	1650	1977	2353	2783	3272	3826	4451	5155	5946	6832	7825	8934
COP [W/W]	2.39	2.58	2.80	3.07	3.39	3.79	4.29	4.93	5.79	7.00	8.82	11.86	17.94	36.21
Efficiency [-]	0.43	0.42	0.41	0.40	0.39	0.37	0.35	0.32	0.28	0.23	0.14	-	-	-

A graph can be made from the data points of the 3 kW heat pump evaporating capacity $\dot{Q}_e$ where a third-power regression line is plotted that fit the points. The same can be done for the evaporating capacity at condensing temperature of 60 °C $\dot{Q}_{e\_60}$ and for the condensing capacity $\dot{Q}_c$ resulting in Figure 16-1.

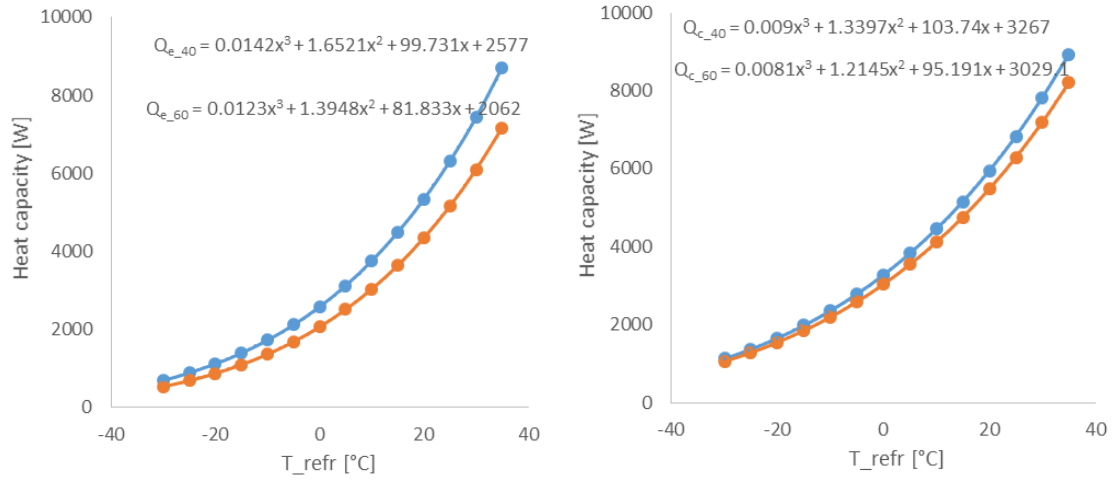

Figure 16-1 Heat capacity in the evaporator Qe (left) and condenser Qc (right) for 40 and 60 °C refrigerant temperature

Tables

The specifications of the heat pumps are presented below.

Table 16.5 Specifications heat pump 3kW capacity and 60 °C condensing temperature

T_refr [°C]	-30	-25	-20	-15	-10	-5	0	5	10	15	20	25	30	35
$\dot{Q}_e$ [W]	540	692	877	1101	1370	1690	2069	2515	3037	3645	4349	5162	6098	7171
$\dot{W}_c$ [W]	570	653	738	825	911	994	1072	1140	1196	1237	1257	1252	1217	1146
$\dot{Q}_c$ [W]	1053	1279	1541	1843	2190	2585	3033	3541	4114	4758	5480	6289	7193	8203
COP [W/W]	1.85	1.96	2.09	2.23	2.40	2.60	2.83	3.11	3.44	3.85	4.36	5.02	5.91	7.16
Efficiency [-]	0.45	0.45	0.44	0.44	0.43	0.42	0.41	0.40	0.39	0.37	0.35	0.33	0.29	0.23

Table 16.6 Specifications heat pump 4kW capacity and 40 °C condensing temperature

T_refr [°C]	-30	-25	-20	-15	-10	-5	0	5	10	15	20	25	30	35
$\dot{Q}_e$ [W]	943	1199	1511	1885	2332	2862	3487	4218	5071	6060	7202	8516	10025	11751
$\dot{W}_c$ [W]	635	715	794	869	936	991	1029	1046	1036	993	909	777	588	333
$\dot{Q}_c$ [W]	1514	1843	2226	2667	3174	3754	4413	5160	6004	6953	8020	9216	10554	12051
COP [W/W]	2.39	2.58	2.80	3.07	3.39	3.79	4.29	4.93	5.79	7.00	8.82	11.86	17.94	36.21

Table 16.7 Specifications heat pump 4kW capacity and 60 °C condensing temperature

T_refr [°C]	-30	-25	-20	-15	-10	-5	0	5	10	15	20	25	30	35
$\dot{Q}_e$ [W]	728	933	1183	1485	1847	2279	2791	3392	4096	4916	5866	6963	8225	9673
$\dot{W}_c$ [W]	769	880	996	1113	1229	1341	1445	1538	1614	1668	1695	1689	1641	1546
$\dot{Q}_c$ [W]	1420	1725	2079	2486	2953	3486	4092	4776	5549	6417	7391	8482	9702	11064
COP [W/W]	1.85	1.96	2.09	2.23	2.40	2.60	2.83	3.11	3.44	3.85	4.36	5.02	5.91	7.16

Table 16.8 Specifications heat pump 5kW capacity and 40 °C condensing temperature

T_refr [°C]	-30	-25	-20	-15	-10	-5	0	5	10	15	20	25	30	35
$\dot{Q}_e$ [W]	1187	1510	1901	2373	2935	3603	4389	5309	6382	7627	9064	10719	12618	14790
$\dot{W}_c$ [W]	799	900	1000	1094	1178	1247	1295	1317	1304	1250	1144	978	740	419
$\dot{Q}_c$ [W]	1906	2320	2801	3357	3995	4725	5554	6494	7556	8752	10094	11599	13284	15167
COP [W/W]	2.39	2.58	2.80	3.07	3.39	3.79	4.29	4.93	5.79	7.00	8.82	11.86	17.94	36.21

Table 16.9 Specifications heat pump 5kW capacity and 40 °C condensing temperature

T_refr [°C]	-30	-25	-20	-15	-10	-5	0	5	10	15	20	25	30	35
$\dot{Q}_e$ [W]	917	1174	1488	1869	2325	2869	3512	4270	5156	6187	7383	8763	10352	12174
$\dot{W}_c$ [W]	968	1108	1253	1401	1547	1688	1819	1935	2031	2100	2134	2125	2066	1946
$\dot{Q}_c$ [W]	1788	2171	2616	3129	3717	4388	5150	6012	6984	8077	9303	10676	12212	13925
COP [W/W]	1.85	1.96	2.09	2.23	2.40	2.60	2.83	3.11	3.44	3.85	4.36	5.02	5.91	7.16

Equations

The complete list of equations for the 3, 4 and 5 kW heat pump are presented below.

3kW heat pump

$$\dot{Q}_{e\_40} = 0.0142{T_{refr}}^3 + 1.6521{T_{refr}}^2 + 99.731T_{refr} + 2577$$

$$\dot{Q}_{e\_60} = 0.0123{T_{refr}}^3 + 1.3948{T_{refr}}^2 + 81.833T_{refr} + 2062$$

$$\dot{Q}_{c\_40} = 0.009{T_{refr}}^3 + 1.3397{T_{refr}}^2 + 103.74T_{refr} + 3267$$

$$\dot{Q}_{c\_60} = 0.0081{T_{refr}}^3 + 1.2145{T_{refr}}^2 + 95.191T_{refr} + 3029.1$$

4kW heat pump

$$\dot{Q}_{e\_40} = 0.0192{T_{refr}}^3 + 2.2284{T_{refr}}^2 + 134.52T_{refr} + 3476$$

$$\dot{Q}_{e\_60} = 0.0166{T_{refr}}^3 + 1.3948{T_{refr}}^2 + 81.833T_{refr} + 2062$$

$$\dot{Q}_{c\_40} = 0.0122{T_{refr}}^3 + 1.807{T_{refr}}^2 + 139.93T_{refr} + 4407$$

$$\dot{Q}_{c\_60} = 0.0109{T_{refr}}^3 + 1.6382{T_{refr}}^2 + 128.4T_{refr} + 4085$$

5kW heat pump

$$\dot{Q}_{e\_40} = 0.0241{T_{refr}}^3 + 2.8047{T_{refr}}^2 + 169.31T_{refr} + 4375$$

$$\dot{Q}_{e\_60} = 0.0208{T_{refr}}^3 + 2.3679{T_{refr}}^2 + 138.93T_{refr} + 3501$$

$$\dot{Q}_{c\_40} = 0.0154{T_{refr}}^3 + 2.2743{T_{refr}}^2 + 176.11T_{refr} + 5547$$

$$\dot{Q}_{c\_60} = 0.0138{T_{refr}}^3 + 2.0618{T_{refr}}^2 + 161.6T_{refr} + 5142$$

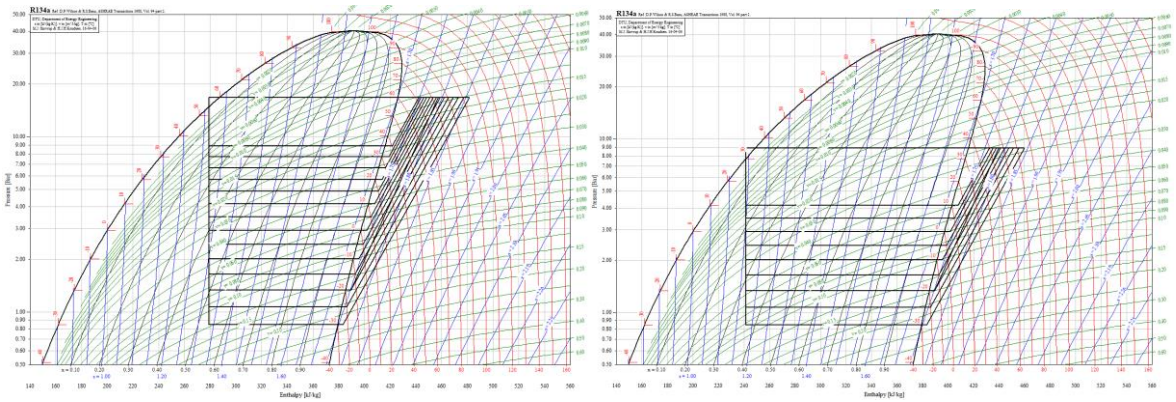

Figure 16-2 Coolpack 28 plotted thermodynamic cycles of R134a for 40 °C (left) and 60 °C (right) condensing temperatures

17. Appendix H – Log P-H diagram R134a

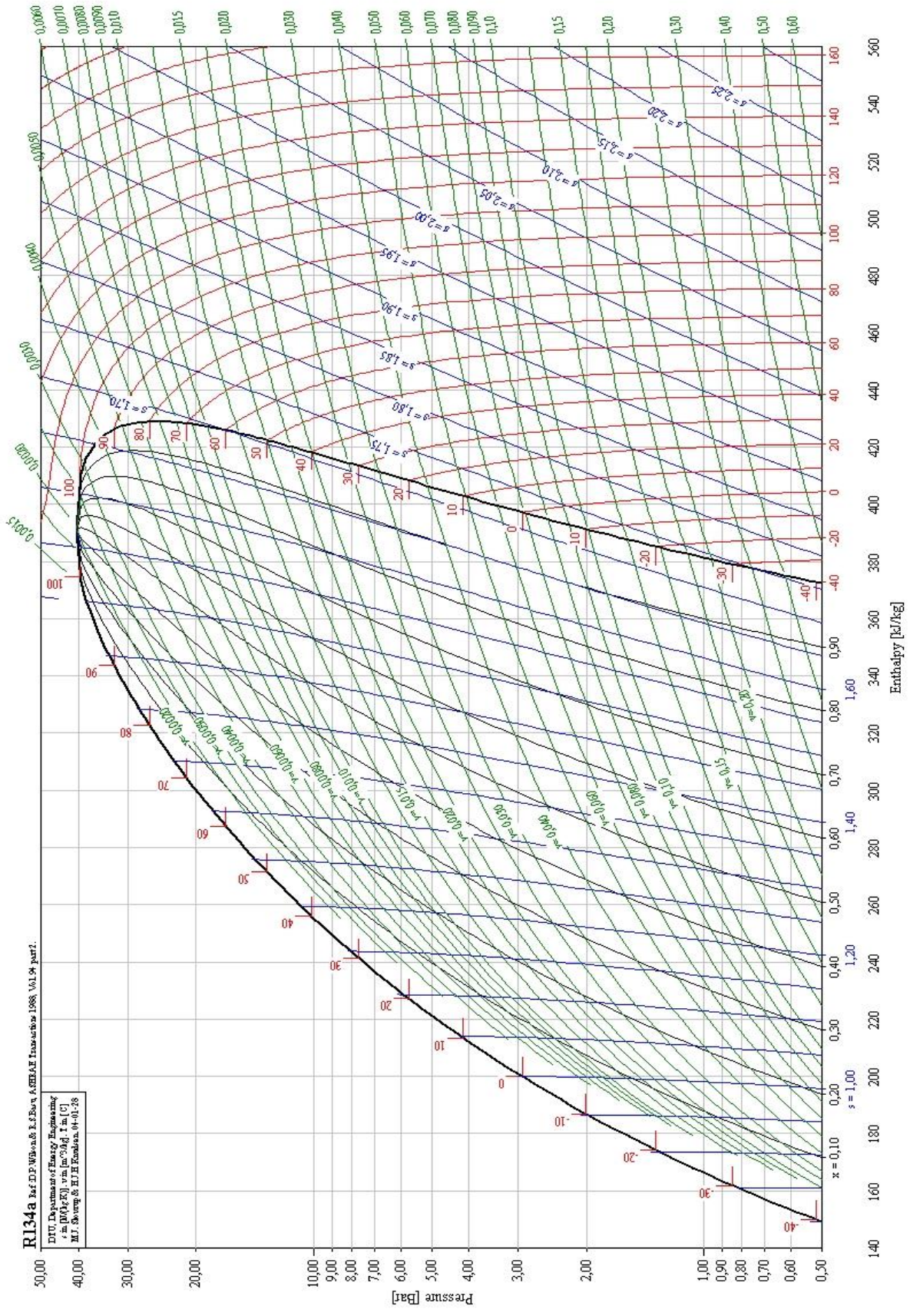

18. Appendix I – Detail drawings

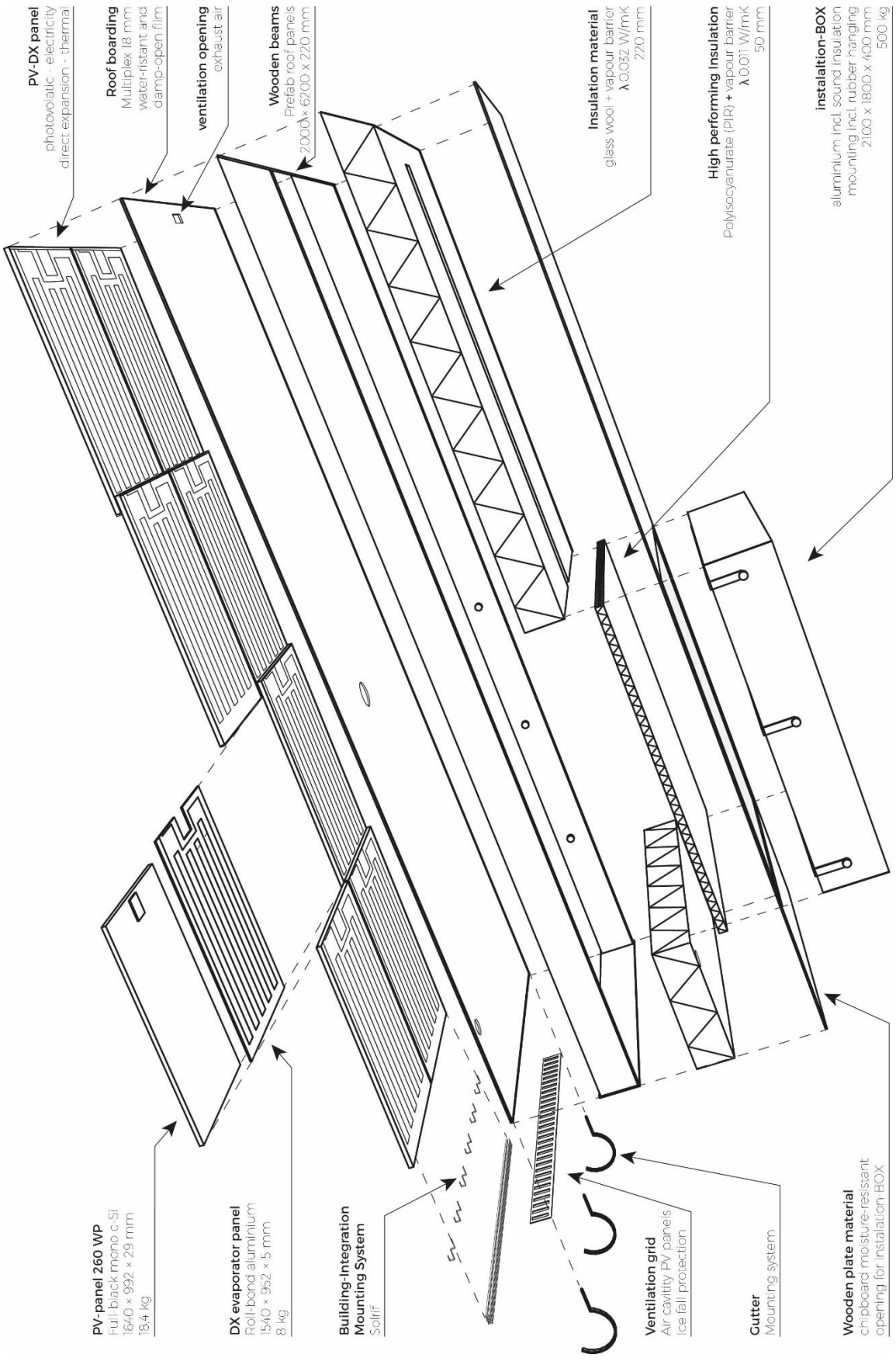

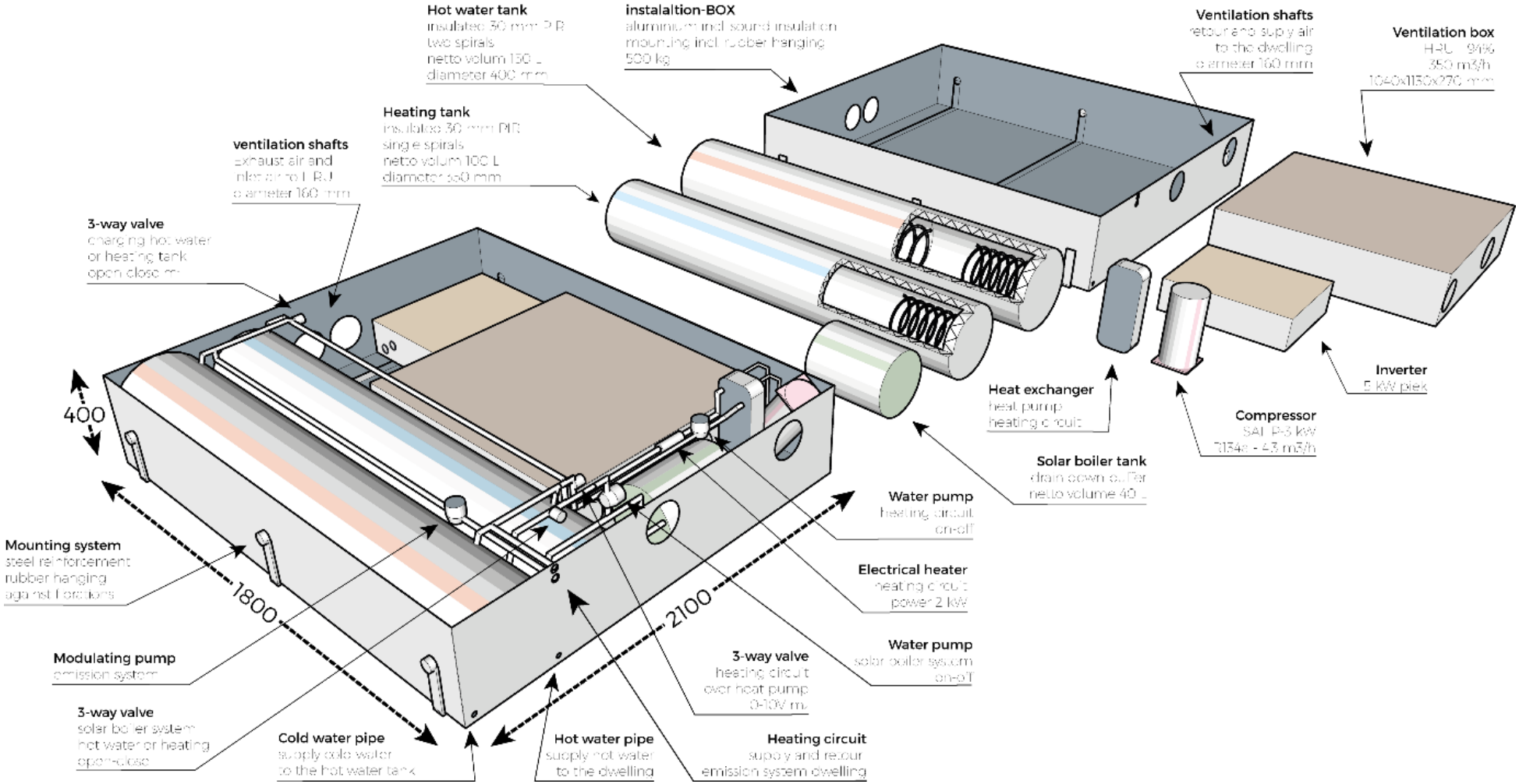
Hot water tank
insulated 30 mm PIR
two spirals
netto volum 150 L
diameter 400 mm
instalaltion-BOX
aluminium and sound insulation
mounting incl. rubber hanging
500 kg
Ventilation shafts
retour and supply air
to the dwelling
diameter 160 mm
Ventilation box
HRU 94%
350 m3/h
1040x1150x270 mm
Heating tank
insulated 30 mm PIR
single spirals
netto volum 100 L
diameter 350 mm
ventilation shafts
exhaust air and
inlet air to HRU
diameter 160 mm
3-way valve
charging hot water
or heating tank
open close m
400
Heat exchanger
heat pump
heating circuit
Inverter
5 kW plex
Compressor
SAT P-5 kW
7134e - 43 m3/h
Solar boiler tank
drain down buffer
netto volume 40 L
Water pump
heating circuit
on-off
Mounting system
steel reinforcement
rubber hanging
against vibrations
1800
2100
Electrical heater
heating circuit
power 2 kW
Water pump
solar boiler system
on-off
Modulating pump
emission system
3-way valve
heating circuit
over heat pump
0-10V m
3-way valve
solar boiler system
hot water or heating
open close
Cold water pipe
supply cold water
to the hot water tank
Hot water pipe
supply hot water
to the dwelling
Heating circuit
supply and recour
emission system dwelling

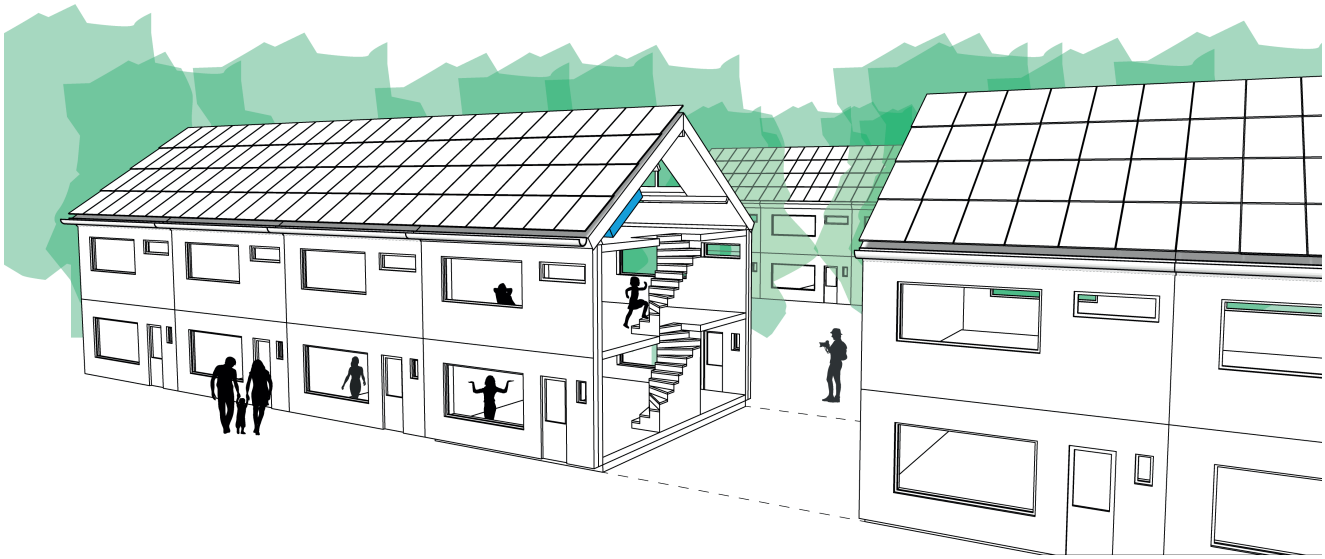

TU Delft

VAN DORP
MET KENNIS EN RESPECT